

**EXPERIMENTAL STUDY OF
LOCAL SCOUR AT THE TOE OF PROTECTED EMBANKMENT**

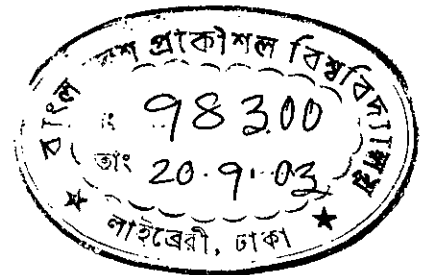
M. M. RABIQUL HASAN

**DEPARTMENT OF WATER RESOURCES ENGINEERING
BANGLADESH UNIVERSITY OF ENGINEERING AND TECHNOLOGY
DHAKA
August, 2003**

EXPERIMENTAL STUDY OF
LOCAL SCOUR AT THE TOE OF PROTECTED EMBANKMENT

M. M. Rabiquil Hasan

A Project submitted to the Department of Water Resources Engineering in Partial
fulfillment of the requirements for the degree of Masters of Engineering in
Water Resources.



#98300#

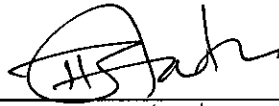
Department of Water Resources Engineering
Bangladesh University of Engineering and Technology
Dhaka

August, 2003

Bangladesh University of Engineering & Technology
Department of Water Resources Engineering

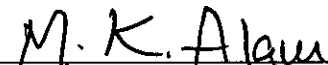
Recommendation of the Board of Examiners

We hereby recommended that the project prepared by M. M. Rabiqul Hasan, Roll No. 100116008 F, Session October, 2001 entitled “**Experimental Study of Local Scour at the Toe of Protected Embankment**” be accepted as satisfactory in partial fulfillment of the requirement for the degree of Master of Engineering in Water Resources.

1. 

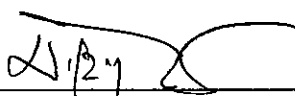
Dr. Md. Abdul Matin
Professor, Department of Water Resources Engineering
Bangladesh University of Engineering and Technology

Chairman
(Supervisor)

2. 

Dr. M. K. Alam
Professor, Department of Water Resources Engineering
Bangladesh University of Engineering and Technology

Member

3. 

Dr. M. Monowar Hossain
Professor, Department of Water Resources Engineering
Bangladesh University of Engineering and Technology

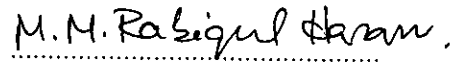
Member

CERTIFICATE OF RESEARCH

This is to certify that except where specific reference to other investigators is made the work described in this thesis is the result of the investigation of the candidate. Neither this thesis nor any part thereof has been submitted elsewhere for the award of any degree or diploma.



.....
(Prof. Dr. M. A. Matin)
Countersigned by the Supervisor



.....
(M. M. Rabiqul Hasan)
Signature of the Candidate

TABLE OF CONTENTS

	Page No.
TABLE OF CONTENTS	v
LIST OF TABLES	vii
LIST OF FIGURES	viii
LIST OF NOTATIONS	xi
ACKNOWLEDGEMENT	xiv
ABSTRACT	xv
Chapter 1 INTRODUCTION	1
1.1 Background	1
1.2 Objective of the Study	2
1.3 Scope and Limitations of the Present Study	3
Chapter 2 LITERATURE REVIEW	4
2.1 Introduction	4
2.2 Scour	4
2.3 According to the Location of the Scour	5
2.3.1 General Scour	6
2.3.2 Contraction Scour	6
2.3.3 Local Scour	6
2.4 According to the Sediment Transport Capacity	7
2.4.1 Clear Water Scour	7
2.4.2 Live Bed Scour	7
2.5 Bed Form	8
2.5.1 Characteristics of Bed Forms	8
2.6 Flow Around Embankment-like Structure at the Flat Bed Condition	10
2.7 Scouring Around Embankment Type Structure	12
2.7.1 Time Scale for Local Scour	13
2.8 Available Prediction Method of Local Scour Around Embankment	17

	2.9	Types of Earthen Embankment	25
	2.10	Method of construction	27
	2.11	Suitable Preliminary Section for Embankment	28
Chapter	3	EXPERIMENTAL SET UP AND	30
	3.1	METHODOLOGY	30
	3.2	Methodology	31
		Experimental Setup and Measurement	31
	3.2.1	Laboratory Channel System	34
	3.2.2	Measuring Devices	36
	3.2.3	Hydraulic parameter	36
	3.2.4	Bed Material	38
	3.3	3.2.5 Types of Structures	39
		Measurements	40
	3.3.1	Discharge	40
	3.3.2	Scour Depth	40
	3.3.3	Scour Area	40
	3.3.4	Velocity	51
Chapter	4	RESULTS AND DISCUSSION	68
	4.1	Shape or Slope Factor	68
	4.2	Scour Profile Variation	73
	4.3	Scour Area and characteristics	76
Chapter	5	CONCLUSION AND RECOMMENDATION	83
	5.1	Conclusion	83
	5.2	Recommendation for Future Studies	84
		REFERENCES	85

LIST OF TABLES		
Table 2.1	Classification of Bed Forms and their Characteristics	Page 9
Table 2.2	Suggested Value of K	Page 18
Table 2.3	Shape/Slope Correction Factor Proposed by Melville	Page 24
Table 2.4	Comparison of Shape/Slope Factors of Melville and Rahaman and Muramoto	Page 25
Table 2.5	U.S.B.R. Recommendations for Free board for Embankment	Page 28
Table 2.6	Terzaghi's side Slope for Earthen Embankment	Page 29
Table 3.1	Test Hydraulic Parameter	Page 37
Table 4.1	Comparison of scour depth with experimented value and equation value	Page 73

LIST OF FIGURE

Figure 2.1	Shield's Diagram for Incipient Motion	Page 4
Figure 2.2	Types of Scour	Page 5
Figure 2.3	Types of Bed form	Page 8
Figure 2.4	Amplification of Shear Velocity as function of b/h	Page 11
Figure 2.5	Verification of Local Scour Depth with Flow Velocity and T	Page 14
Figure 2.6	Temporal Development of Local Scour Depth Around Abutment	Page 15
Figure 2.7	Flow concentration of the restricted region close to the Abutment-like structures	Page 19
Figure 2.8	Concentration of Discharge Fluxes close to the Structure	Page 20
Figure 2.9	Amplification of Shear Velocity close to the Structure	Page 21
Figure 2.10	Critical Shear velocity vs. Particle size graph for Cohesionless Soil	Page 22
Figure 2.11	Homogenous type Embankment	Page 26
Figure 2.12	Zoned type Embankment	Page 27
Figure 2.13	Diaphragm type Embankment	Page 27
Figure 3.1	Layout of Channel System with Embankment type Structure	Page 31
Figure 3.2	Laboratory Channel	Page 32
Figure 3.3	Rehbok Weir and Associated Point Gauge	Page 34
Figure 3.4	P.- E.M.S. Control Unit	Page 35
Figure 3.5	P.- E.M.S. Probes	Page 35
Figure 3.6	Point Gauge	Page 36
Figure 3.7	Grain Size Distribution of Bed Material	Page 38
Figure 3.8	Photograph of Sloping Structure used in the Study	Page 39
Figure 3.9	Photograph of Vertical Structure used in the Study	Page 39
Figure 3.10	Scour for Structure with 1V: 1H Slope	Page 41
Figure 3.11	Scour for Structure with 1V: 2H Slope	Page 42
Figure 3.12	Scour for Structure with 1V: 3H Slope	Page 43
Figure 3.13	Scour for Vertical Structure with $b= 60\text{cm}$	Page 44
Figure 3.14	Scour for Vertical Structure with $b= 40\text{cm}$	Page 45
Figure 3.15	Scour for Vertical Structure with $b= 20\text{cm}$	Page 46
Figure 3.16	Longitudinal Scour Profile for Sloping-wall Structure	Page 47
Figure 3.17	Longitudinal Scour Profile for Vertical-wall Structure	Page 48

Figure 3.18	Lateral Scour Profile for Sloping-wall Structure	Page 49
Figure 3.19	Lateral Scour Profile for Vertical-wall Structure	Page 50
Figure 3.20	Selected points for Vertical Velocity Measurement	Page 51
Figure 3.21	Velocity Vector for 1V: 1H Slope Structure	Page 52
Figure 3.22	Velocity Vector for 1V: 2H Slope Structure	Page 52
Figure 3.23	Velocity Vector for 1V: 3H Slope Structure	Page 53
Figure 3.24	Velocity Vector for 20cm width Vertical Structure	Page 53
Figure 3.25	Velocity Vector for 40cm width Vertical Structure	Page 54
Figure 3.26	Velocity Vector for 60cm width Vertical Structure	Page 54
Figure 3.27to	Vertical Velocity Distribution of different Point of Structure	Page 55
Figure3.31	1V: 1H Slope	
Figure 3.32to	Vertical Velocity Distribution of different Point of Structure	Page 57
Figure 3.36	1V: 2H Slope	
Figure 3.37to	Vertical Velocity Distribution of different Point of Structure	Page 59
Figure 3.41	1V: 3H Slope	
Figure 3.42to	Vertical Velocity Distribution of different Point of Vertical	Page 61
Figure 3.46	Structure, b=60cm	
Figure 3.47to	Vertical Velocity Distribution of different Point of Vertical	Page 63
Figure 3.51	Structure, b=40cm	
Figure 3.52to	Vertical Velocity Distribution of different Point of Vertical	Page 65
Figure 3.56	Structure, b=20cm	
Figure 4.1	Comparison of Experimental data with curves, 1V: 1H Slope Structure	Page 69
Figure 4.2	Comparison of Experimental data with curves, 1V: 2H Slope Structure	Page 70
Figure 4.3	Comparison of Experimental data with curves, 1V: 3H Slope Structure	Page 71
Figure 4.4	Comparison of Experimental data with curves of Vertical Structures	Page 72
Figure 4.5	Longitudinal Scour Variation for Sloping –wall Structures	Page 74
Figure 4.6	Longitudinal Scour Variation for Vertical –wall Structures	Page 74
Figure 4.7	Lateral Scour Variation for Sloping –wall Structures	Page 75
Figure 4.8	Lateral Scour Variation for Vertical –wall Structures	Page 75

Figure 4.9	Scour Area of Different Structure	Page 76
Figure 4.10	Scour Around the 1V:1H Slope Structure	Page 77
Figure 4.11	Scour Around the 1V:2H Slope Structure	Page 78
Figure 4.12	Scour Around the 1V:3H Slope Structure	Page 79
Figure 4.13	Scour Around the Vertical Structure, b=60cm	Page 80
Figure 4.14	Scour Around the Vertical Structure, b=40cm	Page 81
Figure 4.15	Scour Around the Vertical Structure, b=20cm	Page 82

LIST OF NOTATIONS

Symbols	Description
A	Cross sectional area of channel
B	Width of channel
b	Flow restriction width
b_s	Region of amplified flow velocity
C	Constant
D	Sediment diameter
d_s	Scour depth
d_{se}	Equilibrium scour depth
d_{ss}	Maximum scour depth of slope-wall structure
d_{sv}	Maximum scour depth of vertical wall structure
d_{50}	Diameter size for which 50% of the material are finer by weight
d_{90}	Diameter size for which 90% of the materials are finer by weight
f	Silt factor
F_r	Froude number
g	Acceleration due to gravity
h	Water depth
K	Multiplication factor
K_{yB}	Flow depth-foundation size factor
K_{yb}	Flow depth-foundation size factor for structure
K_{yt}	Flow depth-foundation size factor for abutment
K_d	Sediment size factor
K_G	Channel geometry factor
K	Factor
K_{sc}	Muramoto and Rahaman shape/slope factor

K_{sm}	Melville shape/slope factor
K_{sm}^*	Adjusted correlation factor
K_t	Time factor
K_o	Alignment factor
L	Abutment length
m, n	Constant
n	Manning's roughness coefficient
Q	Discharge
q	Discharge per unit width
R	Lacey's regime depth
r	Empirical constant
S	Longitudinal slope of the channel
t	Time
t_e	Time at which equilibrium is reached
u	Approach flow velocity
u_c	Critical velocity
u_*	Bed shear velocity
u_{*c}	Critical bed shear velocity
u_m	Amplified velocity
u_{*m}	Bed shear velocity around structure
V	Approach velocity
X	Longitudinal coordinate of the channel
Y	Lateral coordinate of the channel
y	Approach flow depth
Z	Depth measured from initial bed level
α	Constant
β	Empirical constant
γ	Unit weight of water
γ_s	Unit weight of sediment
ϕ	Angle of repose of bed material
θ	Slope angle of structure made with horizontal
ν	Kinematic viscosity of water
ρ	Water density
τ_*	Bed shear stress
τ_{*c}	Critical bed shear stress

ACKNOWLEDGEMENT

The author expresses his sincere gratitude and respect to Dr. M. Abdul Matin, Professor, Department of Water Resources Engineering, BUET for his constant supervision, valuable suggestions, keen interest and encouragement throughout the work. His constructive comments and expertise helped the author for better understanding of the study from the selection of the topic until the completion.

The author's sincere thanks also goes to the members of the examination board Dr. M. K. Alam, Professor and Dr. M. Monowar Hossain, Professor, Department of Water Resources Engineering, BUET for their thorough examination and criticism of the thesis work without which this paper would not achieve clarity at many places.

The author is very much thankful to M. Anisul Haque, Associate Professor, IWFM, BUET and Engr. M. Shoel Rana, Research Assistant, BUET-DUT Project, Department of Water Resources Engineering for their valuable suggestion and co-operation.

The author is very much grateful to his parents for their continuous prayer and concern. Without their constant support and encouragement the present study could not be completed in time. The author also wishes to give thanks to his family members, friends and laboratory staff.

Above all the author is grateful to the almighty who has given him the opportunity to work hard with pleasure.

M. M. Rabiqul Hasan

August, 2003.

ABSTRACT

Local scour occurs around embankments, spur dikes and abutments because of the obstruction to flow caused by such structures. The scour hole develops as overbank flow reenters the main channel and sets up large vortices to wash sediment away. But in laboratory tests, scour hole seldom stays constant under a constant discharge, because the depth of scour fluctuates with time when there are dunes moving on the alluvial bed. Embankments those are directed downstream have smaller scour holes than those of angled upstream because the scour depth is directly related to the extent of the obstruction to flow. Scour depth around embankment-like structures increases as the value of b/h (b = length of the structure in the lateral direction and h =approach flow depth) increases up to certain extent. A number of scour depth prediction formulae available so far have been analyzed in order to find out appropriate scour predictor around such structures in Bangladesh. The study was made under clear-water condition. The hydraulic parameters were set so that the flow is close to the critical condition of sediment transport that is clear-water condition.

For scour study, three sloping-wall embankment type structures and three vertical-wall embankment type structures were used. These structures were made of half-inch thick particleboards and wood. Around these structures the scour depth, scour contour, scour pattern, scour area, velocity vector and vertical velocity distribution were observed. Bed level variation of each structure was compared with others. Each test was run for 7 hours and 30 minutes. This test running time was selected based on the limitation of laboratory pump and in an attempt to reach equilibrium stage. Results were compared with some existing prediction methods (Lacey 1930, Melville 1992, Rahaman and Muramoto 1999, Liu 1961).

It was found that for vertical-wall structures the results were close to Lacey's (1930) method. Particularly, the value of vertical structure with larger width, $b=60\text{cm}$ was

very close to Lacey's (1930) method. For sloping-wall structures experimented value were near to Lacey's method. For Melville's (1992), Rahaman and Muramoto's and Liu's (1961) cases scour values were higher than Lacey's.

Finally, suggestions have been put forward for further extension of the study.

CHAPTER 1

INTRODUCTION

1.1 Background

Bangladesh is primarily a deltaic riverine and disaster prone country, where floods, embankment failure, sedimentation over the flood plain are regular natural hazards every year during the monsoon. In order to protect people's hearth and home embankment construction has become an established practice in Bangladesh from long before. But unfortunately, every year devastating flood damages hundred of embankments (Islam, 1994). According to Tobin (1995) evidence from aerial photography satellite imagery and flood plain maps suggest that 90% of the area affected by significantly floodplain erosion and sedimentation were those where embankment had been damaged.

Scour occurs around embankments because of the obstruction to flow and the removal of material by running water (Chang, 1988). From the engineering viewpoint, one is always interested in determining the potential scour so that the provisions can be made in design and construction (Chang, 1988). The engineer is often called to design bank protection and conveyance channels that must maintain stability while subject to scour.

Many investigator have studied various aspect of local scour around embankment as a result, a number of prediction methods are available at present, which are inherently empirical in nature. Unfortunately, estimations of scour depth around embankment in alluvial channels are involved with lot of uncertainties. Therefore, engineers often find structures in danger due to excessive scour and they have to seek for some remedial measures to provide safety to the structure.

Local scour can affect the stability of the structure such as riprap embankment and lead to failures if measures are not taken to address the scour (Fischenich and Landers, 1999). One of main reason of embankment failure noted by Tobin (1995) is scouring, this can extended for a mile or downstream for example the failure of several embankment in Hartsburg (Missouri) lead to inundation of the town (Tobin and Ollenburger, 1994).

As per convenient practice of the BWDB (1984) the embankment slope should be 1:2 on the c/s and 1:3 on the r/s. The Local Government and Engineering Department (LGED, 1983)

recommended the side slope of flood embankments both for r/s and c/s to be 1:2 to 1:3 for normal soils (silt and silty clay) and 1:3 to 1:5 for loose sandy soil. Compared with the slope criteria recommended by the BWDB and LGED, both the r/s and c/s slope of the failure embankments studied were inadequate and steep. Safiullah (1977,1982) noted that all the slopes of the Dhaka – Narayanganj – Demra (DND) embankment where toe erosion took place had slopes 1:1.5, 1:1.25, 1:1.38 and 1:1.5 and all of them bellow that required for toe deterioration. It is estimated that about 1200 km of the bank length of the rivers are subjected to erosion and of which about 565 km faces severe erosion problem (BWDB, 1984). During 1985-1995, a detail study was made by IWFM on total fourteen embankment failure location (Islam,1991), none had toe protection arrangement or any internal filter drainage. Therefore, some form of erosion was noted in most of them.

It is important that the design should be safe against scouring. Several embankment protection works have been carried out in our country. Embankment failure resulting in sedimentation over the floodplain and crop damage is a frequent natural disaster in Bangladesh. But unfortunately, very little or no study is available in this regard. Some experimental studies have been done on local scour in the Department of Water Resources Engineering, BUET and those were related on pier and abutment. No mentionable experimental works on embankment scour related to local soil condition have been done. Therefore, in this study an attempt has been made to conduct laboratory study on local scour around embankment type structure for local soil condition.

1.2 Objective of the Study

Following objectives have been set-up for the proposed study:

- To determine the magnitude of scour depth at toe of the protected embankment.
- To compare the observed scour depth with different empirical formula available in the literature.
- Finally to recommend a suitable formula for the design of embankment scour with special reference to Bangladeshi soil condition.

1.3 Scope and Limitations of the Present Study

It is not possible to include everything in a study mainly because of time limitation. However, according to the objectives whatever could be made possible were included. The structures were used in this study were useful to find out the objective. Scour pattern of various structure can be analyzed. This experimental study will also increase on scour around embankment for designing a stabilized stream bank and will evaluate the performance of the protection measure.

In any experimental study there are limitations to specify the boundary conditions and other hydraulic conditions to define the set up of that experiment. Present study also had few limitations. They are describing below:

- 1) The maximum allowable running time for the laboratory pump was 8 hours at a stretch. Moreover, there was no standby pump. In experimental studies, equilibrium phase was not observed until after 50-160 hours (Cardoso, 1999). Therefore, no test could be run up to equilibrium stage.
- 2) Small bed features associated with fine and medium sand are called ripples (Raudkivi, 1997). Ripple formation is associated with fine sand ($D_{50} \leq 0.7mm$) observed in laboratory experiments under clear water conditions (Melville, 2000). Channel bed was prepared with fine sand of $D_{50} = 0.226mm$. As such there was ripple formation. But in this study, these ripple effect was not in consideration.
- 3) The channel was straight. The flow condition was theoretically kept as 'clear-water' by keeping ratio of bed shear stress to critical bed shear stress close to the unity (0.96). There was some local sediment transport due to local bed forms such as ripples, but this was not taken into consideration. This study was made using both slope and vertical-wall embankment type structure.
- 4) The flow depth was maintain at 12cm and discharge 40l/s. The effect of depth and discharge variation was not studied.
- 5) All velocity measurement were taken by P-E.M.S. but its accuracy was not checked by other instrument.

CHAPTER 2 LITERATURE REVIEW

2.1 Introduction:

Local scour around embankments caused by the obstruction to flow of various hydraulic structures. The scour hole develops as over bank flow reenters the main channel and sets up large vortices to wash sediment away. Scour around embankment with different soil condition are discussed in this chapter in brief. The purpose of the chapter is to present an overview of relevant theory, mechanism, influencing factors, countermeasures etc. On local scour as derived from this past studies.

2.2 Scour:

Scour is erosive action of running water in streams, which excavates and carries away material from the bed and banks. Scour criteria are involved with physical conditions pertaining to the threshold of motion for the material. This threshold point of incipient motion can be determined by the universally famous Shield's diagram (Fig. 2.1).

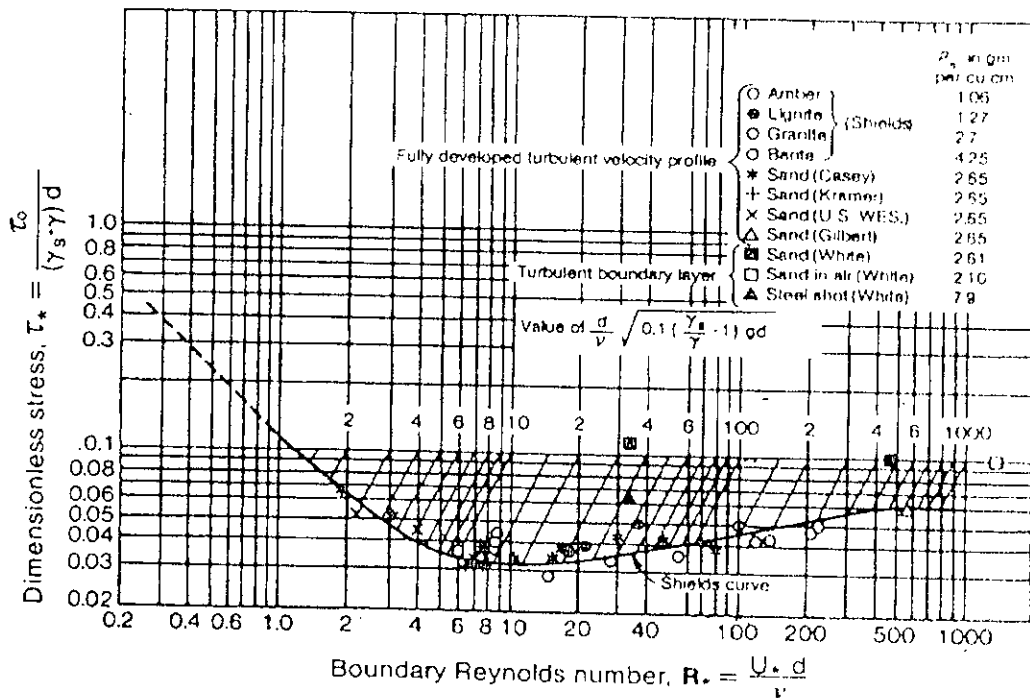


Fig. 2.1 Shield's Diagram for Incipient Motion (Source: Chang, 1988)

Scouring is a lowering of channel bed below on average assumed level generally the result of secondary currents on vortices that occur in conjunction with river features such as bends, at abrupt in flow direction, obstructions, constrictions, confluences, control structures. The severity (depth) and extent of scour is dependent upon the strength of the secondary currents developed at the concerned river features.

'Depth of scour' refers to the material removed below the stated channel bed. Scour depth refers the depth of water above a scour bed under state flow conditions. Scouring is a natural phenomena but the type of scouring can be classified depending on the location and sediment transport capacity of the river and streams.

2.3 According to the location of the scour

According to the location, scouring can be divided as shown in the following diagram:

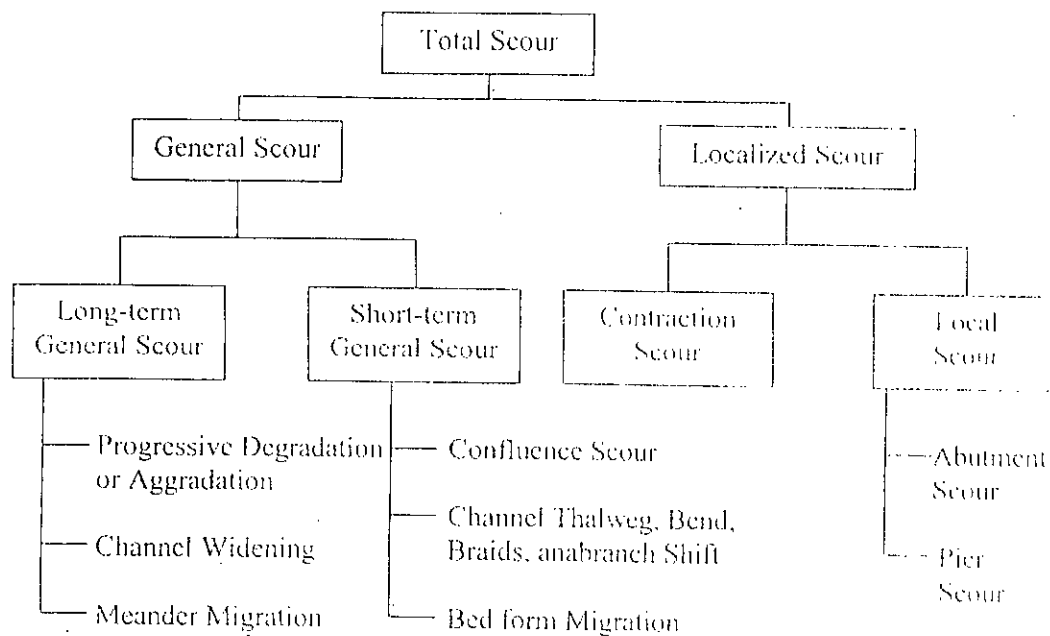


Fig. 2.2 Types of Scour (Melville and Coleman, 2000)

2.3.1 General scour

General scour occurs through a change in the river regime. The result is an overall lowering of the river's longitudinal profile. In many situations, general scour is associated with human investigation through the introduction of some form of barrier at the upstream. The barrier prevents the transport of sediment into the reach. However, the in the river still allows sediment transport, resulting in general degradation of the bed level, dam are common example of this situation. The time frame involved with the human initiated scour is relatively short, but the geomorphologic changes of rivers take long time.

2.3.2 Contraction scour

Contraction or constriction scour caused by a local constriction of the width of a river. When the river flow area is reduced, either by a natural process or human intervention such scour occurs. Decreasing the flow area results in a corresponding increase of average flow velocity and hence an increase in the erosive forces exerted on the bed. Bed materials are removed at a greater rate than it is transported in the reach and overall lowering of the bed elevation can occur. This type of scour situation can result in either long-term degradation or a short-term cyclic event.

2.3.3 Local scour

Local scour occurs near bank protection work like revetments and groynes and other objects that obstruct the flow in different ways. The flow approaches the embankment is deflected down towards the channel bed. At the bed surface strong vortices from which erodes sediment and creates a local scour hole, it continues to deeper until an equilibrium condition is reached. The eroded material is transported downstream.

2.4 According to sediment transport capacity

2.4.1 *Clear Water scour*

Here sediment is removed from the scour hole without replenishment. Clear water scour occurs when the material upstream of the scour hole is not in motion. In this case, the bed shear stresses away from the scour hole will be equal to or less than the critical shear stress τ_c (the shear stress above which the bed particles will begin to be set into motion by the flow) of that particles that make up the bed. Generally, the bed upstream of the scour hole associated with a clear water scour is assumed to be planar. With clear water scour, the depth of the scour hole continues to grow until equilibrium is reached that is when the combination of the temporal mean bed shear stress τ_0 and the turbulent agitation near the bed is no longer able to remove bed material from the scour hole at the pier.

2.4.2 *Live Bed Scour*

Here there is a general movement of sediment both upstream of the scour hole. The bed shear stress in this case is larger than the critical shear stress of the bed. With live bed scour, bed features appear on the approach flow bed. Their formation is dependent on the shear stress excess ($\tau_0 - \tau_c$), flow depth (y), sediment size (d_{50}) etc. equilibrium scour depth in live bed scour is reached when the time average amount of sediment entering the scour hole is equal to the time average amount of sediment leaving the hole.

When the average shear stress on the bed of alluvial channel exceeds the critical tractive stress for the bed material, the particle on the bed begin to move and live bed condition prevails. The rate of sediment transport is dependent on the shape, size and density of the bed particles, and their placement among the surrounding particles. There are two conditions, which determine the amount of sediment transported at a particular cross section of a stream:

- The geology of the country upstream of the particular cross section under consideration, i.e. the supply of sediment.
- The ability of the water or the stream power to transport the sediment.

2.5 Bed Form

Bed forms are flow induced and directly affect the roughness or flow resistance. Therefore, computation of the river stage and flow velocity relies on the determination of bed form roughness. Sediments move with the flow in such a way that bed forms are established. Form of bed roughness observed in the flumes and in alluvial stream are illustrated by Simons and Richardson (1961), as shown in the Fig.2.3 Based on similarities in form, resistance to flow, and sediment transport, these bed forms are divided into categories of lower flow regime, transition zone, and upper flow regime in the order of increasing flow velocity as follows:

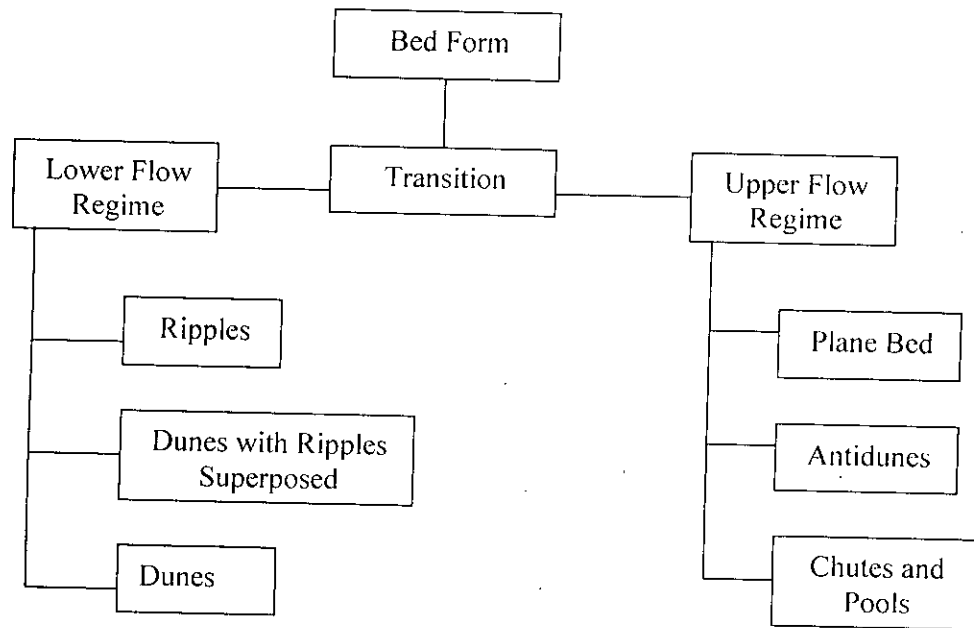


Fig. 2.3 Types of Bed Form

2.5.1 Characteristics of Bed Forms

The characteristics associated with these flow regimes, in terms of bed-material concentration, mode of sediment transport, type of roughness, and phase relation between bed and water surface are compared and summarized in Table 2.1.

Other characteristics features of different bed forms can be recognized on the basis of bed material size and the relative velocity of stream or Froude Number. Ripples are only observed with the fine material (generally with $d < 0.5-0.7$ mm) and do not form

with coarse material (when $d_{50} > 0.9-1.0$ mm). Ripples are independent of depth of flow, but dunes are strongly dependent of flow depth. If the bed material is less than 0.5-0.7 mm, ripples can be superimposed on the top of the dunes. In any case, ripples and dunes are associated with small values of Froude number. With increasing velocity, transition flat bed develop. Transition flat bed can be describe as a bed of washed out dunes. In flume experiments, where the flow depth is relatively small, the transition flat bed condition in fine sand ($d_{50} < 0.4$ mm) normally persists over a significance range of Froude numbers ($0.3 < Fr < 0.8$). however, in case of Fr until the subsequent bed form antidunes appear rather than transition flat bed. In natural rivers transition from dunes to flat bed occurs at relatively lower Froude number, because of great depth. When the Froude number approaches unity, antidunes, chutes and pools are found to develop.

Table 2.1: Classification of Bed Forms and Their characteristics
(After Simons et.al., 1995); (Source: Chang, 1988)

Flow Regime	Bed Form	Bed-material concentration (ppm)	Mode of sediment Transport	Type of Roughness	Phase Relation Between Bed and Water Surface
Lower regime	Ripples	10-200	Discrete steps	Form roughness predominates	Out of phase
	Ripples on dunes	100-1200			
	Dunes	200-2000			
Transition zone	Washed-out dunes	1000-3000		Variable	
Upper Regime	Plane beds	2000-6000	Continuous	Grain roughness predominates	In phase
	Antidunes	Above 2000			
	Chutes and Pools	Above 2000			

2.6 Flow Around Embankment-Like Structure at the Flat Bed Condition

Causes of scouring around embankment-like structures are the subject of many investigations in the laboratory flume. One of the early references of this kind is the study on the flow near groin-like structures by Rajaratnum and Nwachukwn (1983a). They measured detailed flow velocities around narrow vertical-wall abutments in a 37 meter long, 0.92 meter wide and 0.76 deep tilting flume. From their measurement, it was found that the velocity and the bed shear stresses are amplified around the structure up to 5 times of the approach shear stress. Lim (1997) derived an empirical relationship of the bed shear stress amplification using their measured data and expressed by the following equation:

$$\frac{u_{*m}}{u_*} = \left[1.2 \left(\frac{b}{h} \right)^{0.5} + 1 \right] \quad (2.1)$$

here, u_{*m} = bed shear velocity around embankment, u_* = approach bed shear velocity, b = lateral dimension of the structure and h = approach flow depth. The equation (2.1) is applicable within the range of $0.4 \leq b/h \leq 1.0$ and $0.12 \leq Fr \leq 0.29$. here, Fr is Froude number.

It is important to note that scouring would occur at the region where bed shear stress are amplified. Therefore, equation (2.1) is quite useful to estimate the amplification of the bed shear velocity near the structure. The estimation of shear stress or shear velocity may be useful in two ways: (1) to estimate the size of the scour protecting material around the structure and (2) to estimate the scour depth around the structure. However, the applicability of the equation is not tested beyond the boundary condition at which it was derived.

Recently, Molinus, Kheireldin and Wu (1998) studied the distribution of shear stresses experimentally in a 10 meter long, 0.25 meter wide and 0.40 meter deep rectangular flume. They derived an equation to estimate the maximum shear stress at the upstream corner of the embankment type structure considering the effect of width contraction and the effect of vortex and flow systems around the structure separately. The shear stress were amplified up to 10 times the approach shear stress. Their experiments are

within the Froude number of 0.30 to 0.90. The expression for the shear stress amplification around the structure can be written as:

$$\tau_{nose} = \tau_{cont} + \tau'_{nose} \quad (2.2)$$

τ_{nose} = shear stress in the vicinity of abutment nose, τ_{cont} = shear stress due to contraction and τ'_{nose} = shear stress due to presence of abutment structure and its accompanied vortex and flow systems.

Normalizing equation (2.2) by τ_a (a stand for approach flow), it can be written as:

$$A_{nose} = A_{cont} + A'_{nose} \quad (2.3)$$

Equation (2.3) is expressed by Equation (2.4) as below:

$$A_{nose} = \left(\frac{1}{M}\right) \left[1 + 5.46 \left(\frac{1}{M}\right)^{3.89} Fr^{1.74} \left(\frac{b}{h}\right)^{2.5} \right] + \left(\frac{1}{M^2} \sqrt{1 + \tan^2 \alpha_w} - 1\right) \quad (2.4)$$

here, $\alpha_w = 1.485 Fr^{0.13} \left(\frac{b}{h}\right)^{0.06}$, $M = (B-b)/B$, B is the un-contracted channel width

The shear stress amplification in equation (2.4) is not only the function of b/h but also depends on approach Froude number. The shear velocity amplification can be estimated as, $u_{*m}/u_* = \sqrt{A_{nose}}$.

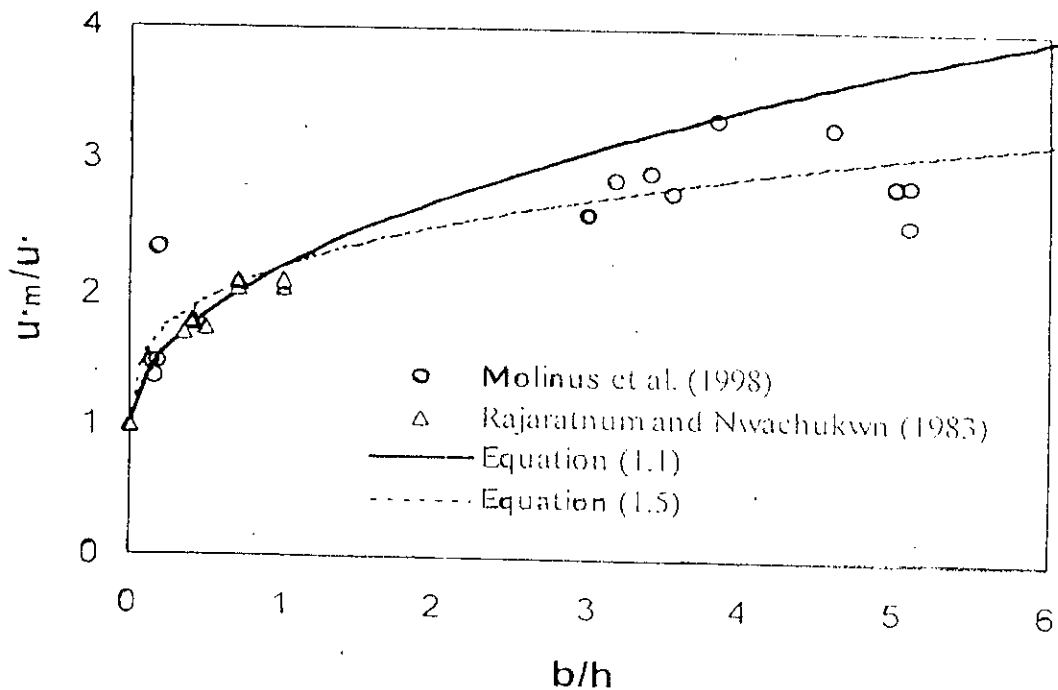


Fig. 2.4 Amplification of shear velocity as function of b/h

Again, applying the empirical relation of Lim (1997) derived from the shear velocity data of Rajaratnum and Nwachukwn (1983) to the measured data of Molinas et al. (1998), it is found that the equation (2.1) fits the entire data range well that can be expressed as shown in Fig. 2.4 and expressed as below:

$$\frac{u_{*m}}{u_*} = 1.2(b/h)^{1/3} + 1 \quad (2.5)$$

The equation (2.5) is applicable within $0.15 \leq b/h \leq 6$ and $0.12 \leq Fr \leq 0.90$ and independent on Froude number at least in the sub-critical flow condition.

2.7 Scouring Around Embankment Type Structure

Due to amplified stresses around the structure scour hole are formed and the maximum scour depth are generally obtain at the nose of the structure. Many experimental studies (as for example, Grade et al. 1961; Laursen, 1963; Rajaratnum and Nwachukwn, 1983b and many others) had been carried out for last 30 years to understand the scouring processes and to estimate the maximum scour depth.

One of the early experiments of this kind was conducted by Grade et al. (1961) in 7.6 meter long and 0.60-meter wide glass sided flume using thin vertical plates with variable width. Bed material sizes were 0.20 mm, 0.45 mm and 1.00 mm and discharge range was set to ensure both the clear-water and live bed condition. It was found from their experiments that in most of the experiments maximum scour was attained after 3 to 5 hours. After this, lowering the bed in too slow to record with the available instruments. It was found that for the same discharge, scour depth is greater in finer sediment as compared with the coarse sediment. In most of the cases, maximum scour depth was found at the upstream corner. The scour hole upstream of the structure was conical in shape, whereas, along the downstream the shallower slope was observed. A deposition bar was formed adjacent to the abutment along the down stream direction in all cases. The ratio of the width and depth of the scour hole varied from 1.8 to 5.0. They proposed an empirical equation for the prediction of the maximum scour depth around the structure as below:

$$\frac{ds}{h} = \frac{k}{M} Fr^n \quad (2.6)$$

here, k and M is a constant depending on flow concentration and angle of inclination of the abutment, d_s is scour depth, h is approach velocity, $n = \text{exponent} = 2/3$, k varied from 2.75 to 5.00.

Again, erosion near the structure had been studied by Rajaratnum and Nwachukwu (1983b). They analyzed the growth of the maximum scour depth with time and found to be similar. Also, the characteristics of the scour hole along the lateral and longitudinal direction at the end had been found to be similar.

2.7.1 Time Scale for Local Scour

The process of local scour is time dependent. Equilibrium between the erosive capability of the flow and the resistance to motion of the boundary materials is progressively attained through erosion of the flow boundary. In fine-grained materials (sands and gravels), the equilibrium or final depth of local scour d_{sc} is rapidly attained in live bed conditions, but rather more slowly in clear water conditions (Melville and Chew, 1999). Clear water scour occurs for mean velocities up to the threshold velocity for bed sediment entrainment, i.e., $V \leq V_c$, while live bed scours for $V > V_c$. The maximum equilibrium scour depth occurs at $V = V_c$. In armored cobble or cohesive sediment bed streams, multiple flood events may be required before the maximum clear water scour is reached. This may take many years. The equilibrium scour depth in live bed condition fluctuates due to the effects of bed form migration. The dashed line in Fig. 2.5 represent the temporal average scour depth under live bed conditions. The diagram also shows the time taken, t_e for the equilibrium scour depth to develop. The equilibrium time, t_e , increases rapidly with flow velocity under clear water conditions but decreases rapidly for live bed scour (Melville and Chew, 1999).

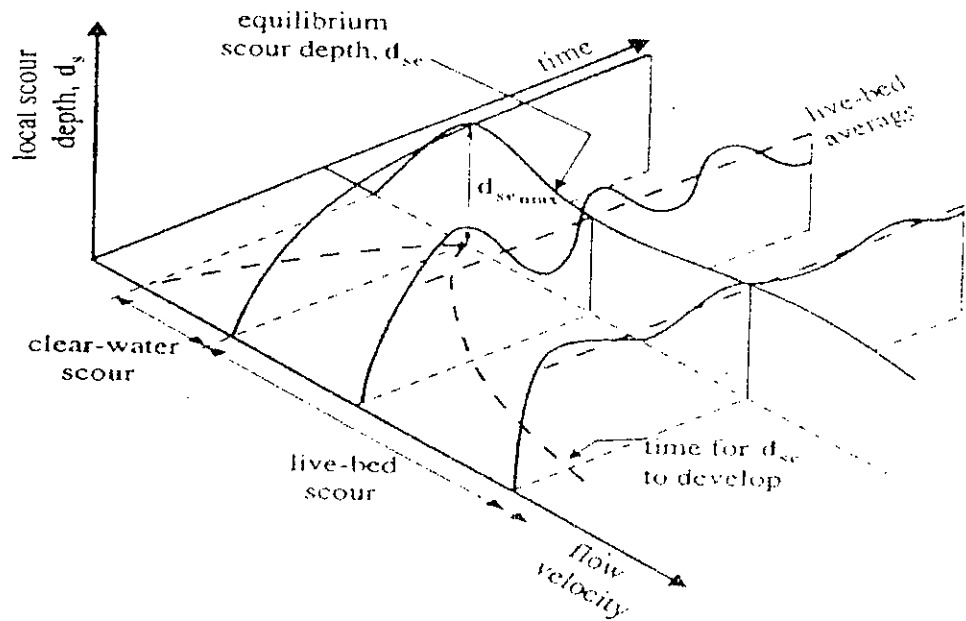


Fig. 2.5 Variation of Local Scour Depth with Flow Velocity and T

(Source: Melville and Chew, 1999)

Existing equation for predicting local scour depth give the equilibrium depth and are therefore conservative regarding temporal effects. For the live bed conditions that typically pertain in floods, equilibrium scour depths are appropriate. However, where clear water condition exit, the equilibrium scour depth may be overly conservative. Peak floods flows may last only one numbers of hours or a few days in the field, and short floods have insufficient time to generate equilibrium depths. The actual scour may be a small fraction of the equilibrium scour depth, which could take weeks to fully develop. Johnson and McCuen (after Melville and Chiew, 1999) developed and analytical model to estimate the temporal process of local scour.

The shape of the flood flow hydrograph is important as well as the flood duration. Typically, the flood duration determines if the equilibrium live bed scour will develop. After the flood peak passes, the flow recedes. The duration of the recession period is also very important. With the flow recession, clear water conditions may prevail,

Time effects are significant when considering poor correlation between the scour depths observed in the field and those measured in the laboratory. In order to achieve equilibrium conditions in small-scale laboratory experiments of clear water scour depth, it is necessary to run the experiments for several days. Data obtain for lesser times, say 10 to 12 hours, can exhibit scour depth less than 50% of the equilibrium depth. Melville and Chiew (1999) have conducted several series of experiments to clarify the effect of time on the development of local scour under clear water conditions. The experiments were conducted for a long period of time to ensure that equilibrium was reached. They have developed method to determine the time (t_e) required for the development of equilibrium scour depth (d_{se}), sediment and approach flow velocity and the concomitant estimation of scour depth at any stage during the development of the equilibrium scour hole. The result show that the scour depth after 10% of the time to equilibrium is between about 50% and 80% of the equilibrium scour depth, depending on the approach flow velocity.

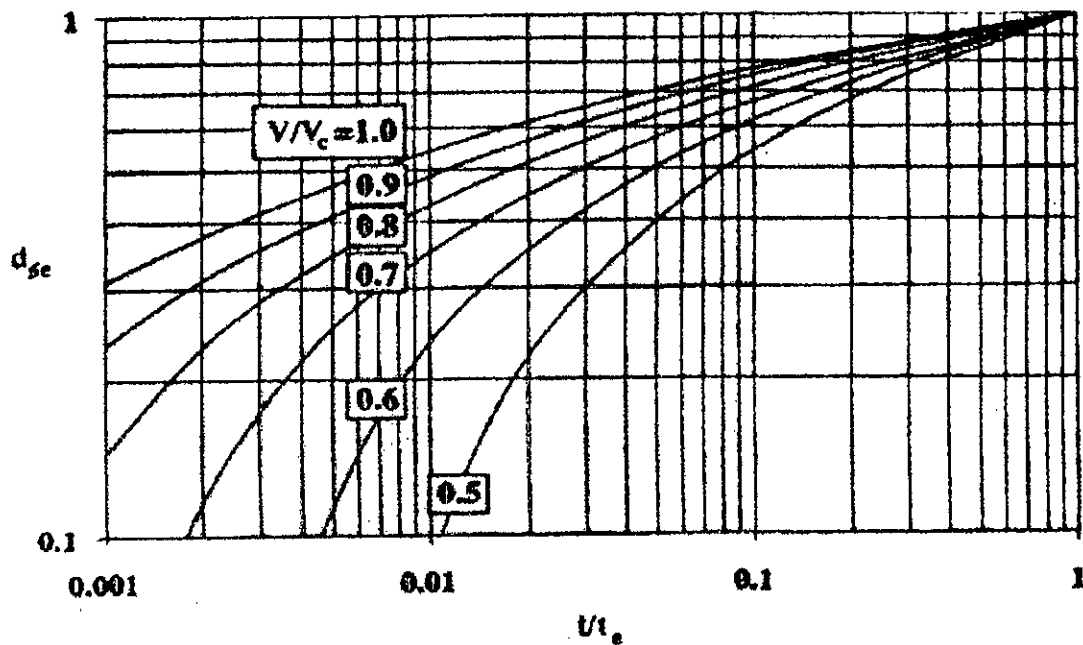


Fig. 2.6 Temporal Development of Local Scour Depth Around Abutment

From the observed laboratory data following equation was fitted, which can be used for the computation of scour depth at any time t , when the equilibrium time (t_e) and the corresponding equilibrium scour depth (d_{se}) are known.

$$\frac{d_s}{d_{se}} = esp \left\{ -0.03 \left| \frac{V_c}{V} \ln \left(\frac{t}{t_e} \right) \right|^{1.6} \right\} \quad (2.7)$$

For $y/D > 6$,

$$t_e (\text{days}) = 48.26 \frac{D}{V} \left(\frac{V}{V_c} - 0.4 \right) \quad (2.8)$$

For $y/D \leq 6$,

$$t_e (\text{days}) = 30.89 \frac{D}{V} \left(\frac{V}{V_c} - 0.4 \right) \left(\frac{y}{D} \right)^{0.25} \quad (2.9)$$

The above equations are valid strictly for $1 \geq V/V_c \geq 0.4$. For non-ripple forming sand ($d_{50} > 0.6\text{mm}$), time for equilibrium scour to develop (t_e) is a maximum at the threshold velocity ($V=V_c$) and when $y/D > 6$. The maximum value is given by:

$$t_{e \max} (\text{days}) = 28.96 \frac{D}{V} \quad (2.10)$$

The time factor introduced by Melville and Chiew (1999) can be applied to the simplified scour depth equation as:

$$d_s = K_{yD} K_t K_d K_i \quad (2.11)$$

Where; K_{yD} represent the factor for flow depth-structure width ratio, K_t represents time factor ($K_t = d_s/d_{se}$), K_i represents the flow intensity factor and K_d represent particle size factor. By the use of equation (2.7) one can obtain scour depth at a particular time t .

2.8 Available Prediction Method of Local Scour around Embankment

Scour depth around embankment-type structures increases as the value of b/h (b =length of the structure in the lateral direction and h = approach flow depth) increases up to certain extent. After that limiting b/h value the observed scour depth remains constant both in alluvial rivers and laboratory channel. A number of prediction methods are available at present, among this method Lacey (1930) and Liu (1961) methods are widely used in Bangladesh. Some of the formulae having the similar expressions are summarized here. It is important to investigate some crucial points on the available prediction methods:

- Whether the methods consider the physical processes of flow and scouring?
- Limitations of each of the methods.
- Difficulty and advantages of using the methods.
- Applicability to the field condition etc.

Lacey's Equation

Lacey (1930) introduced the equation for the prediction of the maximum scour depth (after Rahman et al. 2001). The formula is on the basis of field observation of scouring.

$$\frac{d_s}{h} = 0.47k \left(\frac{Q}{fh^3} \right)^{1/3} - 1 \quad (2.12)$$

Where d_s is the scour depth measured from the initial bed level, h is the approach flow depth, Q is the regime discharge, f is the silt factor is equal to $1.76\sqrt{d_{50}}$, k is the coefficient for local scour depth and d_{50} is the mean diameter of bed sediment in mm. Equation (2.12) is widely used in Bangladesh for the prediction of the local scour depth for different structures using the suggested values of k as shown in Table (2.2)

Table (2.2) Suggested values of k.

Types of structures	k values
Steeply sloping head piers: 1.5:1	3.80
Long sloping head piers: 1:20	2.25
Scour at nose of large radius guide banks	2.75
Maximum scour at rounded bridge pier	2.00
Scour at spurs along river bank	1.70

In a river, the regime discharge Q can be assumed as a constant. Therefore, for a specific type of structure, the maximum scour will be same whatever, the dimension of the structure is. But in practice, the structural dimension, specially, the length of the structure along the lateral direction (b) is the dominant factor for the estimation of the maximum scour depth (Liu, 1961; Laursen, 1963; Melville, 1992; Lim, 1997; Rahman and Muramoto, 1999).

Comments:

- The formula is on the basis of field observation of scouring
- Scour is independent on the size of the structure and only one value of scour depth is obtained for a river reach
- The lateral slope of the structure is not maintained and this equation is not useful to any side slope structure

Modification of Lacey formula

The Lacey equation is very popular in the Indian Sub Continent and in Bangladesh. Designers are using the formula for the estimation of regime depth as well as the local scour depth using a constant factor (k). To overcome the constraint (scour depth does not depend on the dimension of the structure), Lacey equation is modified for the prediction of the maximum local scour depth using the concept of flow concentration (Rahaman and Muramoto, 1999) around the structure.

For $Q = Bhu$, here B = channel width and u = approach flow velocity. Equation (2.12) can be expressed as:

$$\frac{d_s}{h} = 0.47k \left(\frac{Bu}{1.76d_{50}^{0.5}h^2} \right)^{1/3} - 1 = 0.47 \left(\frac{B\psi}{1.76d_{50}^{0.5}h^2} \right)^{1/3} ku^{1/3} - 1 \quad (2.13)$$

where, $u = \psi u_*$, u_* is the approach bed shear velocity, and $\psi = 8.5 + 5.75 \log\left(\frac{h}{k_s}\right)$ for turbulent flow, k_s can be taken as grain roughness $= 2.5d_{50}$.

As the approach flow comes close to the structure, the shear stress amplification will occur. Then, approach shear velocity (u_*) need to be replace by amplified shear velocity (u_{*m}) assuming $k = (u_{*m}/u_*)^{1/3}$ and equation (2.13) can be written as:

$$\frac{d_s}{h} = 0.47 \left(\frac{\psi B}{1.76 d_{50}^{0.5} h^2} \right)^{1/3} u_{*m}^{1/3} - 1 \quad (2.14)$$

The concept of velocity amplification or flow concentration close to the structure adopted by Lim (1997) is very important. But the idea of flow concentration within the entire width of the scour hole region is appropriate (Tsuchiya and Ishizaki, 1966; Kawn and Melville, 1992). Therefore, Rahaman and Muramoto (1999), consider the flow concentration in to restricted region of the scour hole. In the Technical Report-1 (IWF, R03/2002) of the present study, it was observed that the discharge flux becomes highly concentrated close to the structure (Rahaman and Haque, 2002). For the present analysis, idealized flow concentration in to the restricted region is considered in the flat bed condition (Fig. 2.7)

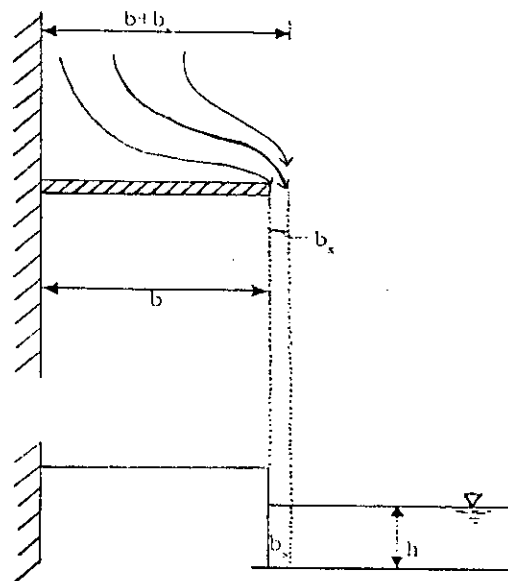


Fig. 2.7 flow concentration of the restricted region close to the abutment-like structures.

From the flow continuity (inflow = out flow)

$$hu(b + b_s) = b_s hu_m \quad (2.15)$$

where u_m = amplified velocity, b_s = region within which flow velocity is amplified.

Equation (2.15) can be expressed as:

$$\frac{u_m}{u} = \left(1 + \frac{b}{b_s}\right) \quad (2.16)$$

Introducing, $u = \psi u_s$, both for the approach and amplified flow, equation (2.16) can be expressed as:

$$\frac{u_{*m}}{u_*} = \left(1 + \frac{b}{b_s}\right) \quad (2.17)$$

From the experimental evidences in the flat bed condition, it was found that b_s can be taken as a function of approach flow depth, i.e., $b_s = \alpha h$, where α is a constant to be determined from experimental results.

$$\frac{u_{*m}}{u_*} = \left(1 + \alpha \frac{b}{h}\right) \quad (2.18)$$

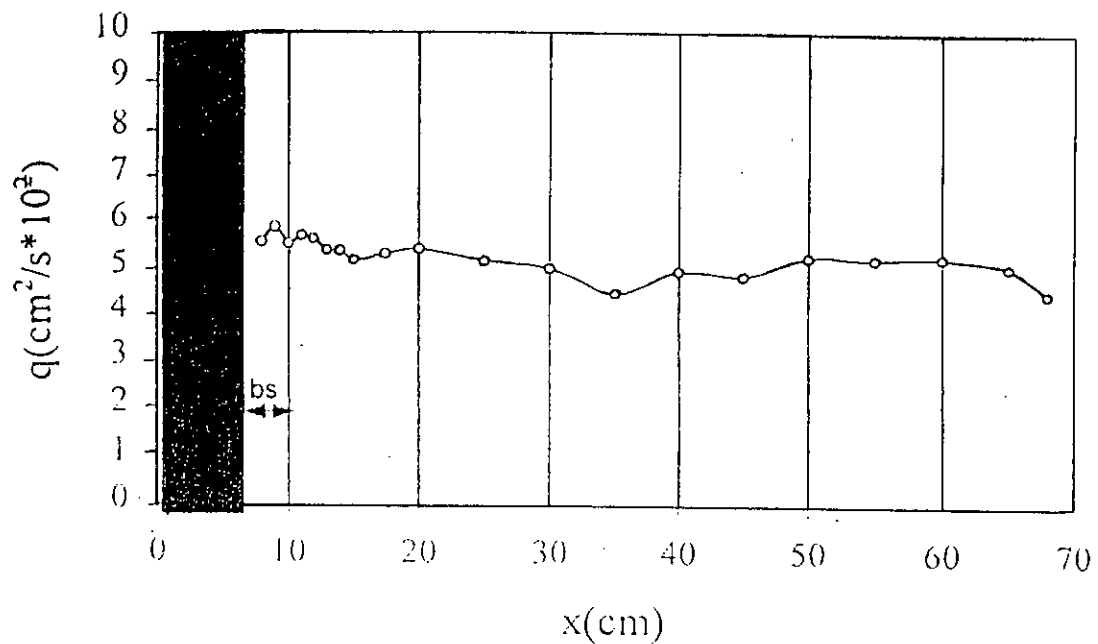


Fig. 2.8 concentration of discharge fluxes close (b_s) to the structure.

From the experimental results of the Rajaratnum and Nwachuwn (1983), $\alpha = 1.5$ Fig. 2.9 and equation (2.18) can be written as:

$$\frac{u_{*m}}{u_*} = \left(1 + 1.5 \frac{b}{h}\right) \quad (2.19)$$

From equation (2.14) and (2.19):

$$\frac{d_s}{h} = 0.47 \left(\frac{\psi B u_*}{1.76 d_{50}^{0.5} h^2} \right)^{1/3} \left(1 + 1.5 \frac{b}{h}\right)^{1/3} - 1 \quad (2.20)$$

For Lacey's non-scouring and non-silting regime condition, $u_* = u_{*c}$ and equation (2.20) can be written for the critical condition of approach flow.

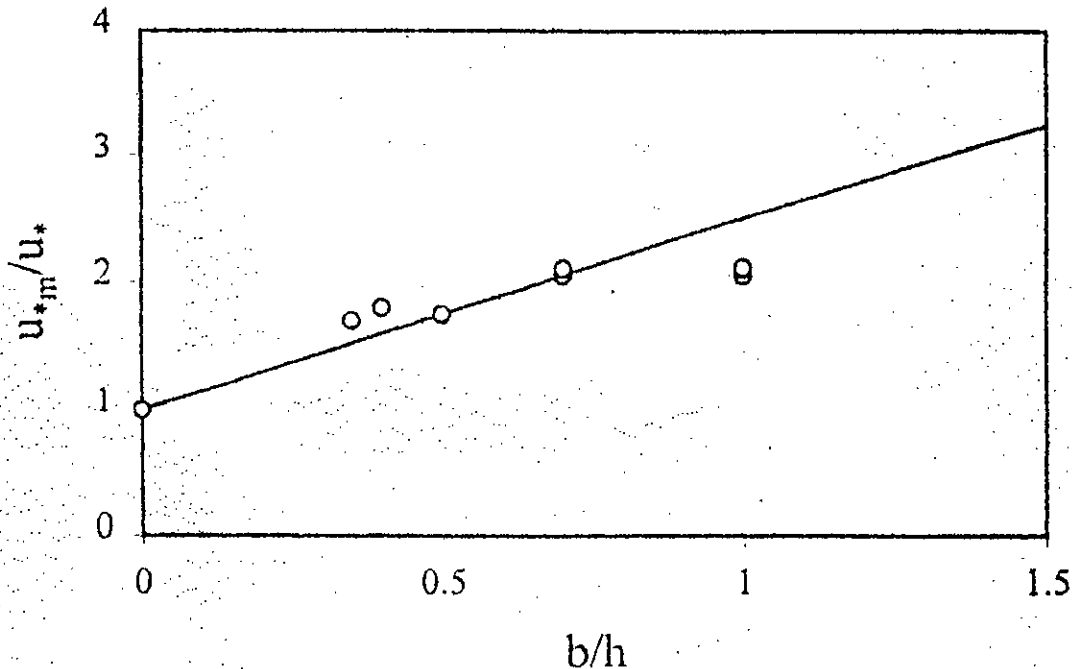


Fig. 2.9 Amplification of shear velocity close to the structure
(Rajaratnum and Nwachuwn, 1983)

$$\frac{d_s}{h} = 0.47 \left(\psi \frac{\varphi B u_{*c}}{1.76 d_{50}^{0.5} h^2} \right)^{1/3} \left(1 + 1.5 \frac{b}{h}\right)^{1/3} - 1 \quad (2.21)$$

Critical shear velocity, u_{*c} (cm/sec), can be estimated using the following relationships when d_{50} is in cm.

$$u_{*c} = 9.0d_{50}^{0.5}$$

when $d_{50} \geq 0.303\text{cm}$

$$u_{*c} = 9.0d_{50}^{0.70}$$

when $0.118\text{cm} \leq d_{50} \leq 0.303\text{cm}$

$$u_{*c} = 7.42d_{50}^{0.5}$$

when $0.0565\text{cm} \leq d_{50} \leq 0.118\text{cm}$

$$u_{*c} = 2.9d_{50}^{0.17}$$

when $0.0065\text{cm} \leq d_{50} \leq 0.0565\text{cm}$

$$u_{*c} = 15d_{50}^{0.5}$$

when $d_{50} \leq 0.0065\text{cm}$

For simplification of calculation, the graphical form of the above relationship can be used as shown in Fig. 2.10.

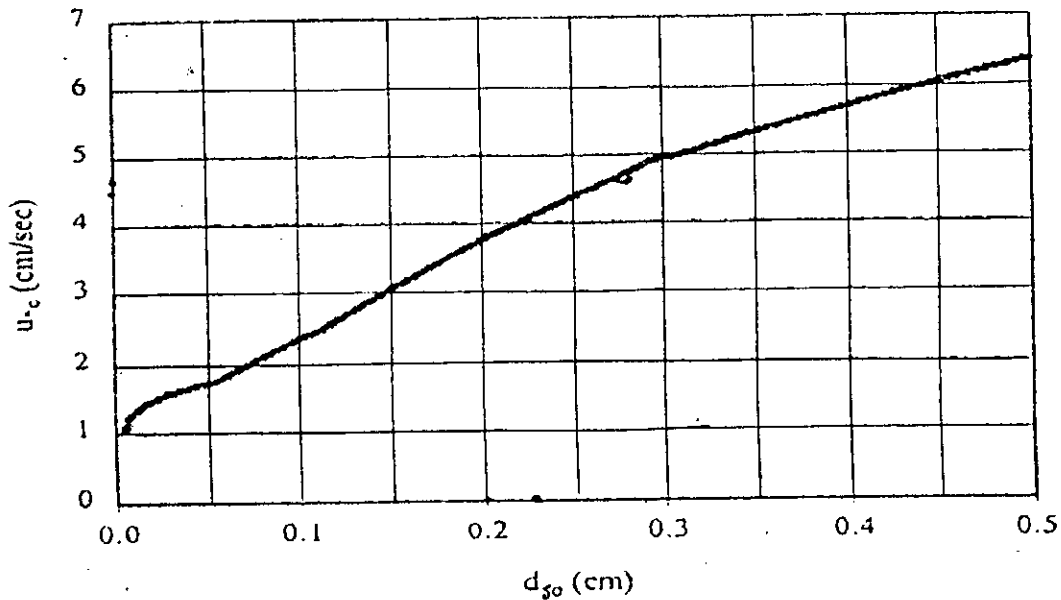


Fig. 2.10 Critical shear velocity vs. particle size graph for cohesion less soil.

Remaining problem of the Modified Lacey:

- Depends on the velocity coefficient that may vary from river to river.
- Produce different prediction line for each of the rivers where channel wide and sediment size remain constant.
- Variable slope parameter can not be introduced. Though Lacey seems to predict for an unknown side slope.

Liu et al. Formula

Liu et al. (1961) presents the following formula for live-bed condition based on the laboratory data, slope of the embankment is known and cannot be used for variable side slope.

$$\frac{d_s}{h} = 1.1 \left(\frac{b}{h} \right)^{0.40} Fr^{1/3} \quad (2.22)$$

Where Fr = Froude number of approach flow.

Melville's formulae

From many experimental data, Melville (1992) proposed the following empirical formulae for the prediction of the maximum local scour depth around embankment type structures by introducing a shape/slope correction factor (k_{sm}).

$$\begin{aligned} b/h < 1: \quad \frac{d_s}{h} &= 2 \left(\frac{b}{h} \right) \\ 1 < b/h < 25: \quad \frac{d_s}{h} &= 2 \sqrt{b/h} \\ b/h > 25: \quad \frac{d_s}{h} &= 10 \end{aligned} \quad (2.23)$$

However, the slope effect becomes less important if the structure becomes relatively longer and the adjusted slope correction factor (k_{sm}^*) is expressed as below,

$$k_{sm}^* = k_{sm} + (1 - k_{sm}) [0.0667(b/h) - 0.667] \quad \text{for } 10 < b/h < 25 \quad (2.24)$$

From this it can be seen that for $b/h > 10$, the influence of slope becomes gradually less important and for $b/h \geq 25$, slope correction factor becomes unity.

Table 2.3 Shape/slope correction factor proposed by Melville (1992) is following:

Slope of embankment (V: H)	Shape/slope factor(K_{sm})
1: 0.5	0.60
1: 1.0	0.50
1: 1.5	0.45

Comments:

- Derived from envelop curves
- No consideration of physical process
- Completely empirical in nature
- Applicable sloped-wall structure using shape/slope factor from Table 2.4
- Not tested with alluvial field data
- Simple to use
- Estimation of constant value of scour depth for long structure is interesting

Rahman and Muramoto Model

Considering the flow concentration into the restricted region of the scour hole, Rahman and Muramoto (1999) proposed an analytical model for the prediction of the maximum local scour depth under clear water around embankment-like structures.

The final form of the expression for the scour depth is:

$$\frac{d_s}{h} = \sqrt{a_3(b/h)} \quad (2.25)$$

$$a_3 = \{\beta / \tan \phi (1 - \beta) + 1/2 \tan \theta\}^{-1}$$

$$\beta = \left\{ 1 + \frac{\left(\frac{d_s}{h}\right)^2 + \frac{d_s}{h}(1 - u/u_c)}{\tan \phi (b/h)(u/u_c)} \right\}^{-1} \quad (2.26)$$

Here, ϕ = angle of repose of the bed sediment and β = is an empirical constant. θ = side slope of the structure.

The slope factor (k_{sc}) is define as the ratio of the maximum scour depth at sloped-wall structure (d_{ss}) and the maximum scour depth at vertical-wall structure (d_{sv}) having the same lateral dimension, then the slope facto can be expressed (Rahaman and Muramoto, 1999) as:

$$K_{sc} = \frac{d_{ss}}{d_{sv}} = \left(1 + \frac{(1-\beta)\tan\phi}{2\beta\tan\theta} \right)^{-1/2} \quad (2.27)$$

The slope/shape factor estimated by above equation of various slope are compared with shape factors for Melville's which is shown in table 2.4.

Table 2.4 Comparison of slope/shape factors from Melville and Muramoto and Rahaman.

Shape/slope factors (d_{ss}/d_{sv})	V1 : H 0.5	V1 : H1	V1 : H1.5
Melville, K_{sm}	0.60	0.50	0.45
Muramoto and Rahaman, K_{vc}	0.80	0.68	0.60

It can be seen that the value of K_{sm}/K_{sc} is nearly constant (=0.75) then the extrapolated value of K_{sm} for 1V:3H slope will be 0.353.

Comments:

- Considering flow and scouring processes observed in the laboratory and field
- The model constant derived from all the available laboratory data and compatible with the field data
- Applicable to vertical as well as sloped structure
- Scour depth increases with the lateral dimension of the structure
- The dead water zone develops in front of the structure are not consider
- The experimental facts reflected ($d_s/h=10$ for $b/h>25$) in the Melville's formulae can not be predicted.

2.9 Types of Earthen Embankment

Earthen embankments are the most ancient type of embankments, as they can be built with the natural materials with a minimum of processing and with primitive equipment. But in ancient days, the cost of carriage and dumping of the dam materials

was quite high. However, the modern developments in earth moving equipments have considerably reduced the cost of carriage and lying of the dam material.

There are following three types:

- Homogeneous Embankment Type.
- Zoned Embankment type.
- Diaphragm type.

Homogeneous Embankment Type

The simplest type of an earthen embankment consists of a single material and is homogeneous throughout. Sometimes, a blanket of relatively impervious material may be placed on the upstream face. A purely homogeneous section is used, when only one type of material is economically or locally available. Such a section is used for low to moderately high dams and for levees.

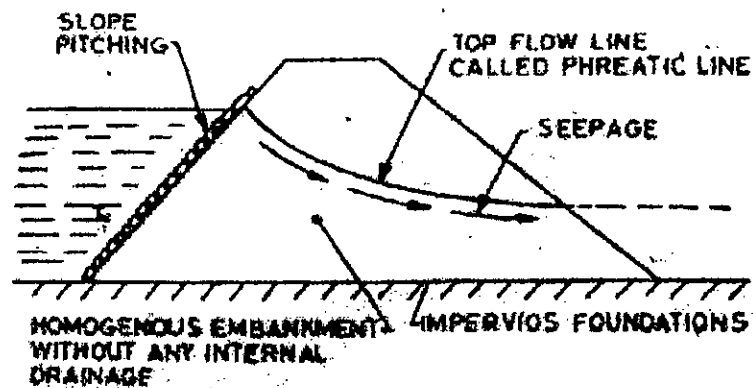


Fig. 2.11 Homogenous type embankment.

A purely homogenous section poses the problem of seepage, and huge sections are required to make it safe against piping, stability, etc. due to this, a homogeneous section is generally added some training work like riprap protection, block protection, geotextile filter etc.

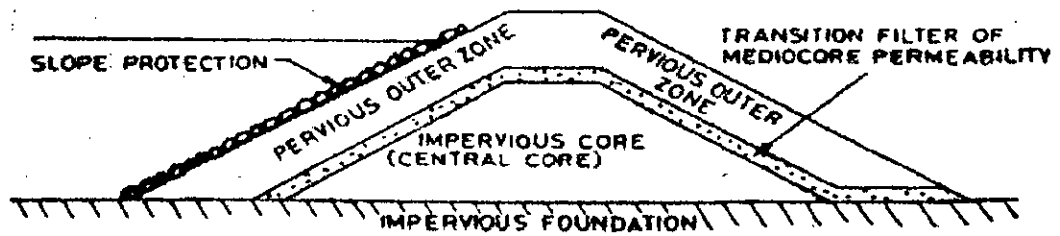


Fig. 2.12 Zoned type embankment

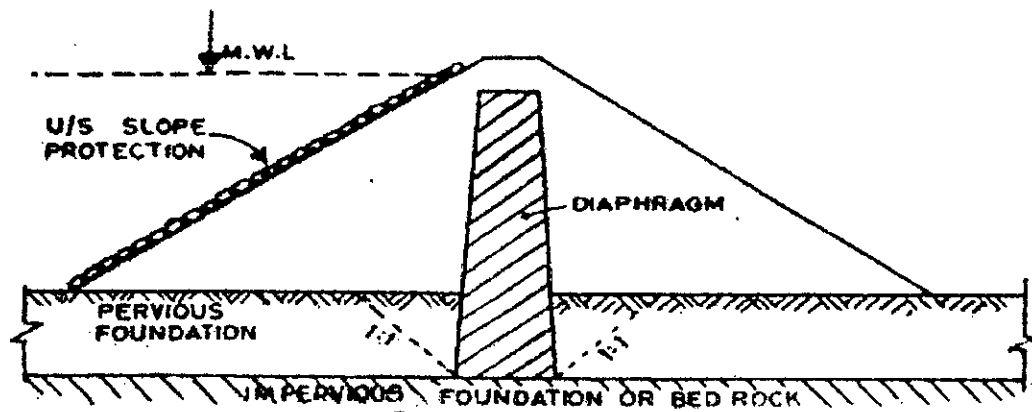


Fig. 2.13 Diaphragm type embankment

2.10 Method of Construction

There are two methods of constructing earthen embankment:

- Hydraulic- fill Method
- Rolled- fill Method

Hydraulic- fill Method

In this method of construction, the dam body is constructed by excavating and transporting soils by using water. Pipes called flumes, are laid along the outer edge of the embankment. The soil material are mixed with water and pumped into these flumes. The slush is discharged through the out lets in the flumes at suitable intervals along their lengths. The slush flowing towards the centre of the bank, tends to settle at the centre, forming a zoned embankment having a relatively impervious central core. Hydraulic- fill method is, therefore, seldom adopted these days. Rock- fill method for constructing earthen dams is, therefore, generally and universally adopted in these modern days.

Rolled-fill Method

The embankment is constructed by placing suitable soil materials in thin layers (15 to 30 cm.) and compacting them with rollers. The soil is brought to the site from borrow pits and spread by bulldozers, etc. in layers. These layers are thoroughly compacted by rollers of design weights. Ordinary road rollers can be used for low embankment. The moisture content of soil material must be controlled. The best compaction can be obtained at a moisture content somewhere near the optimum moisture content (The optimum moisture content is the moisture required for obtaining optimum density in the fill). Compaction of coarse gravels cannot be properly done by rolling and is best done by vibrating equipment.

2.11 Suitable Preliminary Section for Embankment

A few recommendations for selecting suitable values of top width, free board, u/s and d/s slopes are given below for preliminary design:

Freeboard

Freeboard or minimum freeboard is the vertical distance between the maximum reservoir level and top of the embankment. The minimum height of the freeboard for wave action is generally taken to be equal to $1.5h_w$.

Where, $h_w = 0.032\sqrt{V.F} + 0.76 - 0.271(F)^{1/3}$ for $F < 32$ km.

$$h_w = 0.32\sqrt{V.F} \text{ for } F > 32 \text{ km.}$$

V = wind velocity in km/hr.

F = Straight length of water expanse in km.

Values of freeboard for various heights are given in table 2.4.

Table 2.5 U.S.B.R. recommendations for freeboard for embankment

Spillway type	Height of Embankment	Minimum freeboard Over MWL
Uncontrolled (<i>i.e.</i> Free) spillway	Any height	Between 2m to 3m
Controlled spillway	Height less than 60 m	2.5m above top of gate
Controlled spillway	Height more than 60 m	3m above top of gate

Width

The top width of the large embankment should be sufficient to keep the seepage line well within the dam, when reservoir is full. It should also be sufficient to withstand earthquake shocks and wave action. For small embankment, the top width is generally governed by minimum roadway width requirements.

The top width (A) of the earth dam can be selected as per the following recommendations:

$$A = \frac{H}{5} + 3 \text{ for every low embankment}$$

$$A = 0.55\sqrt{H} + 0.2H \text{ for embankment lower than 30m}$$

$$A = 1.65(H + 1.5)^{\frac{1}{3}} \text{ for embankment higher than 30m}$$

H = height of the embankment.

Slopes

The side slopes depends upon various factors such as the type and nature of the embankment, foundation of the materials, height of the embankment etc. The recommended values of side slopes are tabulated below:

Table 2.6 Terzaghi's side slopes for earth embankment

Type of material	U/S slopes (H:V)	D/S slope (H:V)
Homogenous well graded.	2.5 : 1	2 : 1
Homogenous course graded.	3 : 1	2.5 : 1
Homogenous silty clay: 1. height less than 15m 2. height more than 15m	2.5 : 1 3 : 1	2 : 1 2.5 : 1
Sand or sand and gravel with a central clay core.	3 : 1	2.5 : 1
Sand or sand and gravel with R.C. diaphragm.	2.5 : 1	2 : 1

CHAPTER 3

EXPERIMENTAL SET UP AND METHODOLOGY

3.1 METHODOLOGY

To carry out the Experimental Study in a laboratory channel, at first the objectives were selected. At the same time the scope and limitations of the study were defined. The whole experiment was done at Hydraulics and River Engineering laboratory of DWRE, BUET, Dhaka and the existing laboratory facilities were used.

During the laboratory channel preparation and the test run other experimental structure were constructed at pattern shop for example sloping-wall and vertical-wall structure. Depending on the flow volume, estimated scour depth, pump capacity, measuring devices, reservoir capacity and duration for test runs etc, hydraulic parameters were selected. Bed material was analyzed. The experiment was decided to run at clear water condition. Because of the bed material size, there was ripple formation. The effect of ripple on the result was not considered in the study but its characteristics for each structure were analyzed.

The scour study was carried out both for different sloping-wall and for different width of vertical structure. During the scour study, the change of depth was measured every after one hour. It was observed that after six hours of flow run the scour depth was approximately steady condition. However, it was noticed that to get equilibrium condition of scour depth it would need twenty to twenty-four hours flow run. But in the present experiment, each flow was run for seven hours and thirty minutes for every structure. Moreover, there was no stand by pump in the laboratory and the only available pump can run for maximum eight hours continuously. Before the pump was run, every day the channel was backfilled with required water depth.

The scour study was carried out to see the scour geometry and the scour depth developed in each experiment within seven hours and thirty minutes. For this study, total six structure were selected. First three was sloping structure with same flow restriction width, $b=60\text{cm}$ and variable slope (1V:1H, 1V:2H and 1V:3H slope) and the last three structures were vertical but variable with ($b=60\text{cm}$, $b=40\text{cm}$, $b=20\text{cm}$, flow restricted width). Each structure was 1m length.

3.2 Experimental Setup and Measurement

The experiment is conducted in the physical model bed at the Hydraulic and River Engineering Laboratory of Water Resources Engineering Department, Bangladesh University of Engineering and technology (BUET), Dhaka. Experimental setup and the measuring techniques are described in details in the following articles. General layout of the setup is shown in Fig. 3.1.

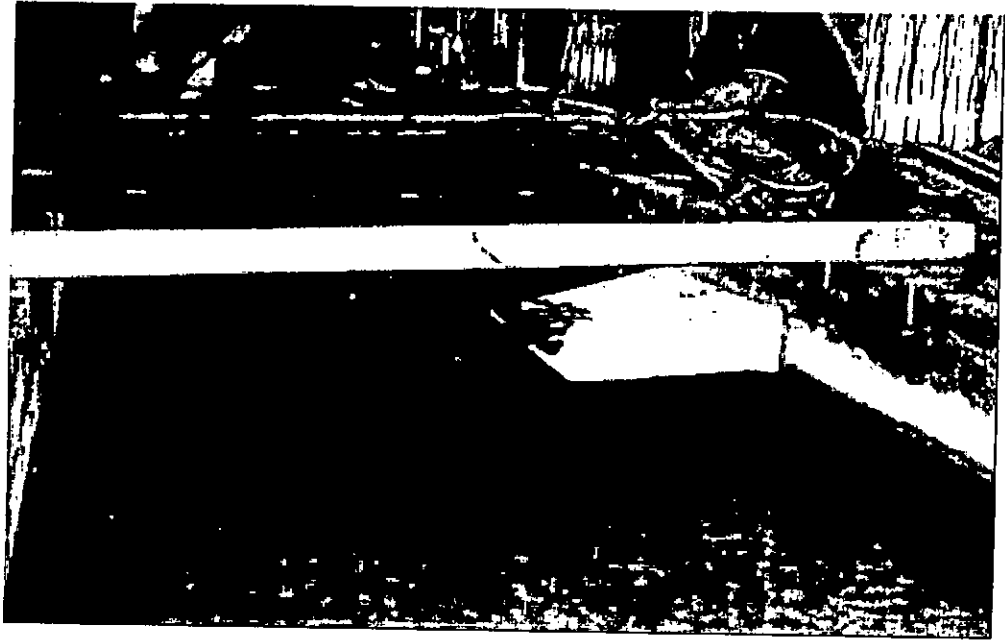


Fig. 3.1 Layout of Channel System with Embankment type Structure

3.2.1 Laboratory Channel System

The Experiment were carried out in a 11m long, 2m wide rectangular channel. Water entered the channel smoothly from an inlet reservoir, and a secondary reservoir was placed at the end which was connected by a tailgate. Though the tailgate water goes to a sump. From this sump, the water was recirculated through a return system. From the tailgate, water was allowed to fall into the sump through a rehbok weir for measuring the flow.

The main channel was made of plastered brick wall and brick soling. Plastering was carried out with sand-cement mortar of ratio 5:1 (sand:cement) to ensure no water seepage and at the same time the wall can be easily broken for remodeling the channel for other tests. The channel is shown in fig. 3.2

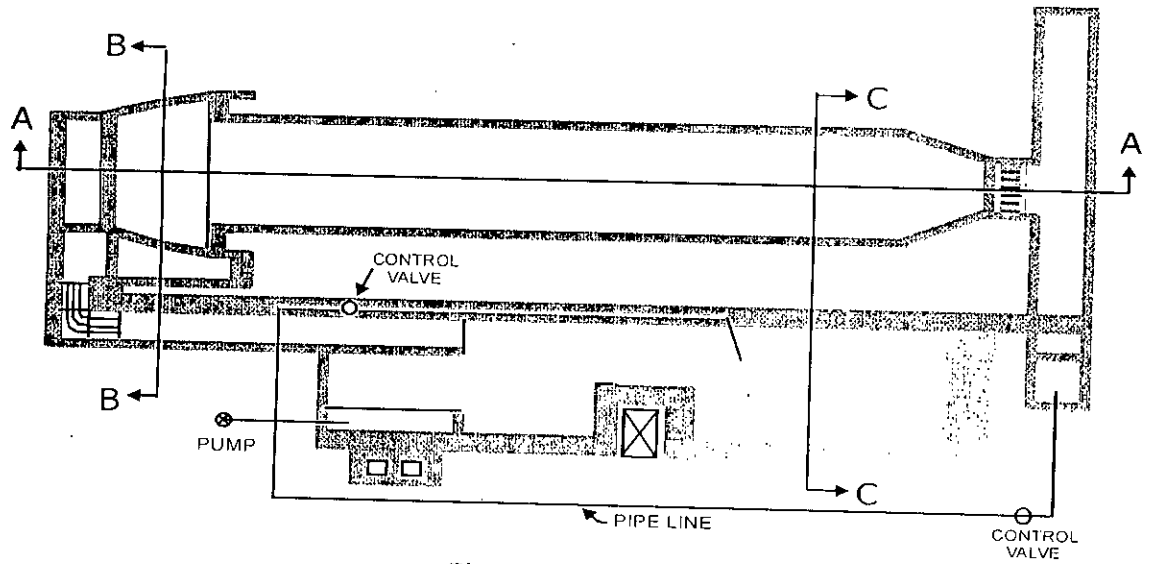


Fig. 3.2a: PLAN

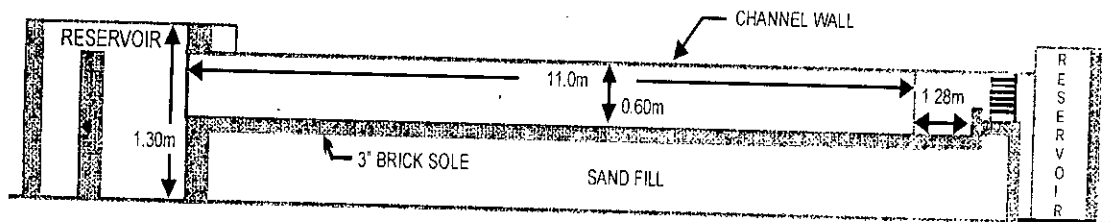


Fig. 3.2b SECTION A-A

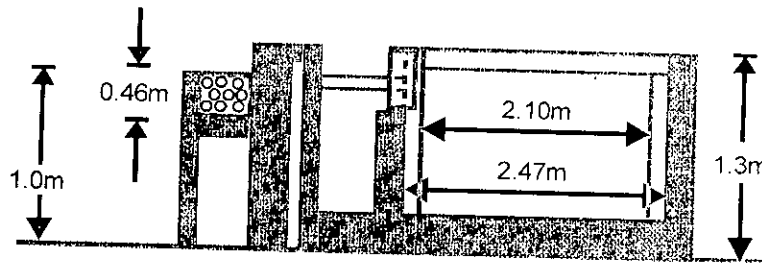


Fig. 3.2c: SECTION B-B

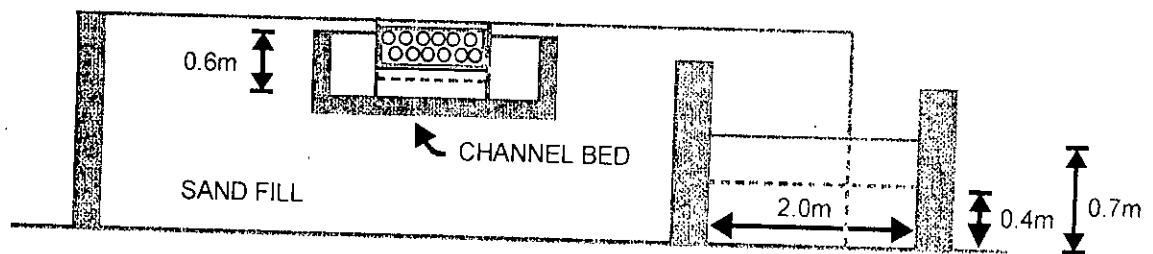


Fig. 3.2d: SECTION C-C

Fig. 3.2 Laboratory Channel

Silt Trap

A reservoir is placed at the end of the channel to act as silt trap. The silt trap precedes a tailgate, which retains the washed out sediments from the channel bed. From this sump, water is transported to the large downstream reservoir through channel system for recirculation

Pipe Line

The pump sucks water from the downstream reservoir into the pipeline. The T-joint on top of the pump divides the water over the excess discharge pipe and the delivery or supply pipe.

Regulating System

Pump

A centrifugal pump with maximum discharge capacity of 70 l/s draw water from downstream reservoir and supplies it to the pipeline. The pump used for the study, can run for 8 hours at a stretch.

Tail Gate

The tailgate is located at the downstream end of the channel. It is made of cast iron and surrounded by rubber flaps. A wheel attached to the gate helps to rotate it up and down and thereby performs the downstream regulation. For a particular discharge, if the tailgate is raised it increases the water level and vice versa.

Valves

Two gate valves are attached to the circulation network: one is in the delivery pipe and another is in the excess discharge pipe. The flow in the channel is controlled by adjusting these values. At the end of the suction pipe, a check valve is attached with a screen. The screen restricts debris, leaves and other relatively large unwanted foreign particles from entering into the pipeline.

PVC Pipe

When the water discharge from the delivery pipe into the upstream reservoir, turbulence is created. A series of PVC pipes are placed on the upstream end of the channel to dampen the turbulence and to aid the development of uniform flow.

3.2.2 Measuring Devices

Measuring devices used in the present study are as follows:

Rehbok Weir

A rehbok weir is attached at the end of the channel that delivers water to the downstream reservoir. The Rehbok weir is calibrated to measure the discharge directly by observing the head above the weir only. The head above the weir is measured by a point gauge setup.

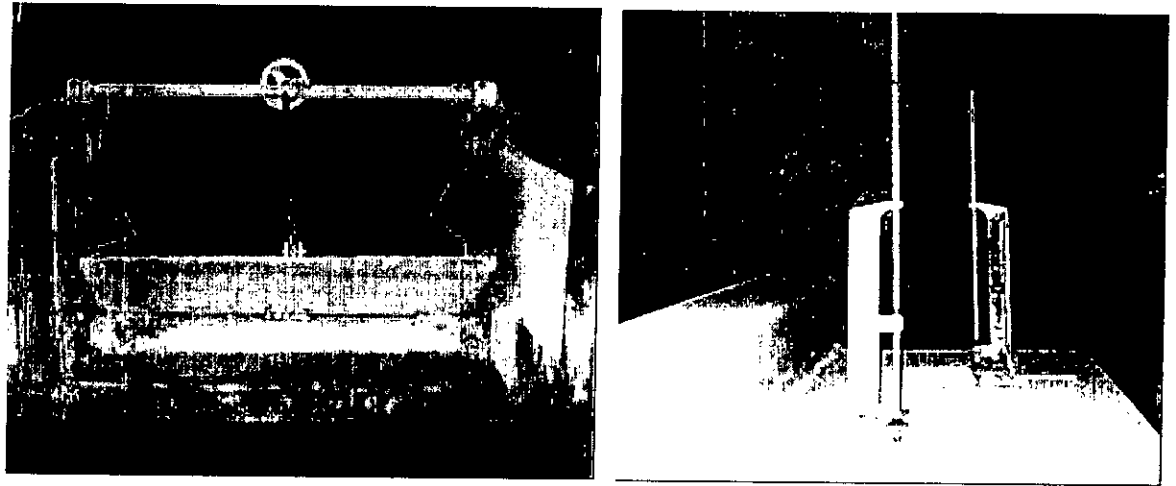


Fig. 3.3 Rehbok Weir and Associated Point Gauge

P. -E.M.S. Velocity Meter

Programmable Electromagnetic Liquid Velocity Meter (P. -E.M.S.) is used for the purpose of velocity measurement. The programmable E.M.S. employs Faraday's Induction Law for measurement of the velocity of a conductive liquid moving through a magnetic field. The magnetic field is inducted by a pulse current through a small coil inside the body of the sensor. Diametrically opposed platinum electrodes sense the Faraday-induced voltages produced by the flow past the sensor.

The sensor has been designed in such a way that these voltages are proportional to the sine (V_y) and cosine (V_x) of the magnitude of the liquid velocity (V) parallel to the plane of the electrodes. Velocity ranges for the meter is 1.0 m/s to 2.5 m/s. This magnitude of the velocity and its direction can be derived by application of common trigonometry.

The instrument consists of three basic parts.

- a. The probe, with built-in amplifier
- b. The control unit in the universal carrying case
- c. Connection cable

The P -E.M.S. measures continuously the velocity components of the liquid in which the probe is immersed, processes the signals obtained and presents them as analogue voltages. For data display a measuring period has to be selected. The period is selectable from 0.1 to 9999.9 seconds. Via menu different types of data presentation can be selected, e.g. mean, actual or standard deviation values of X and Y or total speed and angle. P -E.M.S. unit can be connected to a personal computer, terminal etc. Thus, the P -E.M.S. can return the data measured.

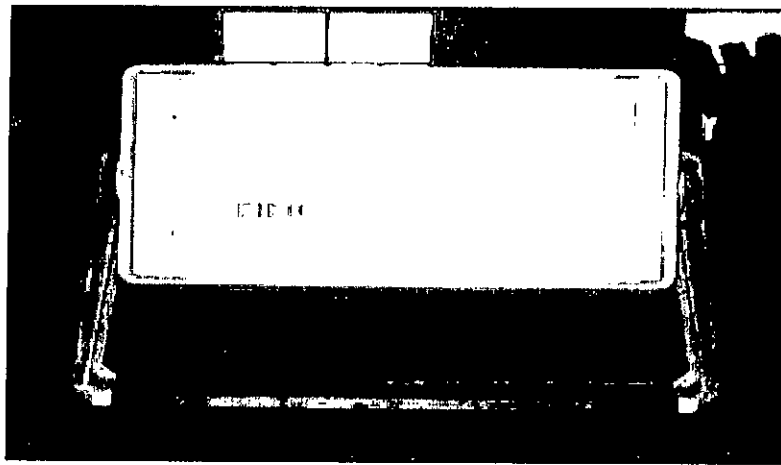


Fig. 3.4 P. - E.M.S. Control Unit

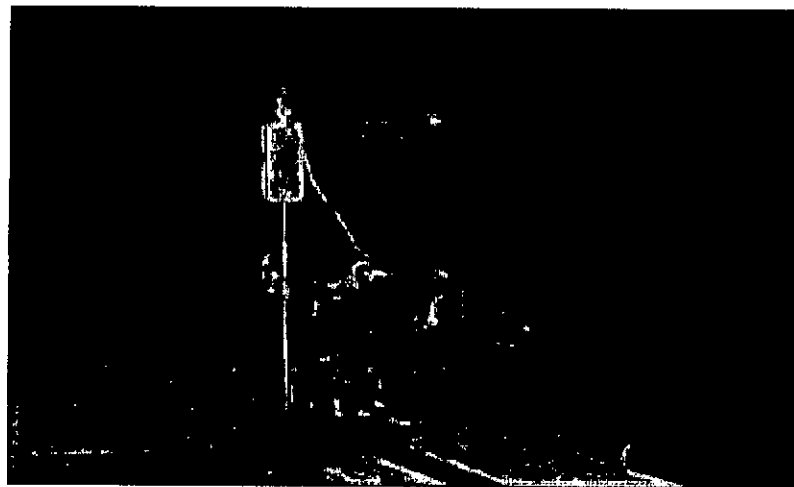


Fig. 3.5 P. - E.M.S. Probes

Point Gauge

The water level and bed level are measured with the help of a point gauge. The gauge is mounted on a frame laid across the width of a channel. The whole structure of point gauge can be moved over the sidewalls. The point gauge can measure with 0.1 mm accuracy.

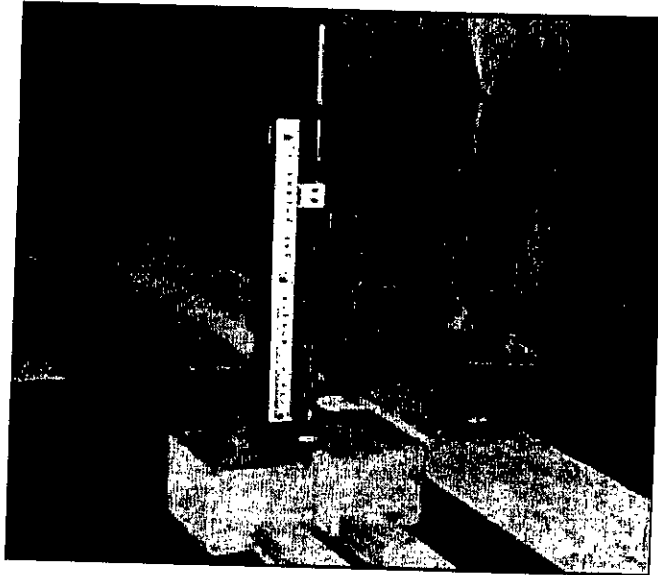


Fig. 3.6 Point Gauge

3.2.3 Hydraulic Parameter

This channel can be supplied a maximum discharge of 70 l/s. If two tailgates are being used, the capacity could be increased to 90 l/s. In that case, clear-water condition would not have been maintained. Considering different hydraulic parameters like flow-rate, velocity, bed shear stress, freeboard, water depth, etc. a discharge of 40 l/s were selected. Summary of different hydraulic parameters that were considered are shown in Table 3.1. the selected parameters are shown as highlighted color in the table.

Since maximum scour at $\tau_b/\tau_{*c} \approx 1$, this was the main, consideration in selecting discharges for the test. The pump used for water circulation can be run for eight hours at a stretch. No stand by pump was available with the system.

3.2.4 Bed Material

The bed material used was fine sand. Uniformity co-efficient was 3 therefore the sand was uniform. D_{50} was 0.226mm and D_{90} was 0.46mm. the grain size chart is shown as fig. 3.7. This bed material formed ripples, as D_{50} was less than 0.7mm (Breusers and Raudkivi, 1991 and Melville and coleman, 2000).

Table 3.1 TEST HYDRAULIC PARAMETER

B	h	A	Q	u	D	n	S	u _*	u _{*c}	u _* /u _{*c}	τ _* /τ _{*c}	Bed level
(m)	(cm)	(m ²)	(l/s)	(m/s)	(mm)			(m/s)	(m/s)			diff. (mm)
2	5	0.1	30	0.172	0.226	0.0117	0.00021	0.0101	0.013	0.776	0.59	2.1
2	8	0.16	30	0.171	0.226	0.0117	0.00011	0.0093	0.013	0.715	0.51	1.1
2	10	0.2	30	0.125	0.226	0.0117	0.00004	0.0062	0.013	0.476	0.22	0.4
2	12	0.24	30	0.121	0.226	0.0117	0.00003	0.0059	0.013	0.453	0.2	0.3
2	15	0.3	30	0.1	0.226	0.0117	0.00002	0.005	0.013	0.384	0.14	0.2
2	20	0.40	30	0.035	0.226	0.0117	0.00001	0.0046	0.013	0.353	0.12	0.1
2	9	0.2	40	0.301	0.226	0.0117	0.0003	0.0162	0.013	1.246	1.55	3
2	10	0.2	40	0.3	0.226	0.0117	0.00026	0.0159	0.013	1.22	1.49	2.6
2	12	0.24	40	0.25	0.226	0.0117	0.00014	0.0128	0.013	0.984	0.96	1.4
2	15	0.3	40	0.22	0.226	0.0117	0.00008	0.01	0.013	0.769	0.59	0.8
2	20	0.40	40	0.19	0.226	0.0117	0.00004	0.008	0.013	0.615	0.37	0.4
2	10	0.2	50	0.312	0.226	0.0117	0.00028	0.017	0.013	1.338	1.71	2.8
2	12	0.24	50	0.281	0.226	0.0117	0.00018	0.014	0.013	1.077	1.16	1.8
2	15	0.3	50	0.25	0.226	0.0117	0.0001	0.012	0.013	0.92	0.85	1
2	20	0.40	50	0.216	0.226	0.0117	0.00005	0.01	0.013	0.769	0.6	0.5

CONSIDERATION AND FORMULAE

In this table, following consideration and formulae are used:

$$B = 2m; \quad h = 5, 8, 9, 10, 12, 15, 20 \text{ cm}; \quad Q = 30, 40, 50 \text{ l/s}; \quad u = \left(\frac{1}{n}\right) (h^{2/3} * S^{1/2})$$

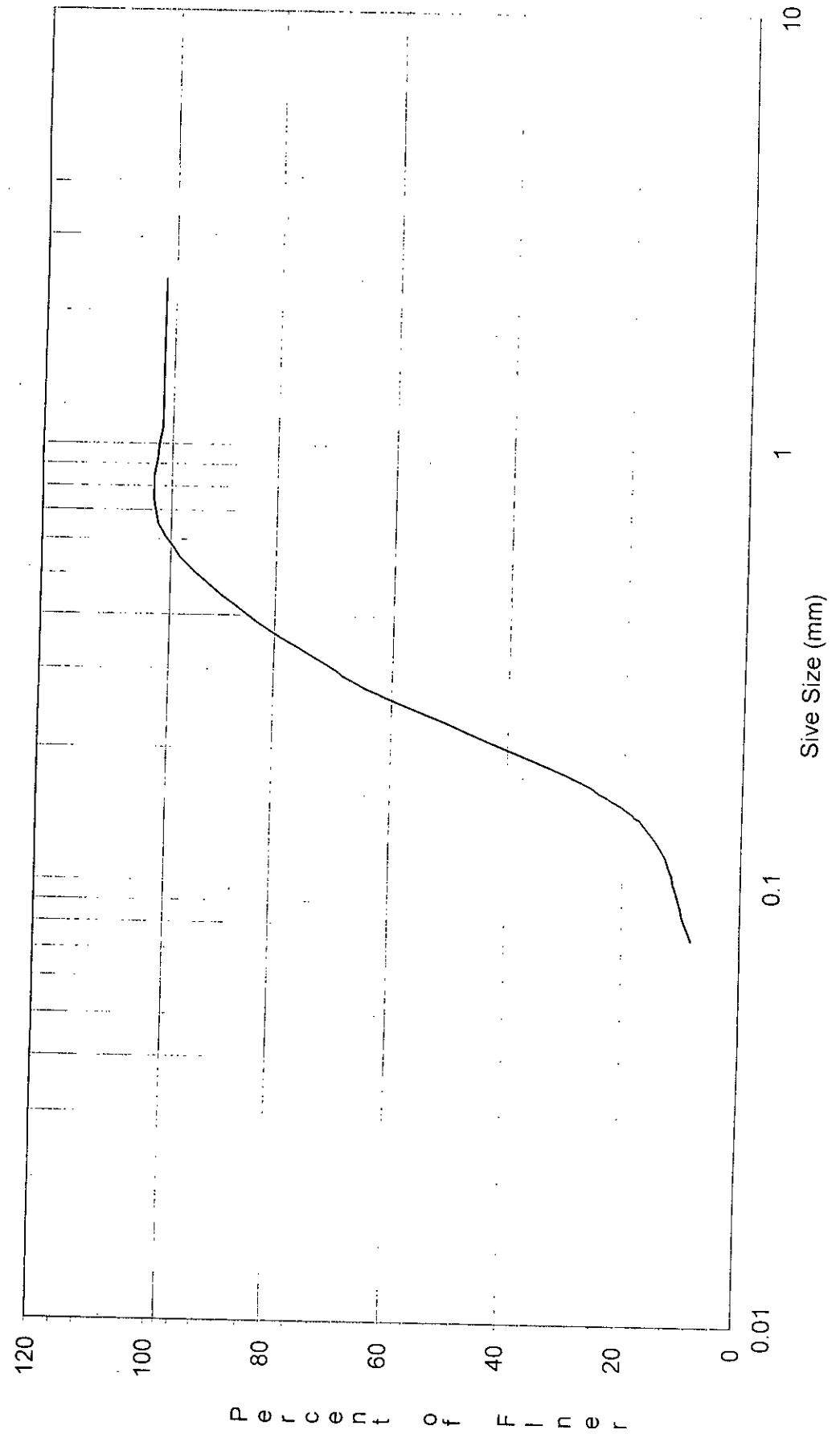
$$n = (1/21.1) (d/1000)^{1/6}; \quad S = \left[\frac{\{(u) * (n)\}}{h^{2/3}} \right]^2; \quad u_* = \text{SQRT}(ghs) = \text{SQRT}(8.4 * D^{11/32});$$

u_{*c} = from graph (fig.2.10); Bed level difference upstream and down stream ends = S * 10 * 1000

$$\tau_* = \rho u_*^2; \quad u_* / u_{*c} = 0.9 \approx 1.0; \quad \tau_* / \tau_{*c} = 0.8 \approx 1.0;$$

The highlighted row shows the selected parameters that were used in this study.
B is the channel width.

Fig. 3.7 Grain Size Distribution for Bed Material



3.2.5 Types of Structures

Two types of structures were used in this study, that's were sloping and vertical embankment like structure. The sloping structure were in three types, that were variable slope of 1V:1H, 1V:2H, 1V:3H but were of same length (100cm) and width (60cm). These structures were made of wooden framework shown in fig. 3.7.

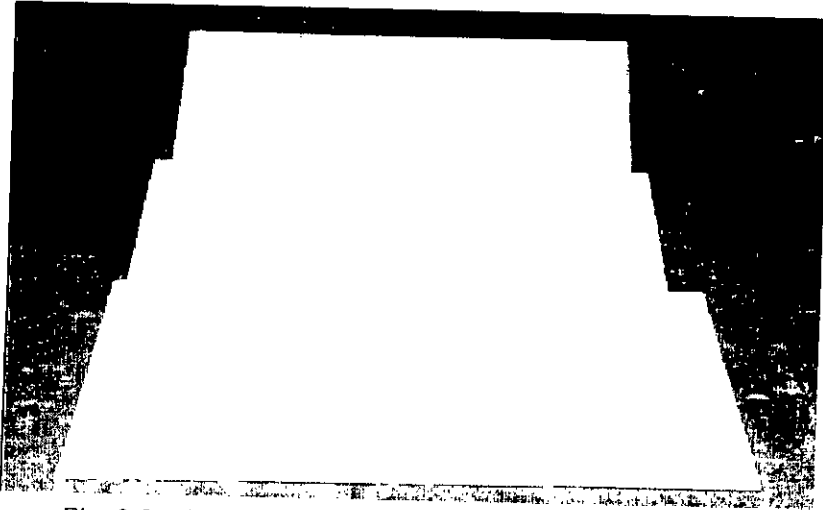


Fig. 3.8 Photograph of sloping structure used in the study

The vertical structure were also in three types, that were variable width of 60cm, 40cm, 20cm but were of same length 100cm. They were made of $\frac{1}{2}$ inch thick particleboard shown in fig.3.9. To make them stable in the channel flow, extra weights were placed inside them. Finally extensive painting was carried out on both inside and outside of all the structure. Thereby, the structures were made waterproof. The joint of the structures were made waterproof by applying putty.

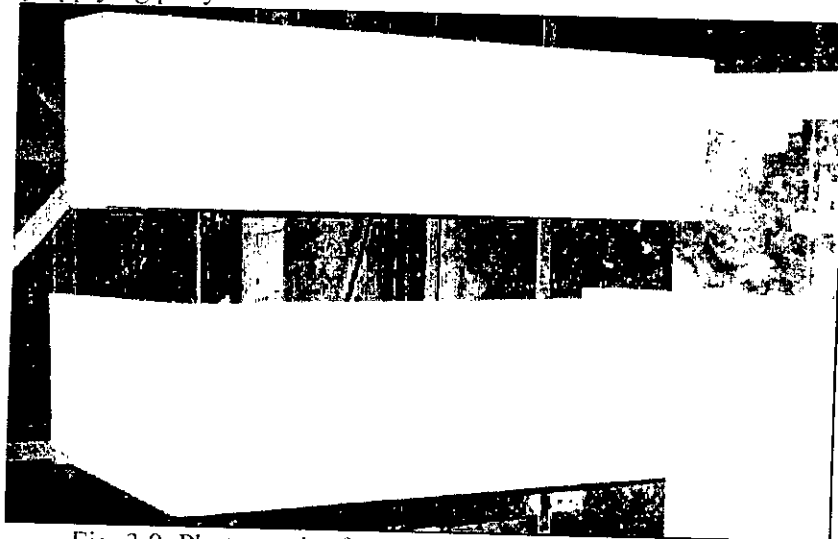


Fig. 3.9 Photograph of vertical structure used in the study

3.3 Measurements

Following measurements were taken in the present study:

3.3.1 Discharge

Discharge in the channel was measured with the help of Rehbok weir. It was calibrated with the point gauge reading. Therefore, only point gauge readings were taken and the corresponding discharges were observed from the calibration table.

3.3.2 Scour Depth

Scour depth were measured with the help of a point gauge, mounted on a platform that slides over the sidewalls at the location of the structure. An area was selected around the structure, where scour is considerable and data were collected from this grid points. In this study, the considerable area was longitudinally 1.6m and laterally 1.0m. The mid point of longitudinal length was considered as center point (0,0). From this center point u/s direction considered as -(ve) axis and d/s direction as +(ve) axis. The total area was divided into grids area of 5cm×10cm. The point gauge measurement was taken from every grid point. As longitudinal grid interval was only 5cm, so every important data came into count. The initial bed level was used as reference for the measurement of maximum scour depth. Any data found to be below this reference level was taken as negative value and indicated scour. Similarly any data found to be above the reference level were taken as positive and indicated deposition. This data were processed for constructing spectral scour (contour) map by Surfer Software. These measurement were used to study the scour pattern, maximum scour depth and its location.

3.3.3 Scour Area

Scour area around the structure was measured with the help of scale. This measurement was done every next day of the experiment. At first scour area were divided in to grids and then every grids area were measured.

Scour Contour for structure with IV: 1H Slope

Contour Unit : cm
Initial Bed Level : 0
(+) ve : Deposit
(-) ve : Scour
Flow Restriction, b : 60cm

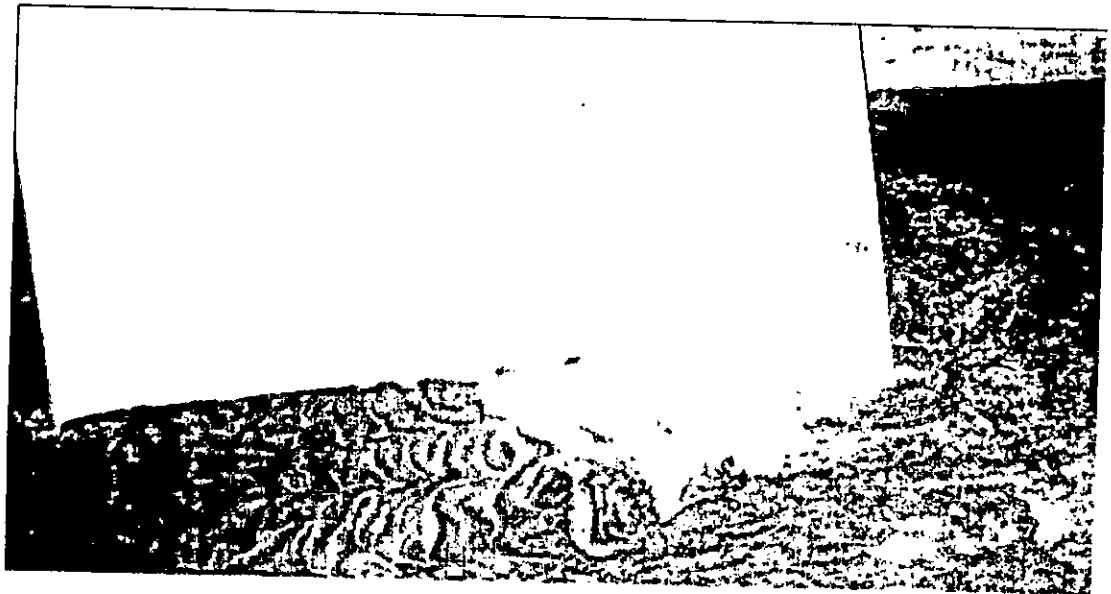
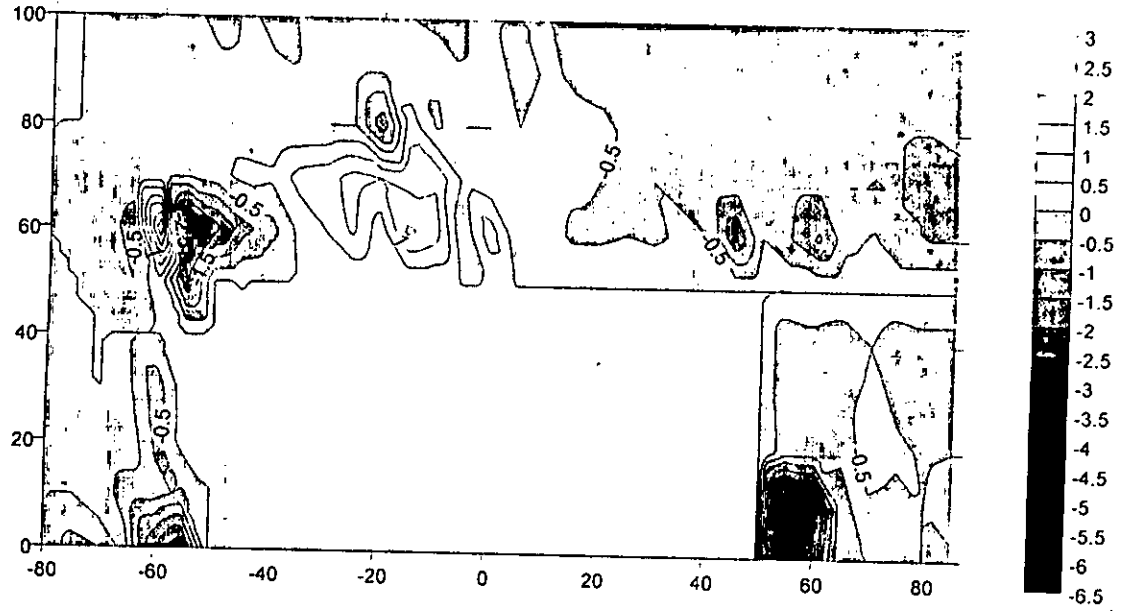


Fig. 3.10 Scour for structure with IV: 1H slope

Scour Contour for structure with 1V: 2H Slope

Contour Unit : cm
Initial Bed Level : 0
(+) ve : Deposit
(-) ve : Scour
Flow Restriction, b : 60cm

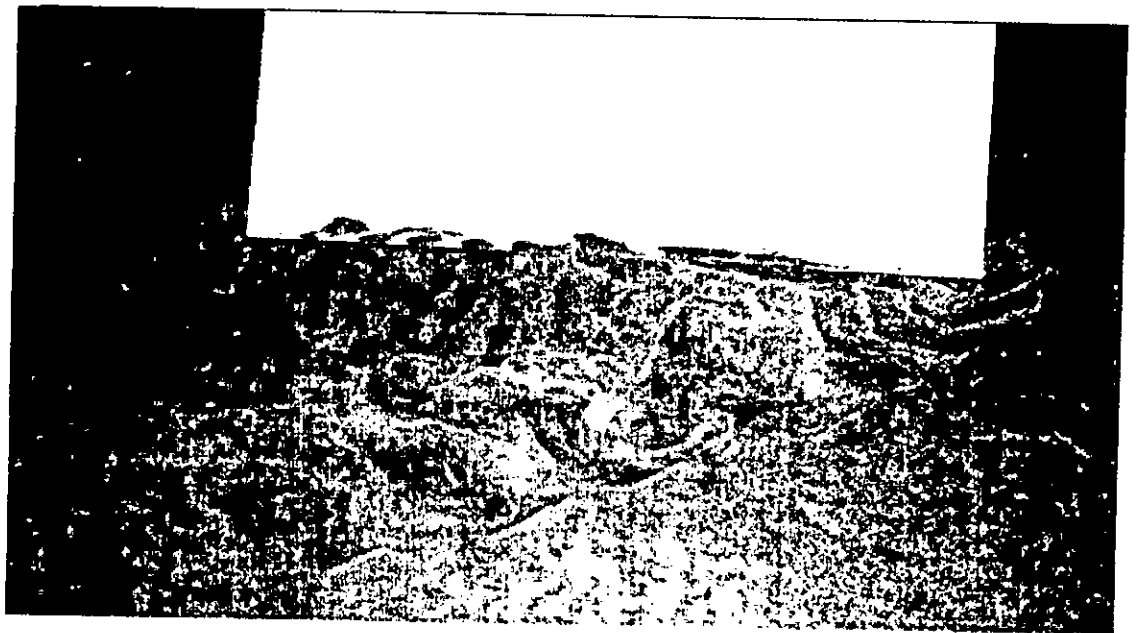
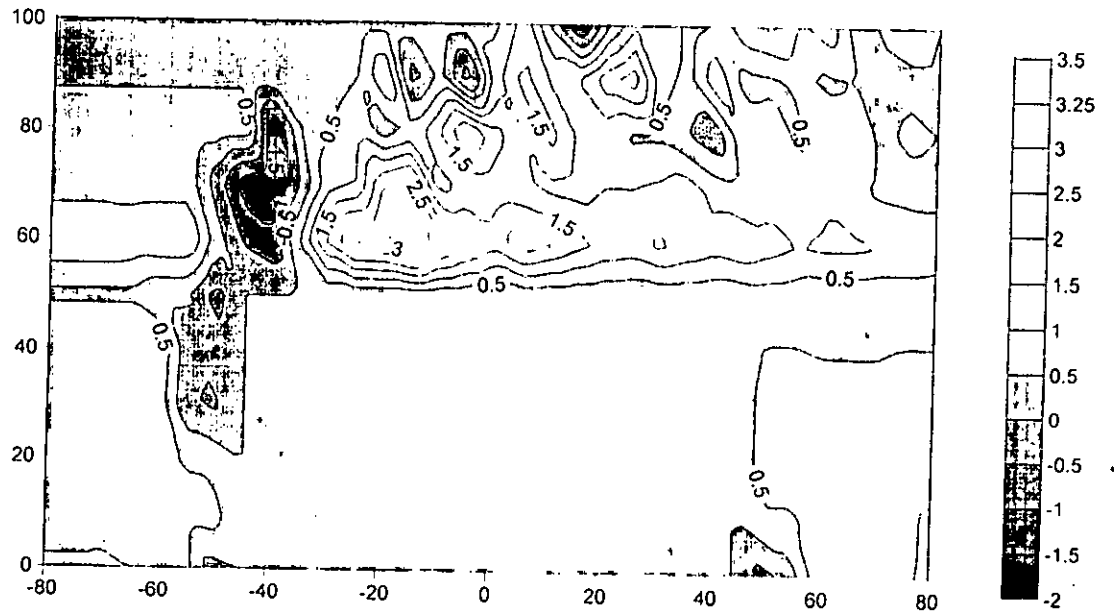


Fig. 3.11 Scour for structure with 1V: 2H slope

Scour Contour for structure with 1V: 3H Slope

Contour Unit : cm
Initial Bed Level : 0
(+) ve : Deposit
(-) ve : Scour
Flow Restriction, b : 60cm

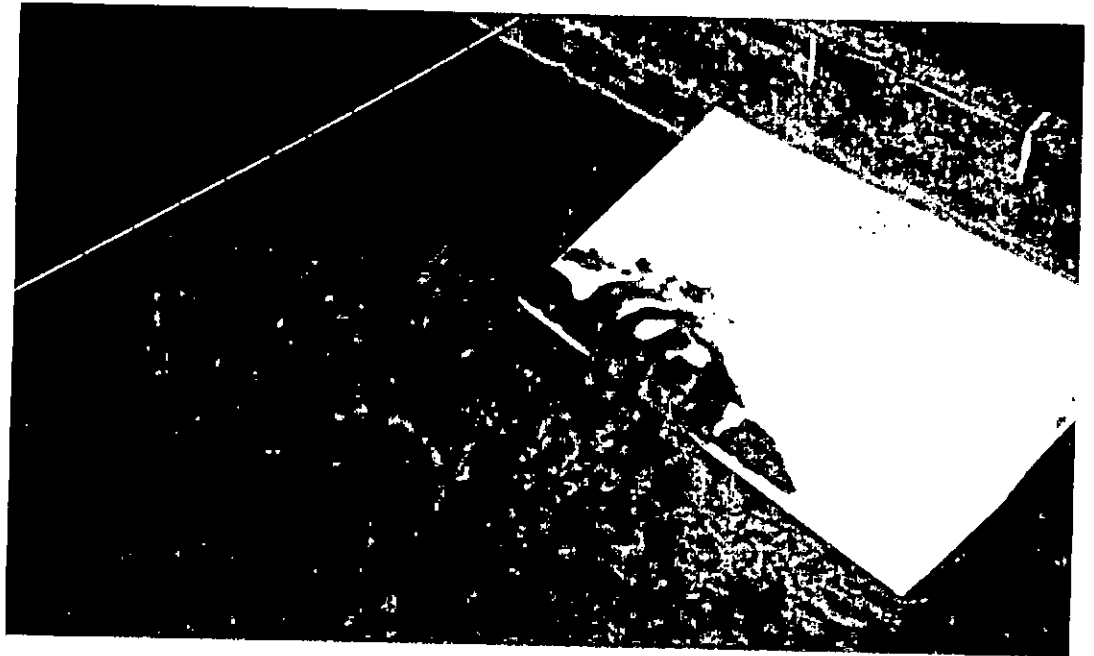
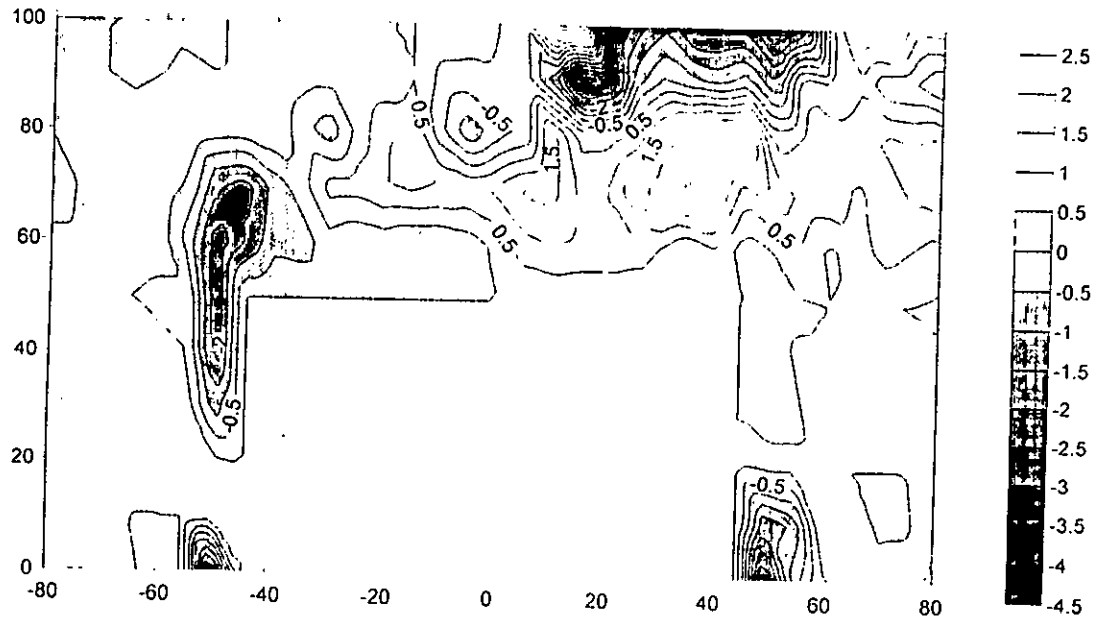


Fig. 3.12 Scour for structure with 1V: 3H slope

Scour Contour for vertical structure

Contour Unit : cm
Initial Bed Level : 0
(+) ve : Deposit
(-) ve : Scour
Flow Restriction, b : 60cm

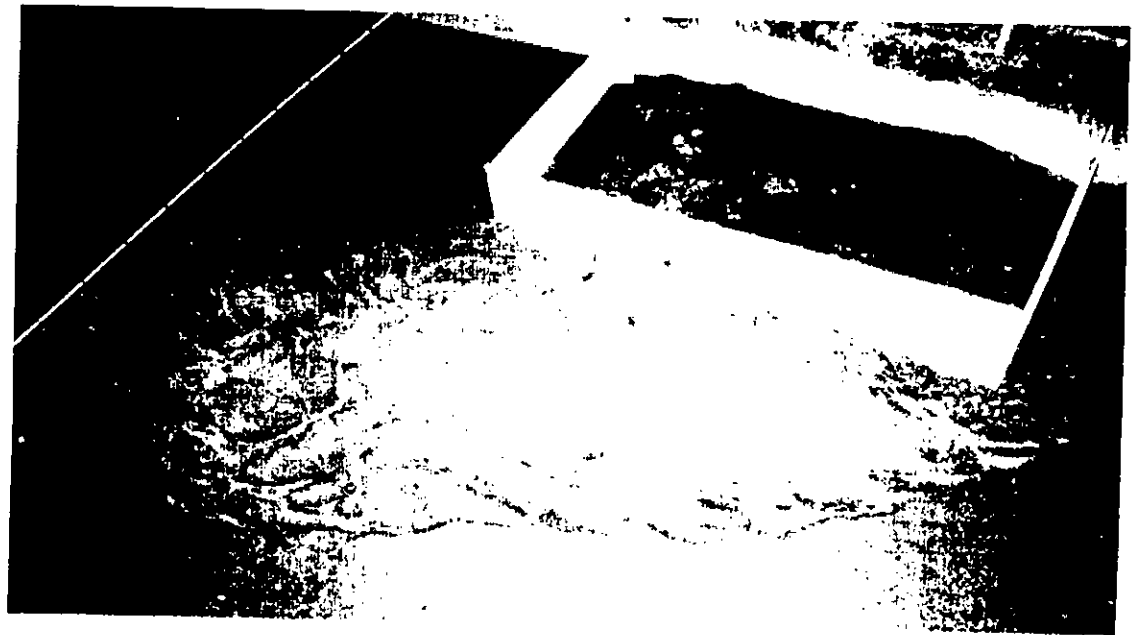
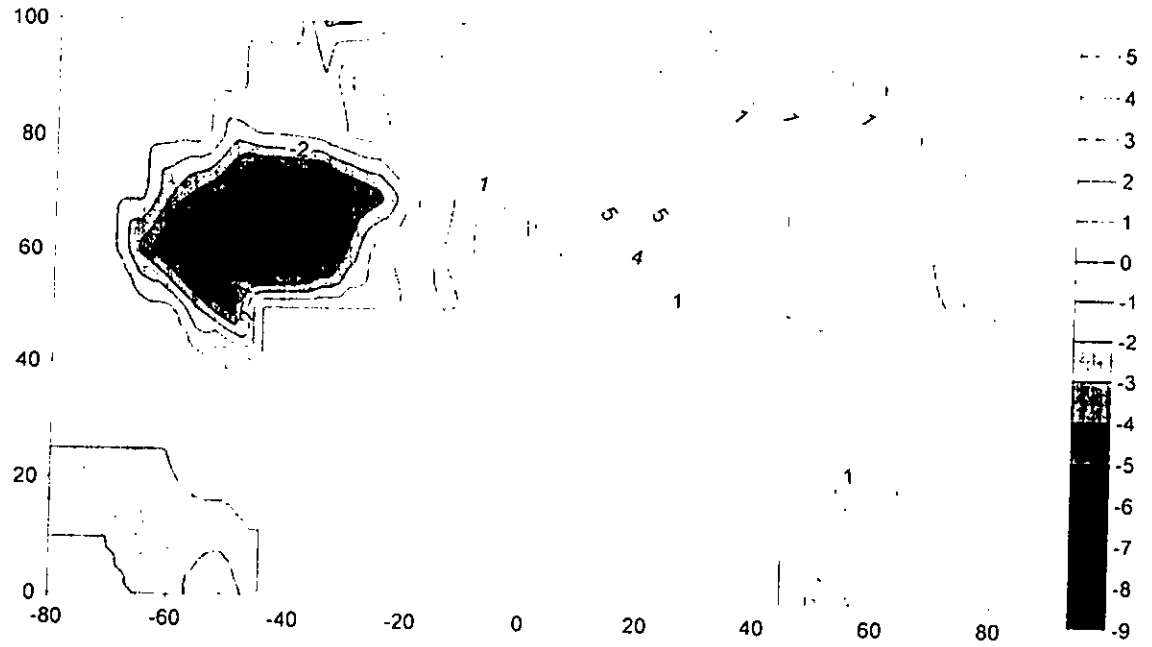


Fig. 3.13 Scour for vertical structure with $b=60\text{ cm}$

Scour Contour for vertical structure

Contour Unit : cm
Initial Bed Level : 0
(+) ve : Deposit
(-) ve : Scour
Flow Restriction, b : 40cm

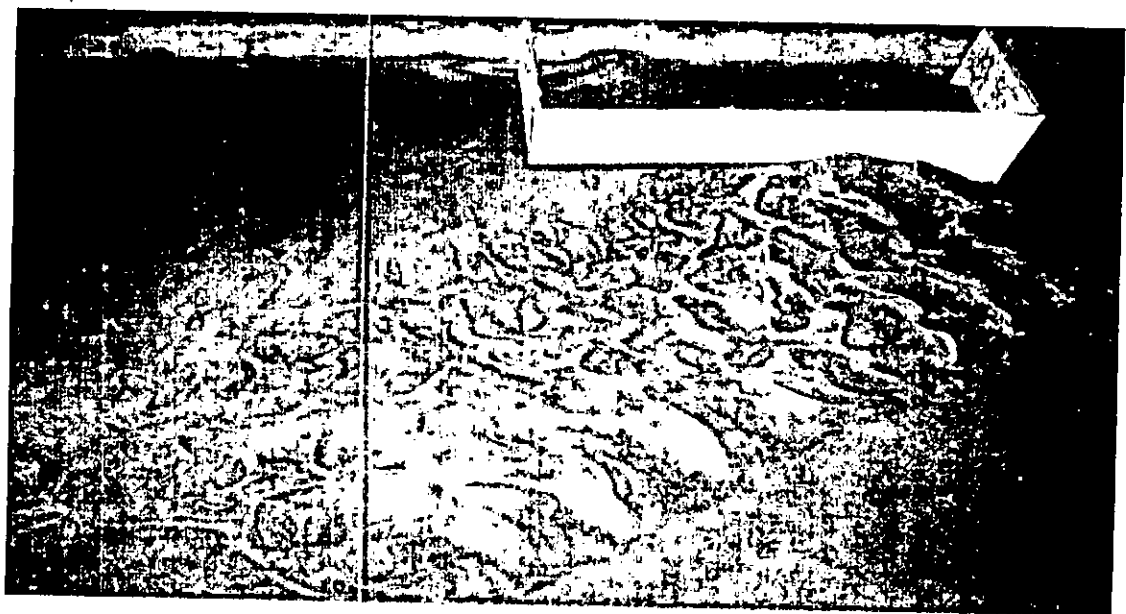
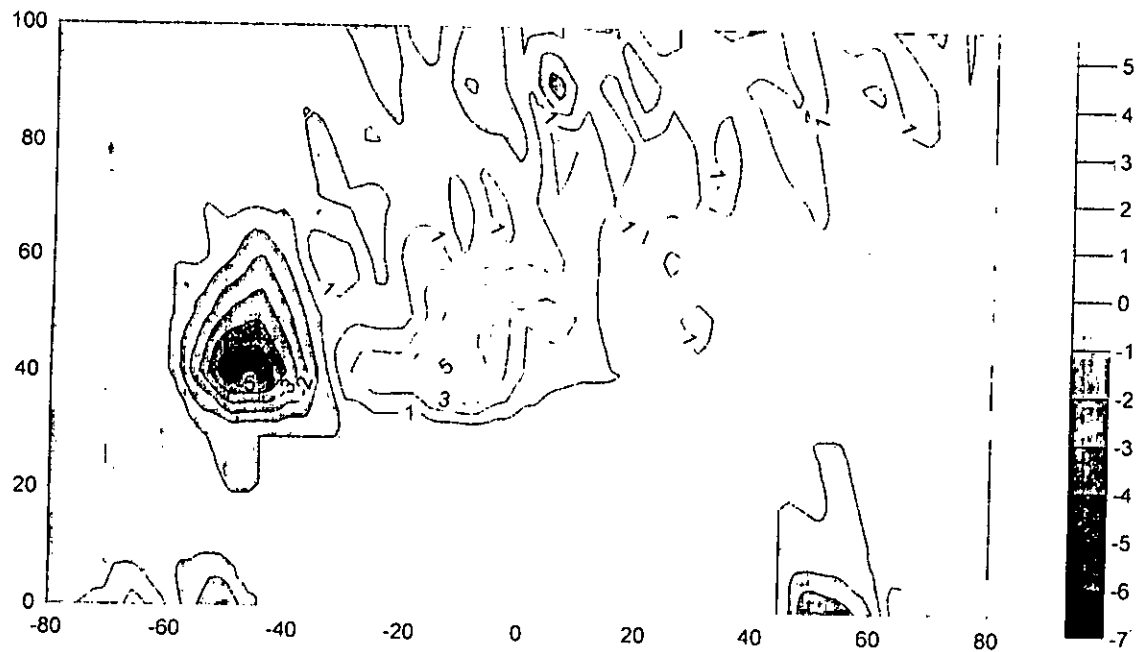


Fig. 3.14 Scour for vertical structure with $b=40\text{ cm}$

Scour Contour for vertical structure

Contour Unit : cm
Initial Bed Level : 0
(+) ve : Deposit
(-) ve : Scour
Flow Restriction, b : 20cm

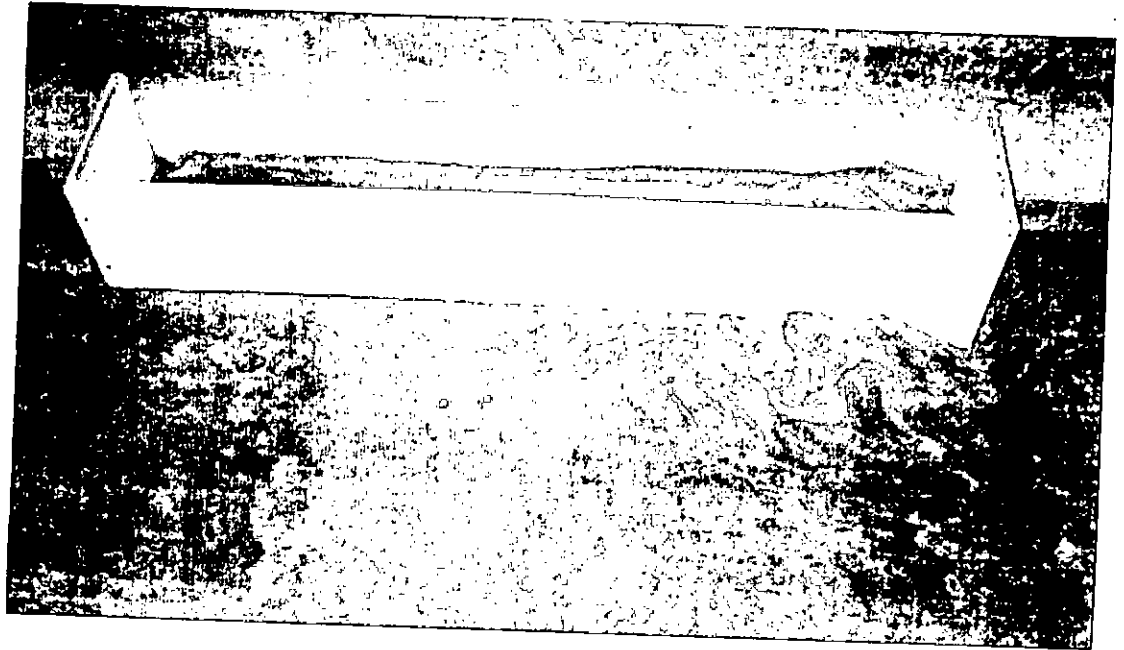
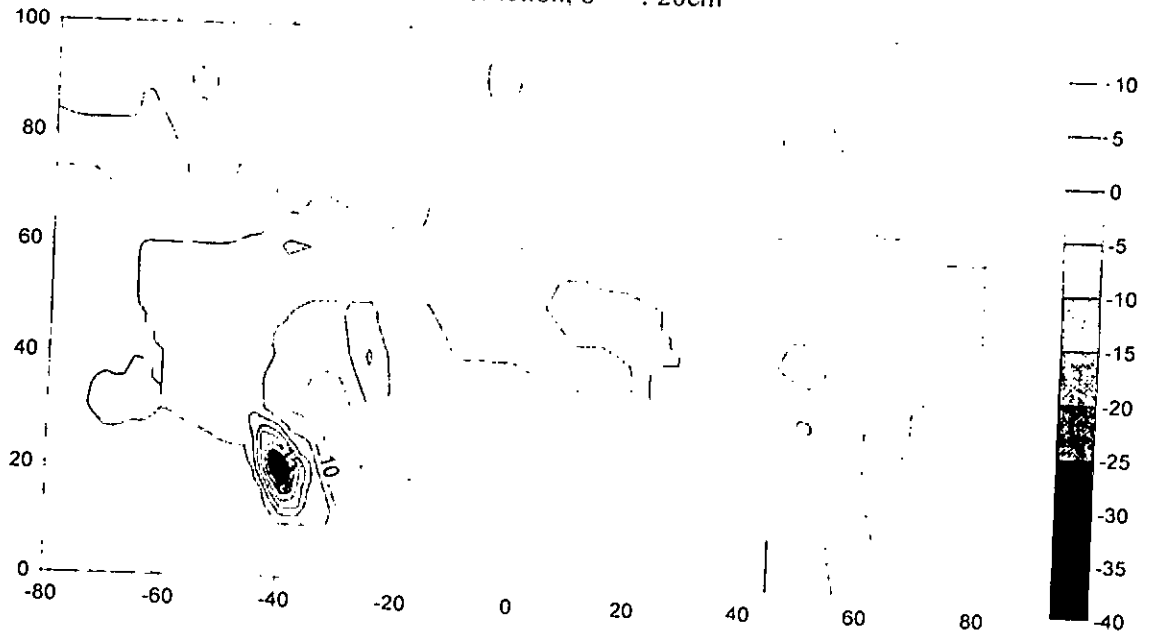
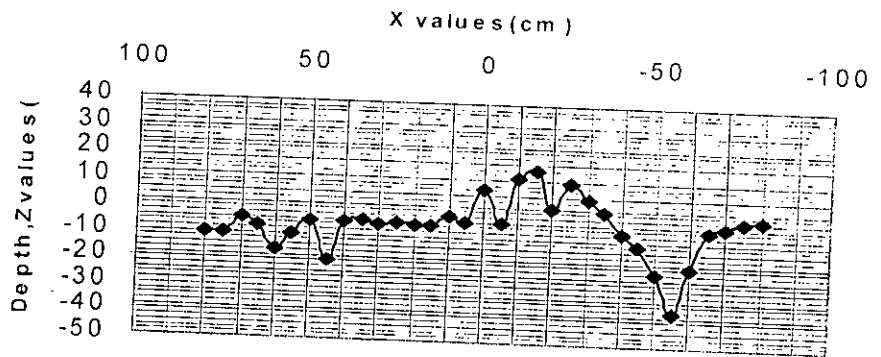
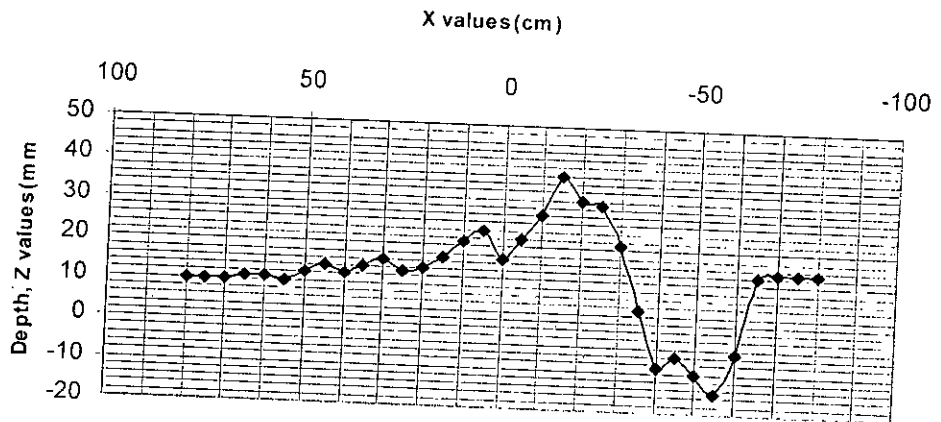


Fig. 3.15 Scour for vertical structure with $b=20\text{cm}$

X vs Z at Y=60cm from right bank
(Slope 1:1, b=60cm)



X vs Z at Y=60cm from right bank
(Slope 1:2, b=60cm)



X vs Z at Y=60cm from the right bank
(Slope 1:3, b=60cm)

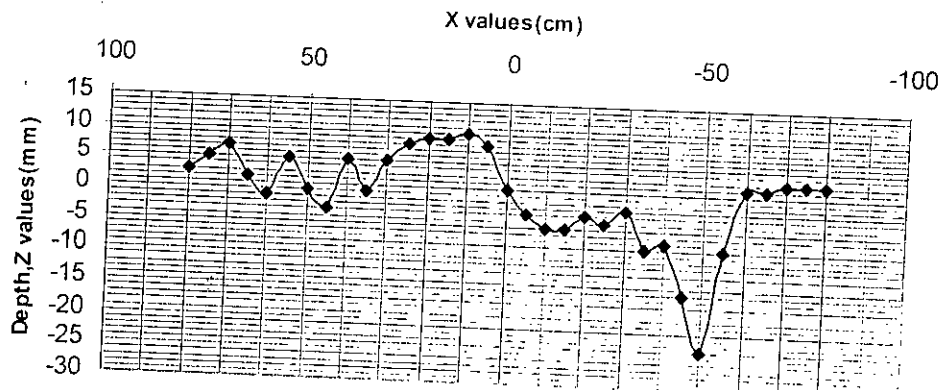
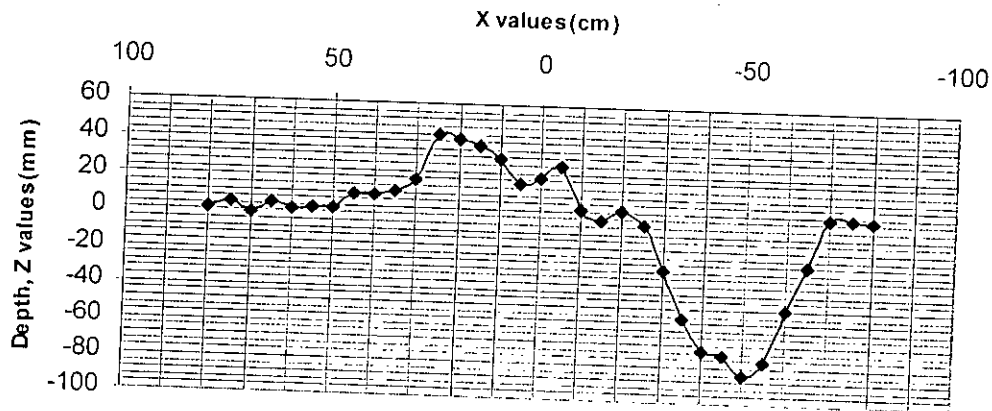
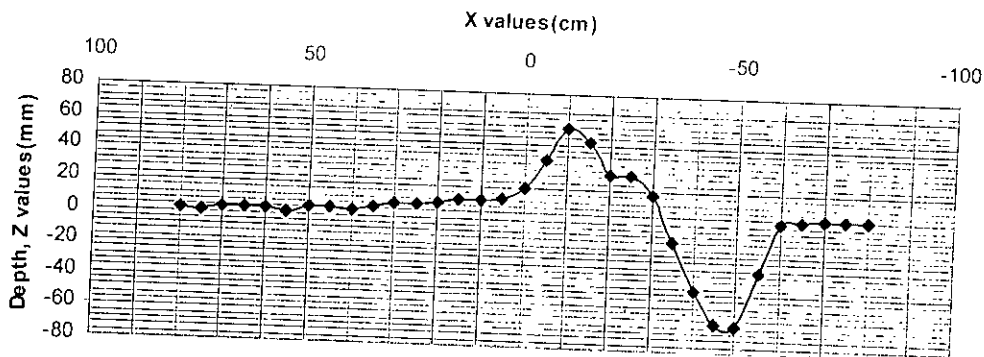


Fig. 3.16 Longitudinal scour profile for sloping-wall structure

X vs Z at Y=60cm from right bank
(Vertical, b=60cm)



X vs Z at Y=40cm from right bank
(Vertical, b=40cm)



X vs Z at Y=20cm from right bank
(Vertical, b=20cm)

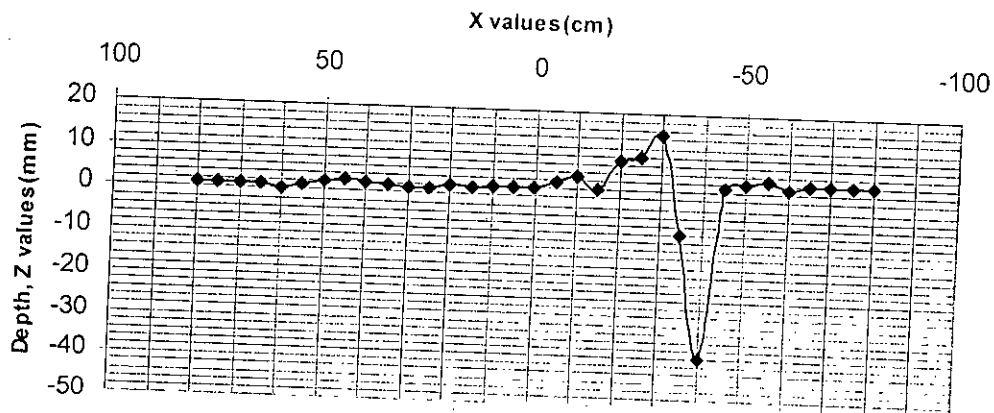
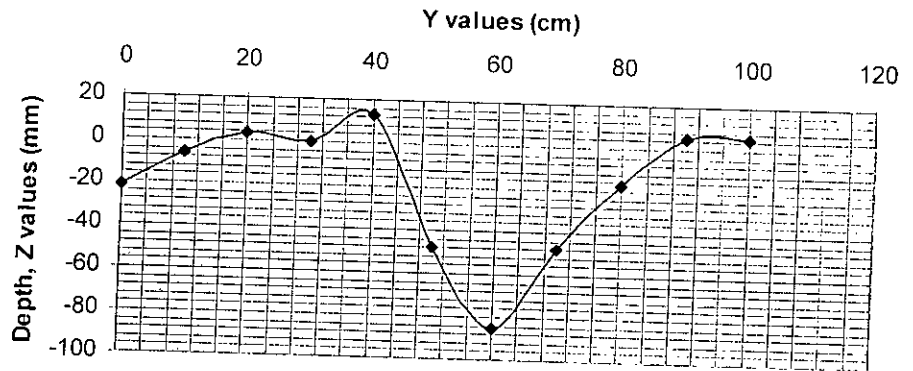
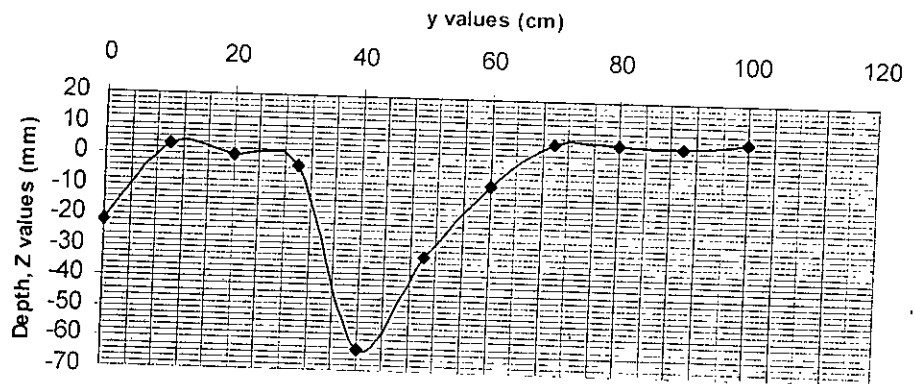


Fig. 3.17 Longitudinal scour profile for vertical-wall structure

Y va Z at X=-50cm location
(Slope 1:1, b=60cm)



Y vs Z at X=-50cm location
(Slope 1:2, b=60cm)



Y vs Z at X =-50cm location
(Slope 1:3, b=60cm)

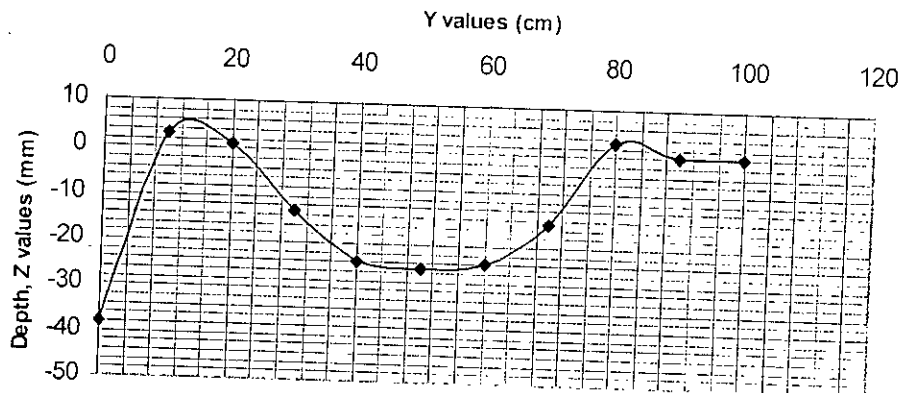
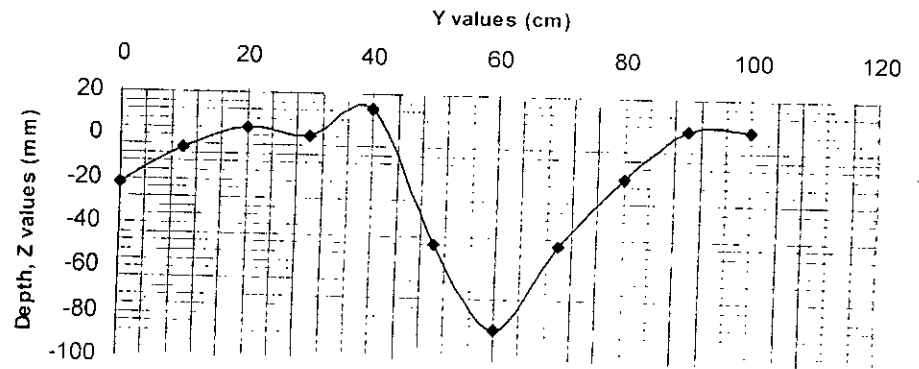
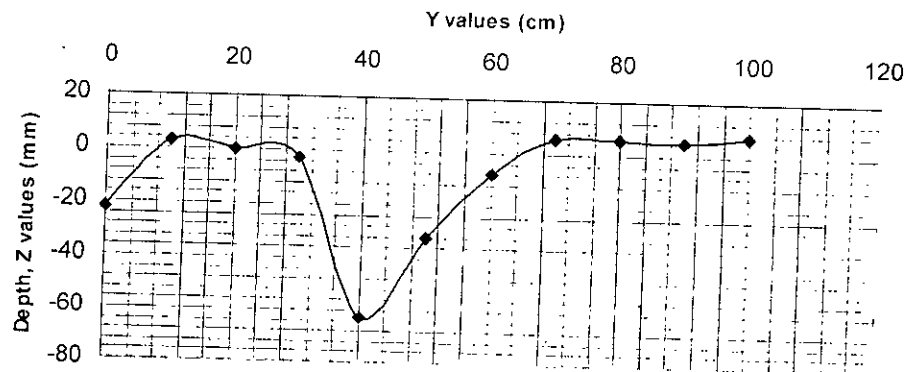


Fig. 3. 18 Lateral scour profile for sloping-wall structure

Y vs Z at X = -50cm location
Vertical, b=60cm



Y vs Z at X=-50cm location
Vertical, b=40cm



Y vs Z at X=-50cm location
Vertical, b=20cm

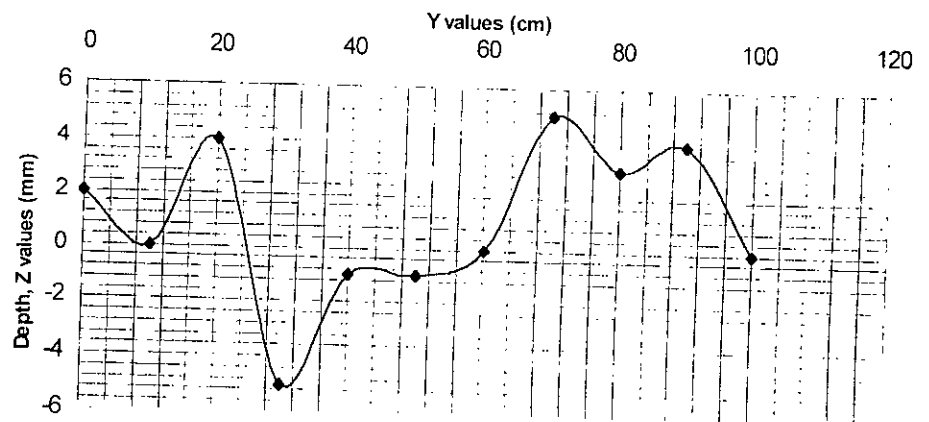


Fig. 3.19 Lateral scour profile for vertical-wall structure

3.3.2 Velocity

Velocity probe was placed at a constant depth of $0.6y$ from the top surface of the water level to obtain the average velocity in all experiments. The area selected for velocity measurement was $0.8m$ u/s to 0.8 d/s from the center of the structure in the longitudinal direction and $1.0m$ traverse direction for the right bank (for both slope and vertical structure). The total area was divided into grid of $10cm \times 10cm$. The data were collected from all the grid point from after four hours of flow run. Vertical velocity from the surface of water at $2cm$ interval were also collected around the structure. Total five points were selected around the structure shown in fig. 3.19 for this measurement. These data were processed by the use of Standford Graphics Software to produce velocity vector.

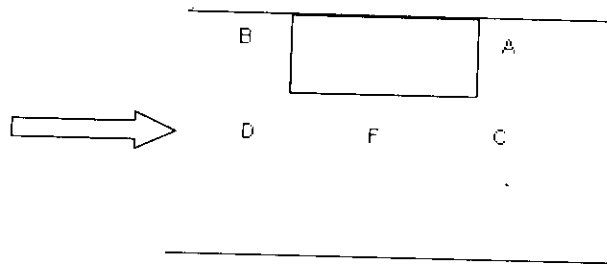


Fig.3.20 Selected points for vertical velocity measurement

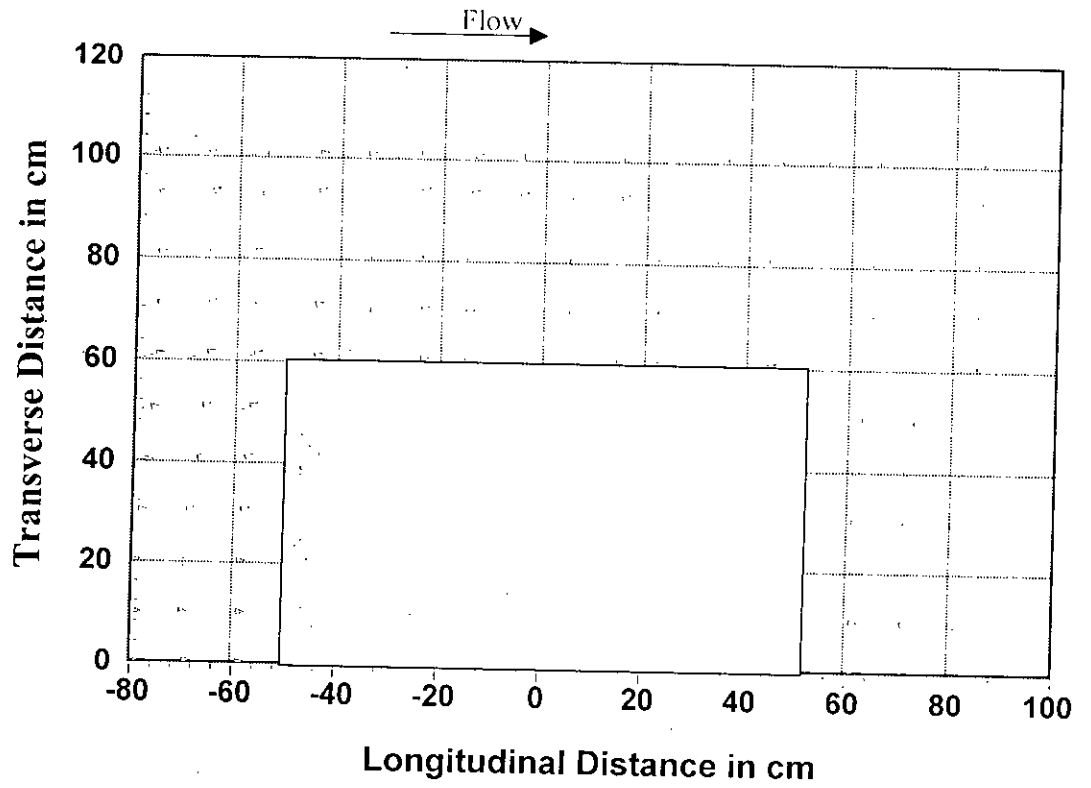


Fig: 3.21 Velocity Vector for 1:1 Slope Structure

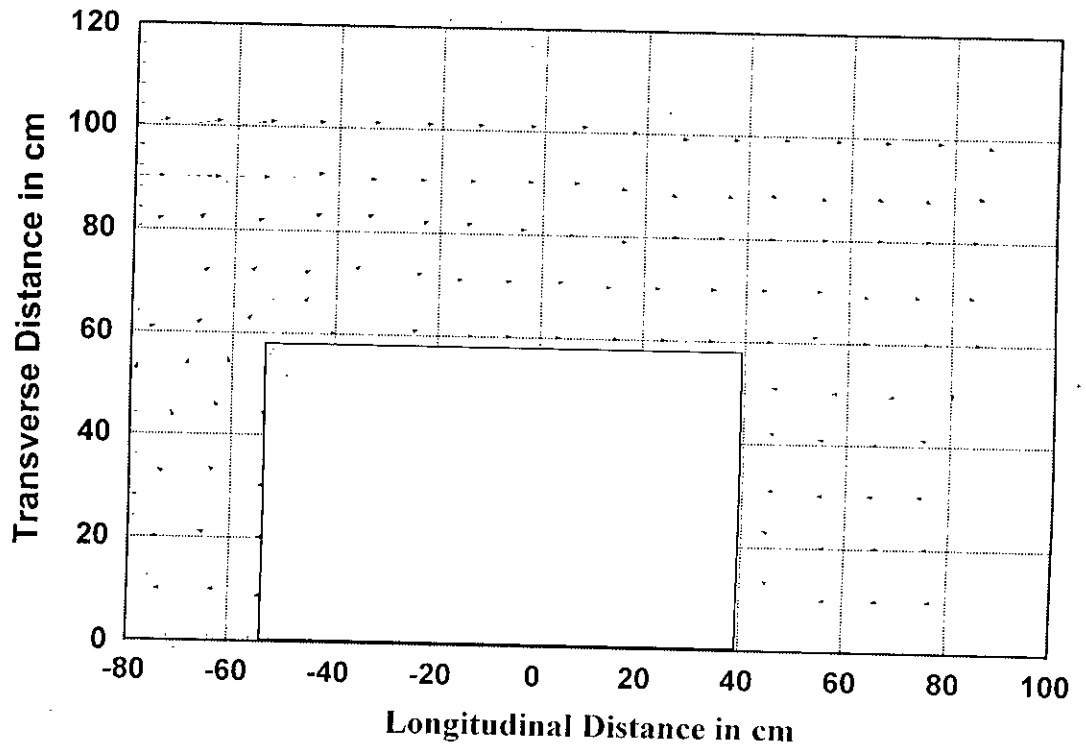


Fig: 3.22 Velocity Vector for 1:2 Slope Structure

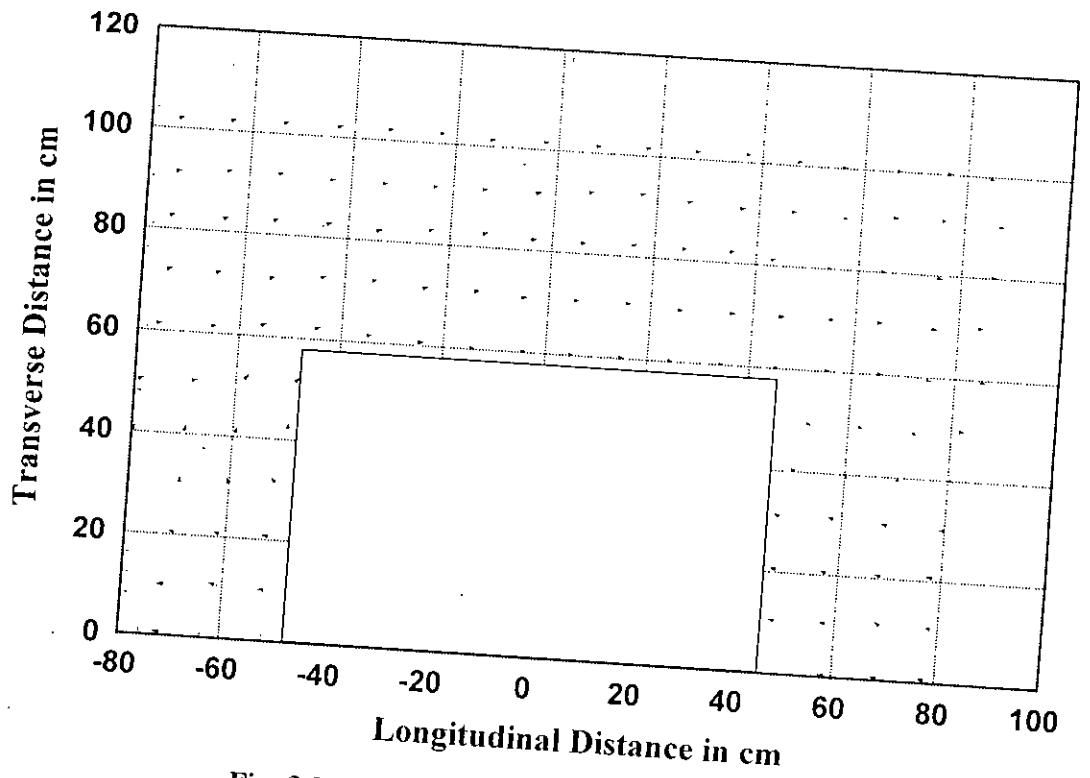


Fig: 3.23 Velocity Vector for 1:3 Slope Structure

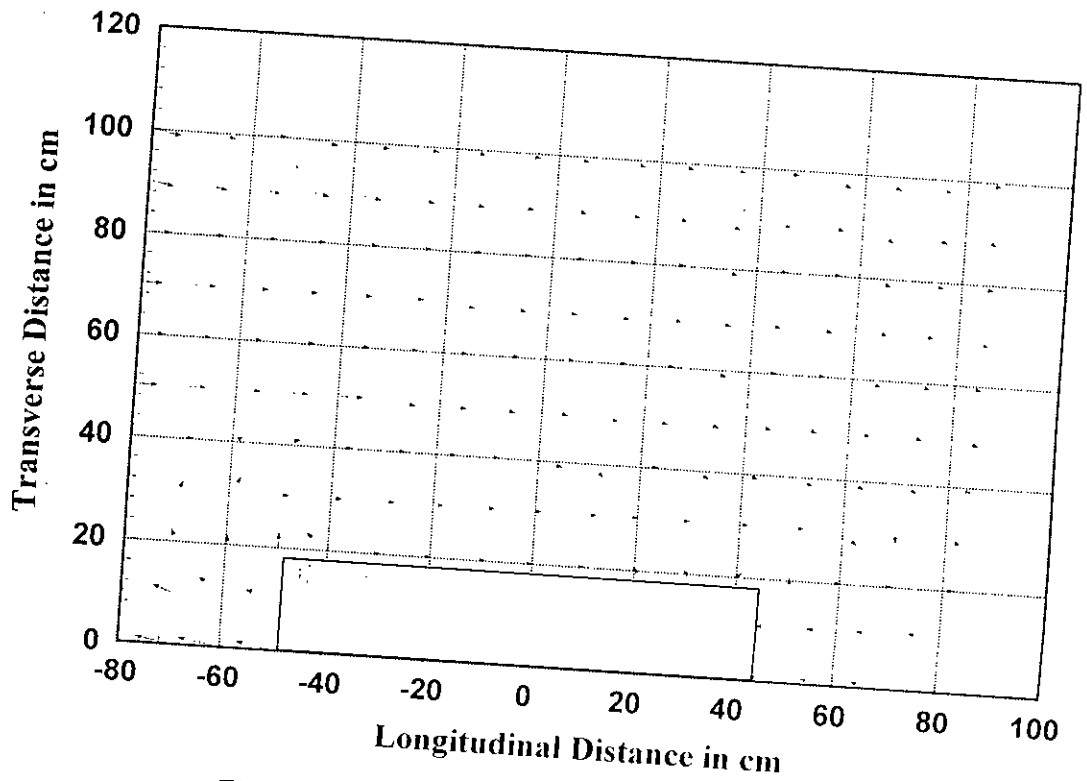


Fig: 3.24 Velocity Vector for 20cm wide Structure

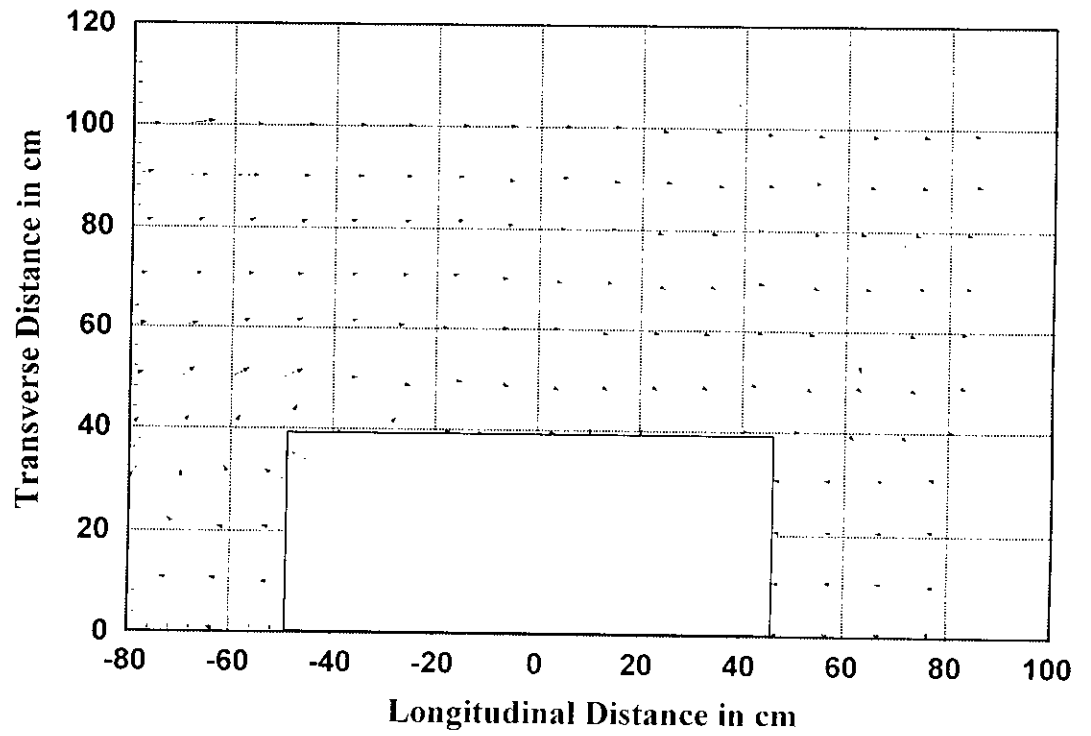


Fig: 3.25 Velocity Vector for 40cm wide Structure

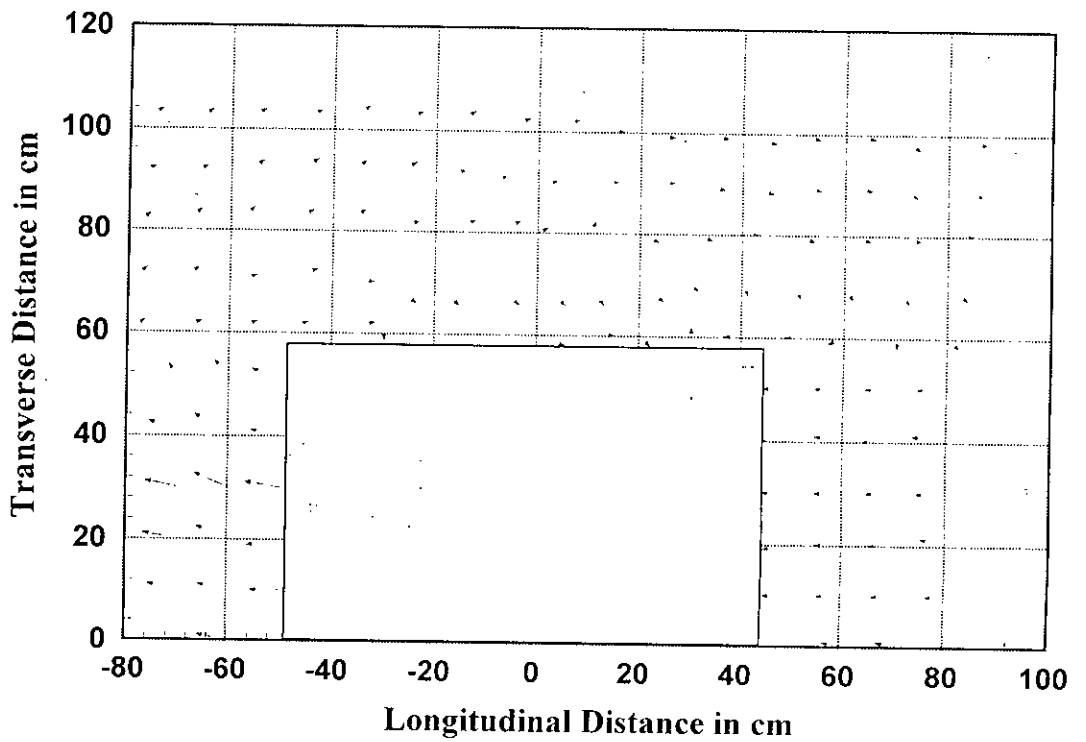


Fig: 3.26 Velocity Vector for 60cm wide Structure

Vertical Flow Direction of structure with 1V:1H slope

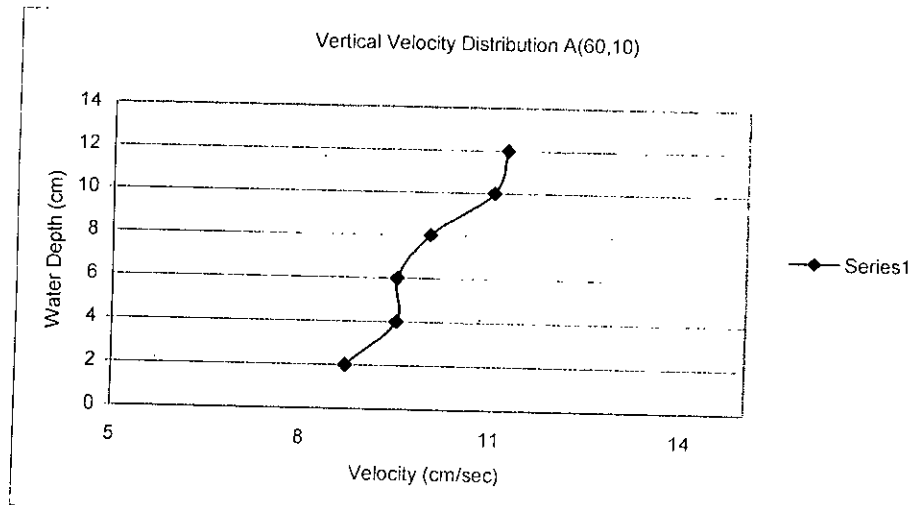
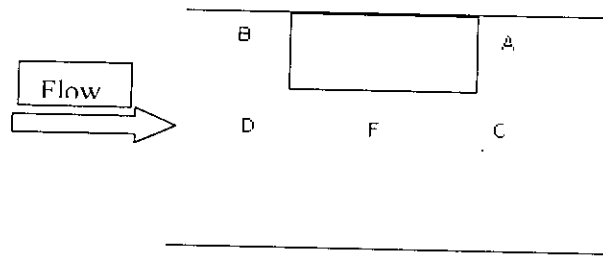


Fig. 3.27 Vertical Velocity Distribution at point 'A' of the structure

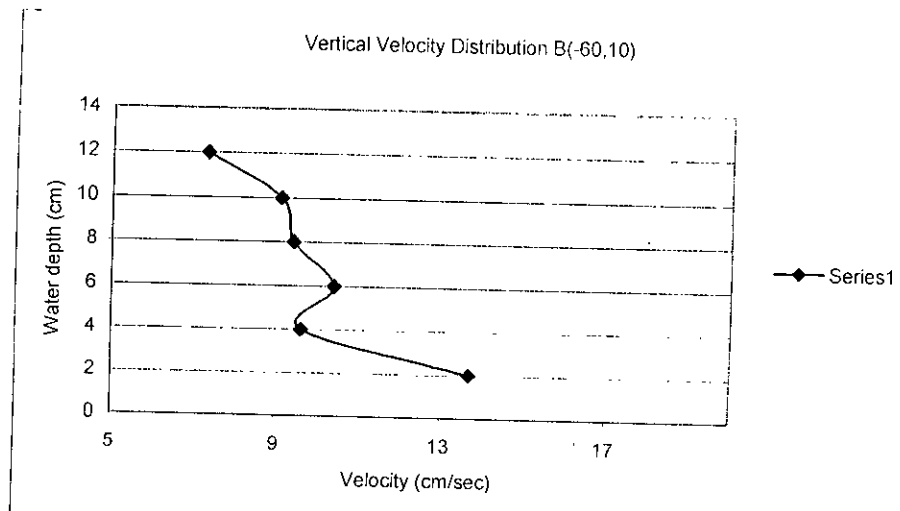


Fig. 3.28 Vertical Velocity Distribution at point 'B' of the structure

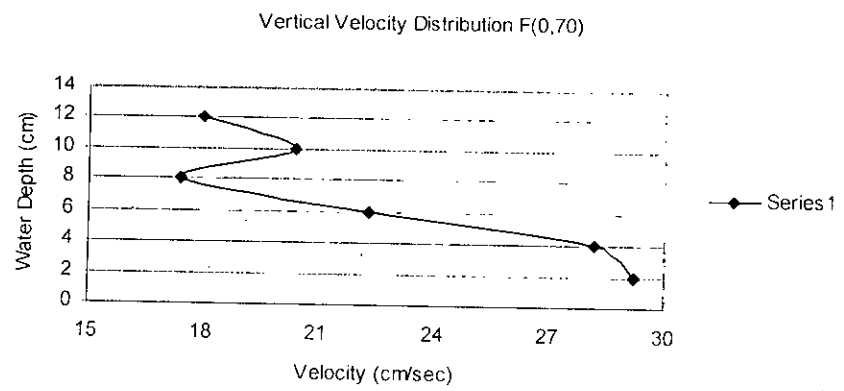


Fig. 3.29 Vertical Velocity Distribution at point 'F' of the structure

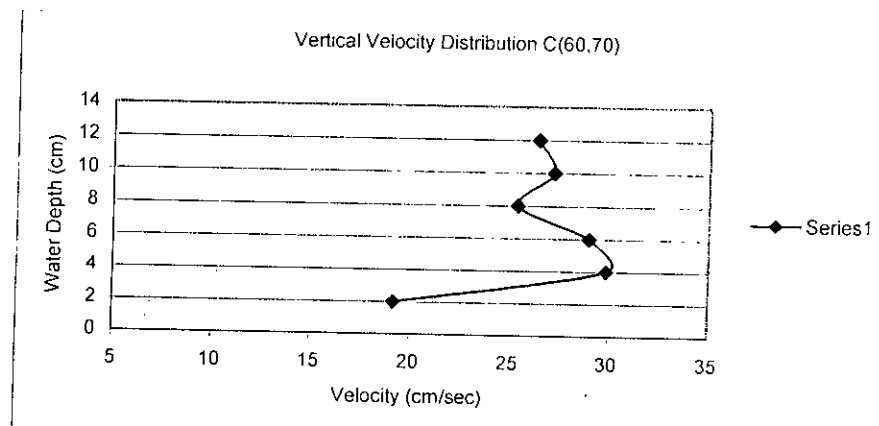


Fig. 3.30 Vertical Velocity Distribution at point 'C' of the structure

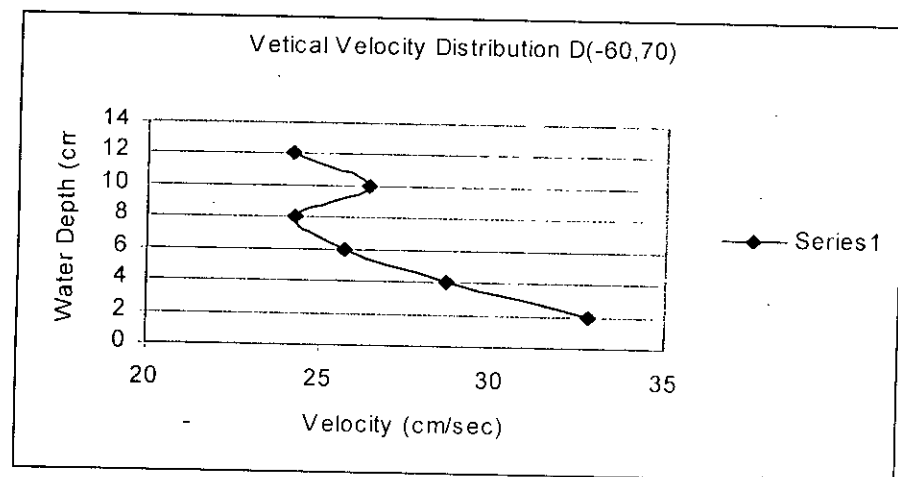
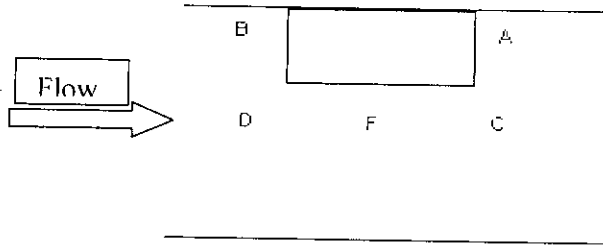


Fig. 3.31 Vertical Velocity Distribution at point 'D' of the structure

Vertical Flow Direction of structure with 1V:2H slope



Vertical velocity Distribution A(60,10)

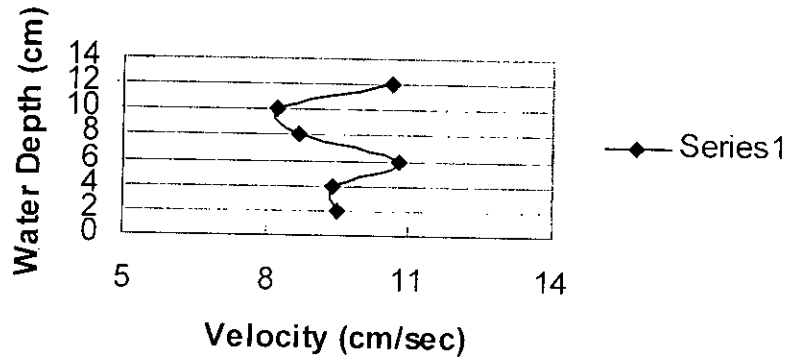


Fig. 3.32 Vertical Velocity Distribution at point 'A' of the structure

Vertical Velocity Distribution B(-60,10)

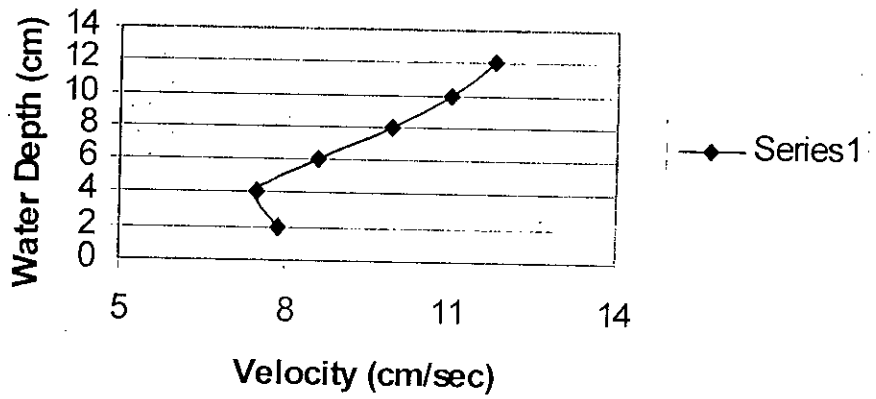


Fig. 3.33 Vertical Velocity Distribution at point 'B' of the structure

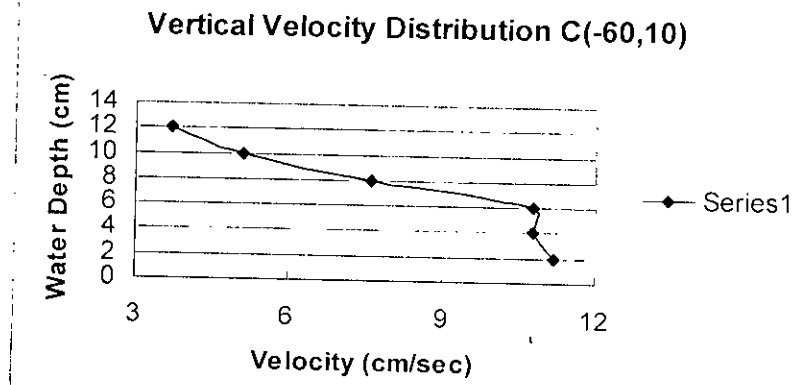


Fig. 3.34 Vertical Velocity Distribution at point 'C' of the structure

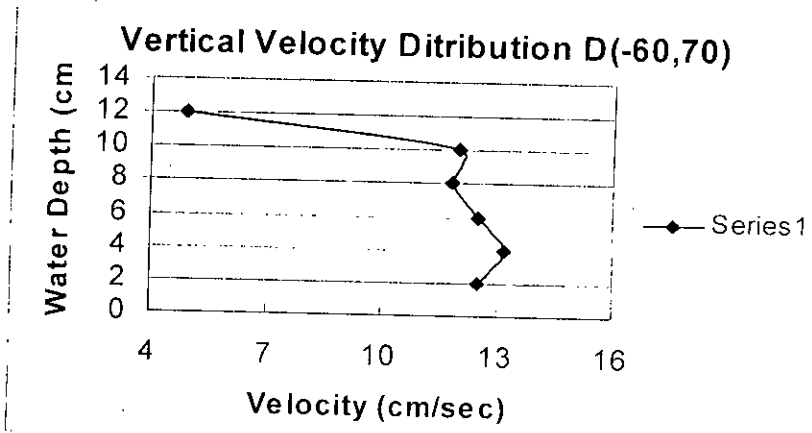


Fig. 3.35 Vertical Velocity Distribution at point 'D' of the structure

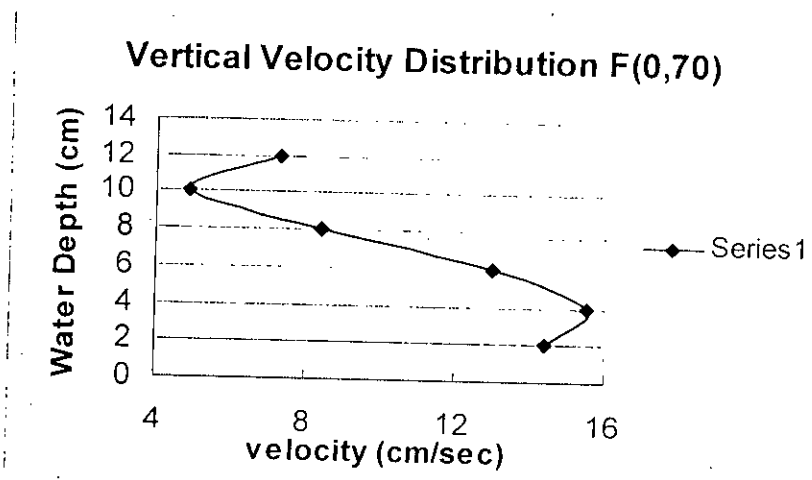


Fig. 3.36 Vertical Velocity Distribution at point 'F' of the structure

Vertical Flow Direction of structure with 1V:3H slope

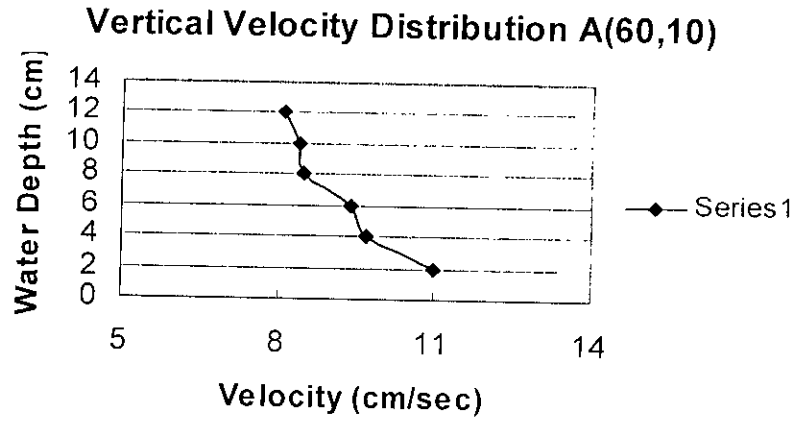
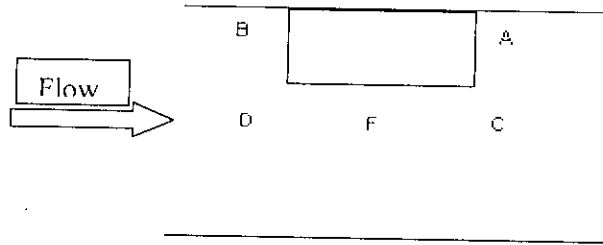


Fig. 3.37 Vertical Velocity Distribution at point 'A' of the structure

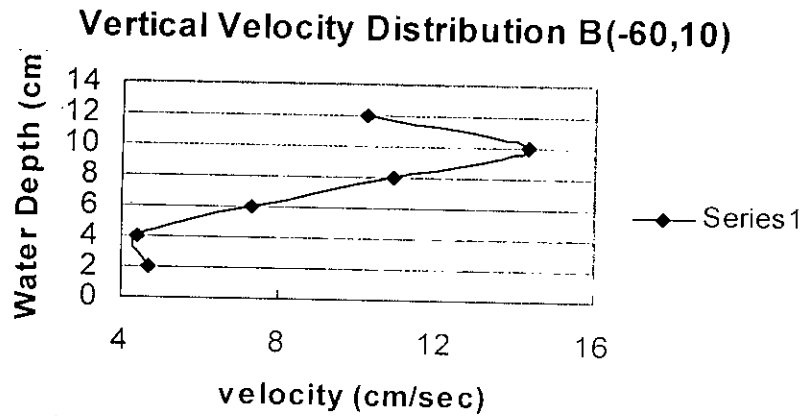


Fig. 3.38 Vertical Velocity Distribution at point 'B' of the structure

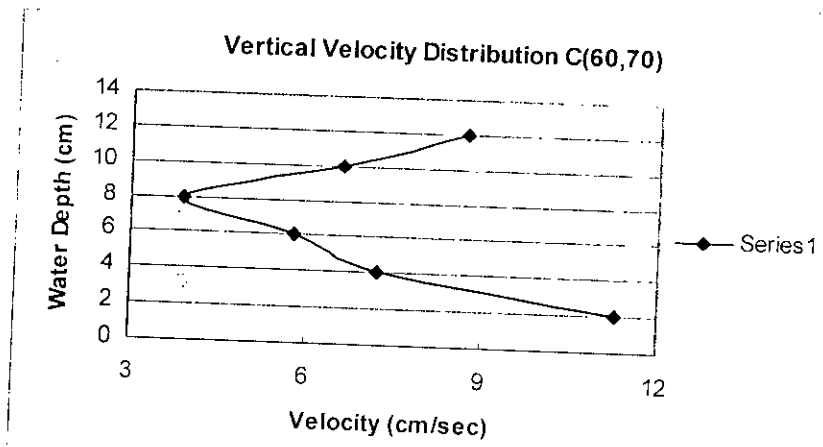


Fig. 3.39 Vertical Velocity Distribution at point 'C' of the structure

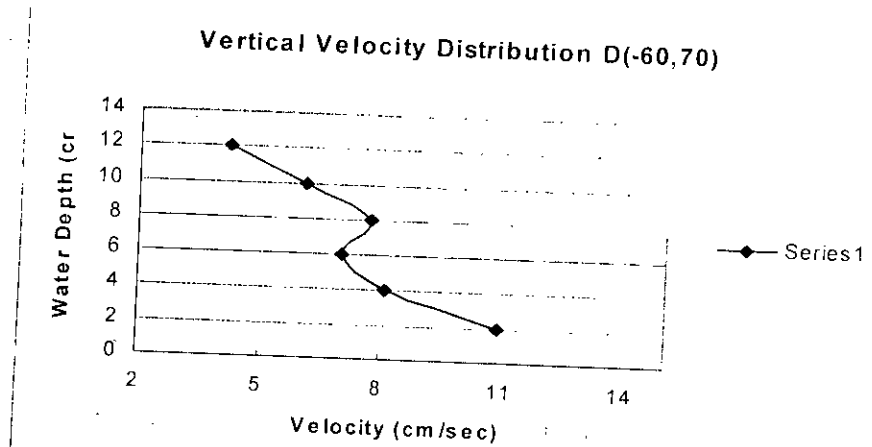


Fig. 3.40 Vertical Velocity Distribution at point 'D' of the structure

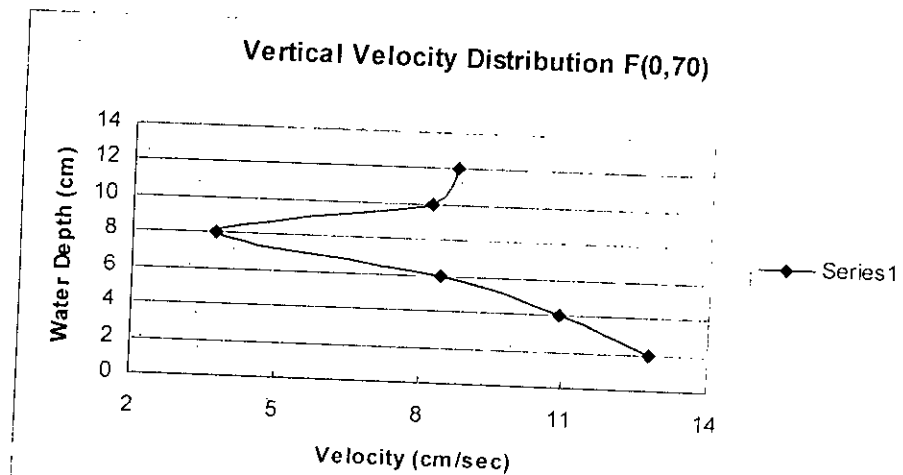


Fig. 3.41 Vertical Velocity Distribution at point 'F' of the structure

Vertical Flow Direction of vertical structure, $b=60\text{cm}$

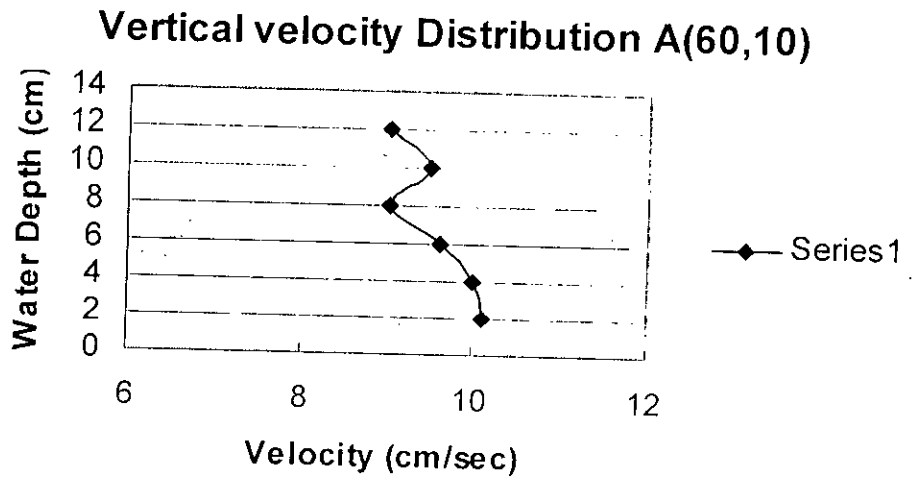
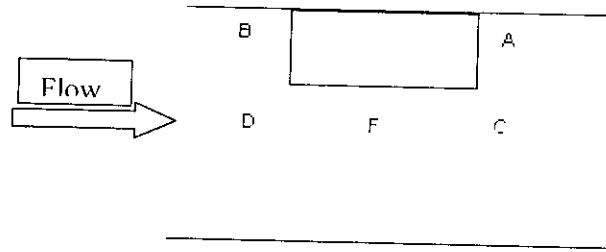


Fig. 3.42 Vertical Velocity Distribution at point 'A' of the structure

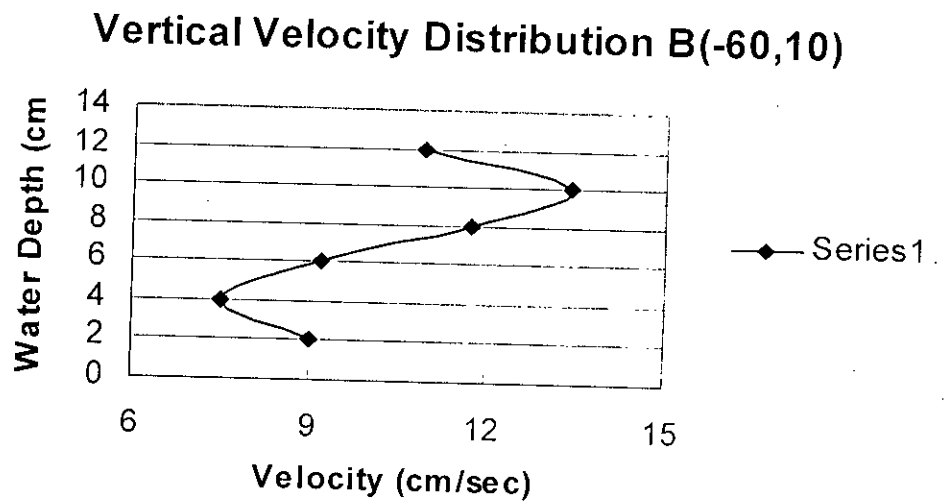


Fig. 3.43 Vertical Velocity Distribution at point 'B' of the structure

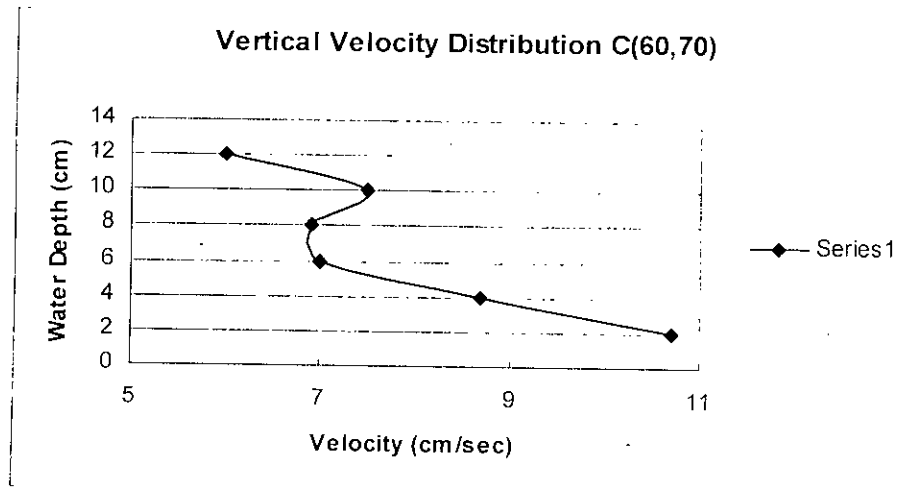


Fig. 3.44 Vertical Velocity Distribution at point 'C' of the structure

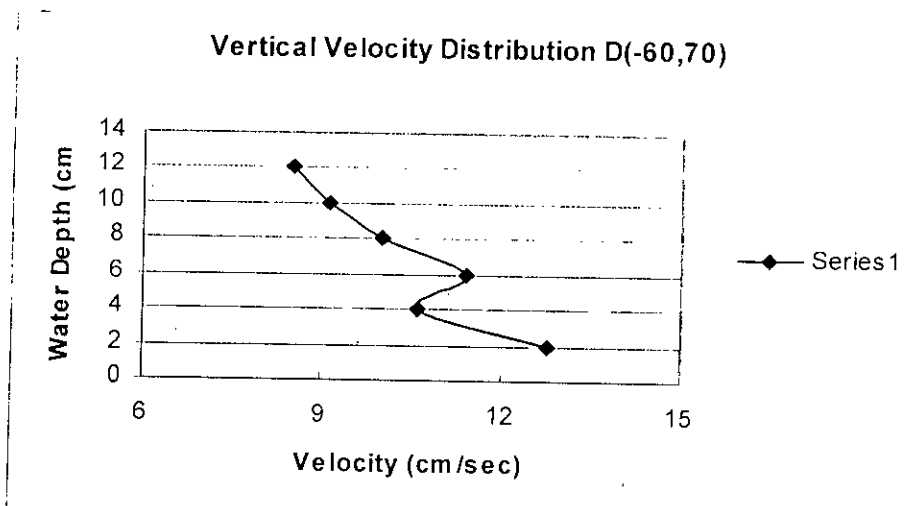


Fig. 3.45 Vertical Velocity Distribution at point 'D' of the structure

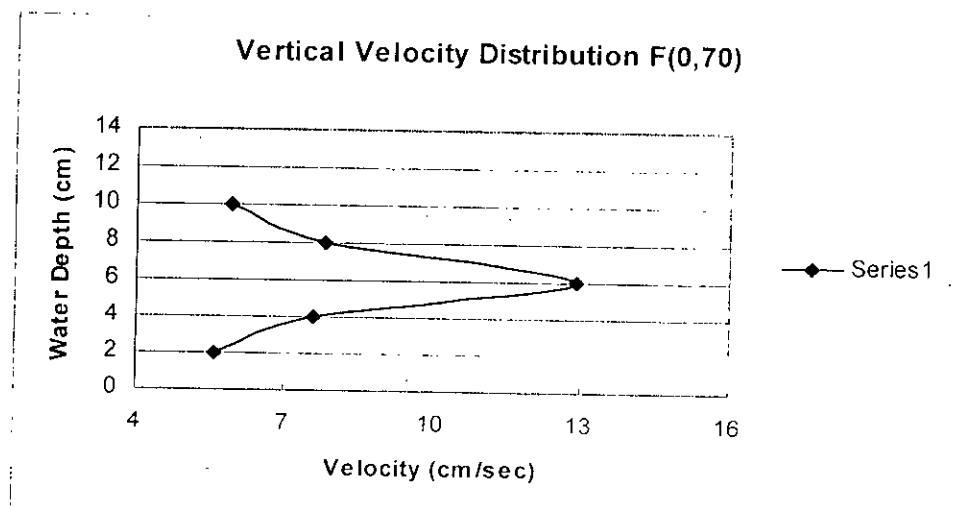
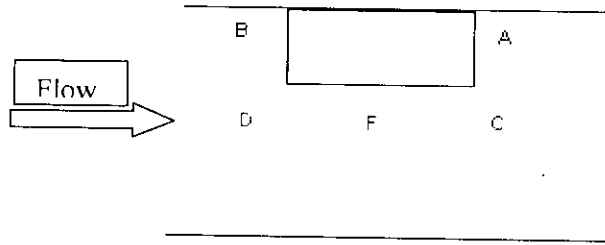


Fig. 3.46 Vertical Velocity Distribution at point 'F' of the structure

Vertical Flow Direction of vertical structure, $b=40\text{cm}$



98300

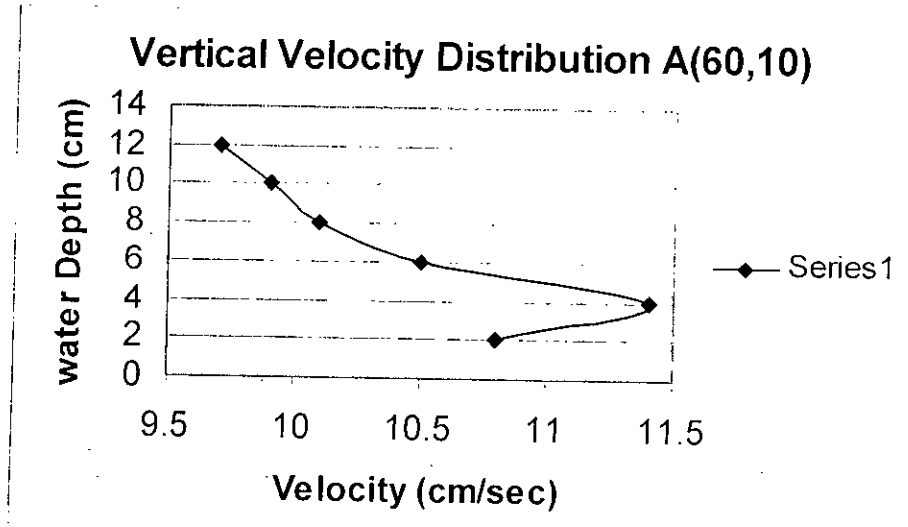


Fig. 3.47 Vertical Velocity Distribution at point 'A' of the structure

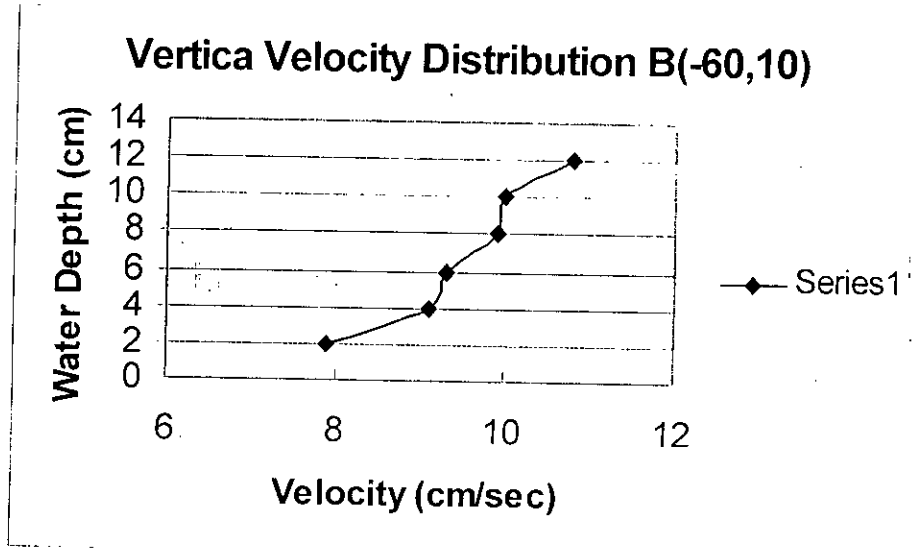


Fig. 3.48 Vertical Velocity Distribution at point 'B' of the structure

Vertical Velocity Distribution C(60,50)

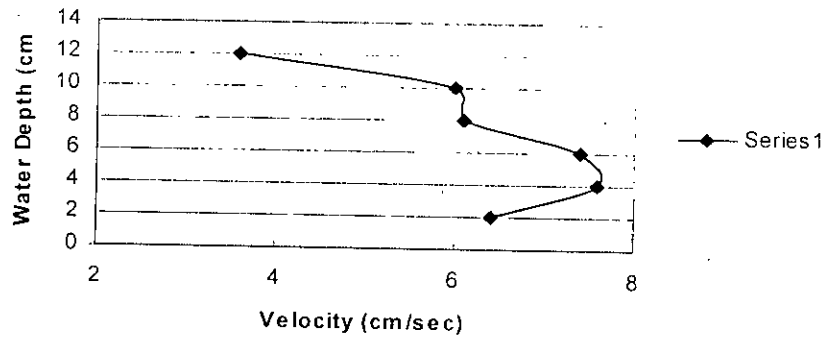


Fig. 3.49 Vertical Velocity Distribution at point 'C' of the structure

Vertical Velocity Distribution D(-60,50)

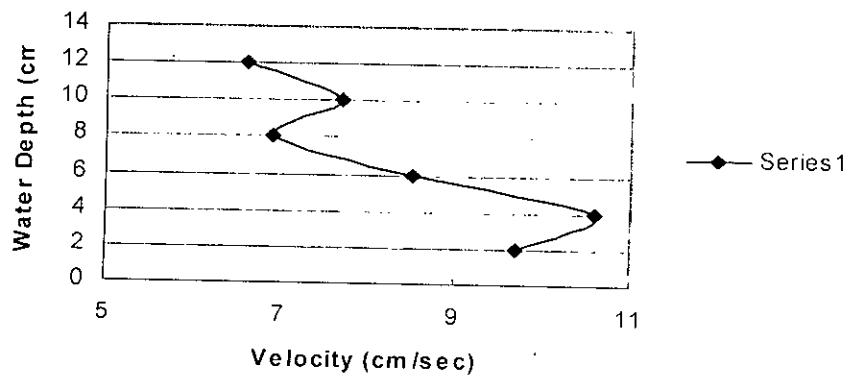


Fig. 3.50 Vertical Velocity Distribution at point 'D' of the structure

Vertical Velocity Distribution F(0,50)

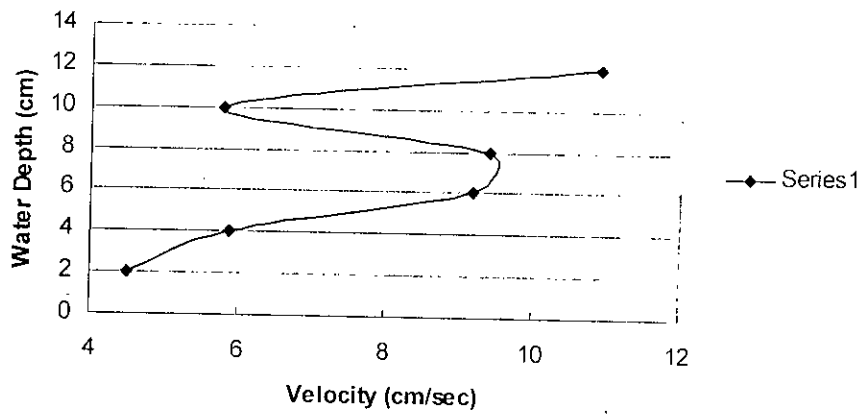
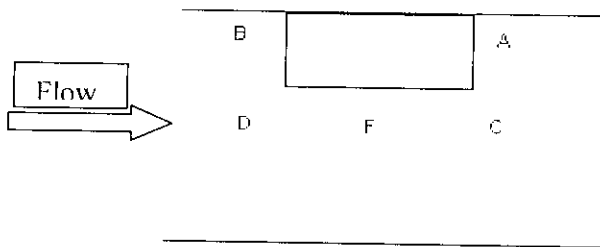


Fig. 3.51 Vertical Velocity Distribution at point 'F' of the structure

Vertical Flow Direction of vertical structure, b=20cm



Vertical Velocity Distribution A(60,10)

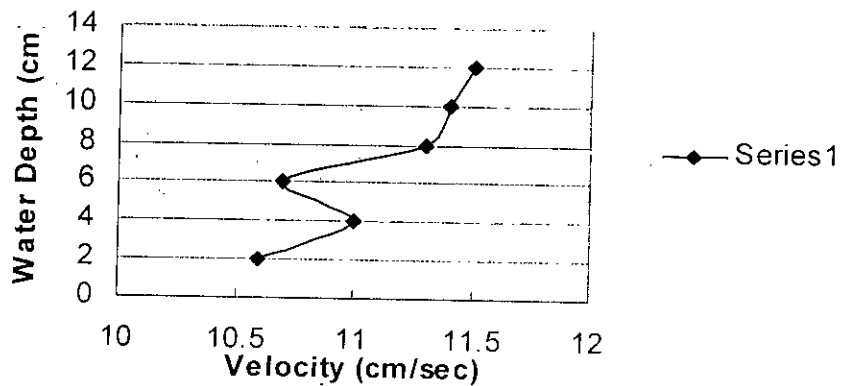


Fig. 3.52 Vertical Velocity Distribution at point 'A' of the structure

Vertical Velocity Distribution B(-60,10)

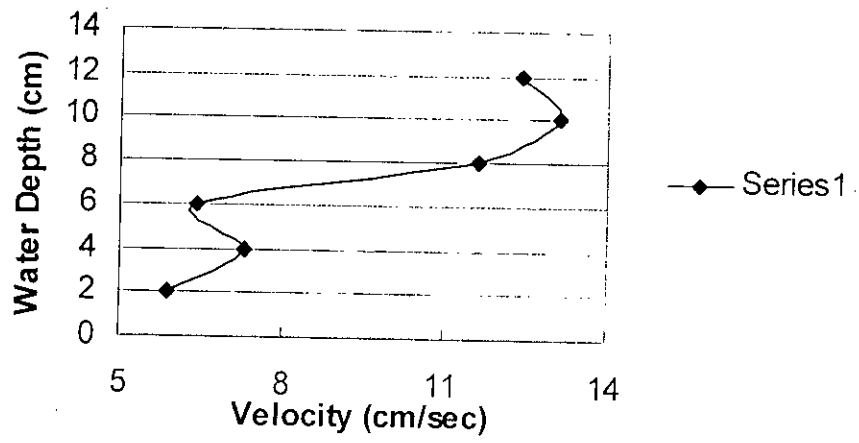


Fig. 3.53 Vertical Velocity Distribution at point 'B' of the structure

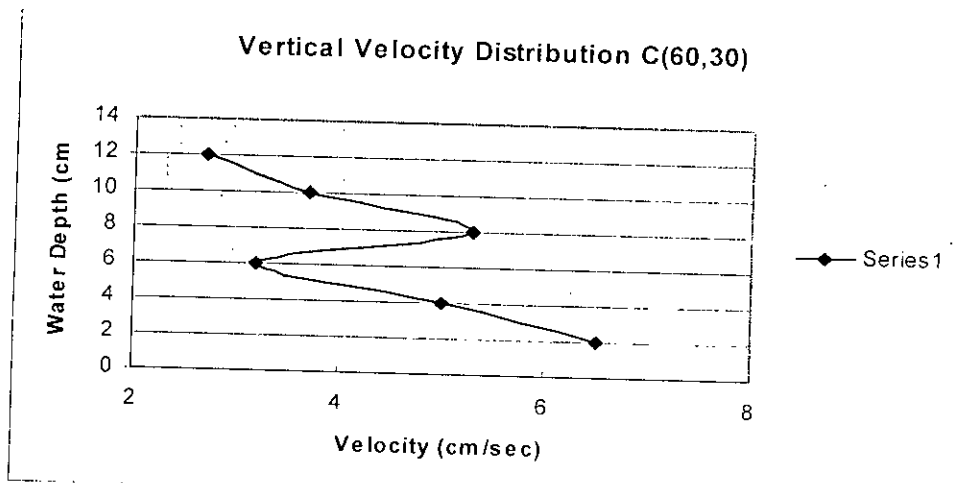


Fig. 3.54 Vertical Velocity Distribution at point 'C' of the structure

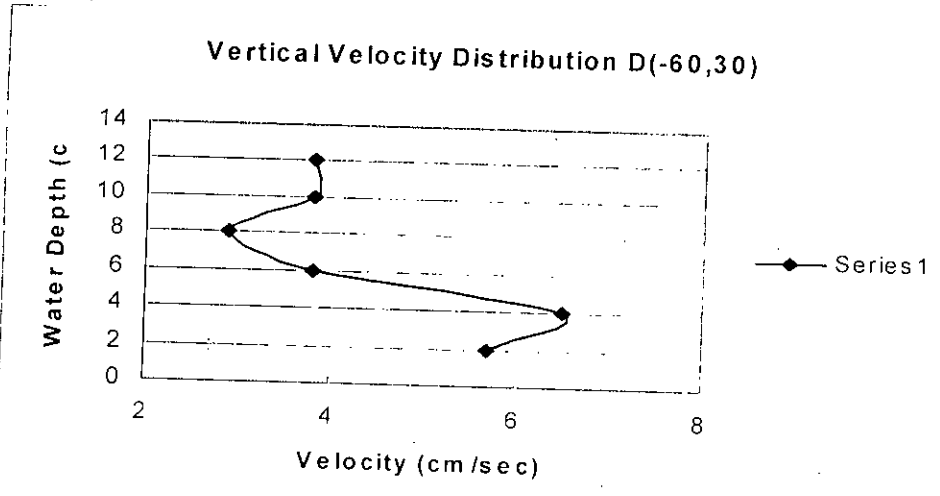


Fig. 3.55 Vertical Velocity Distribution at point 'D' of the structure

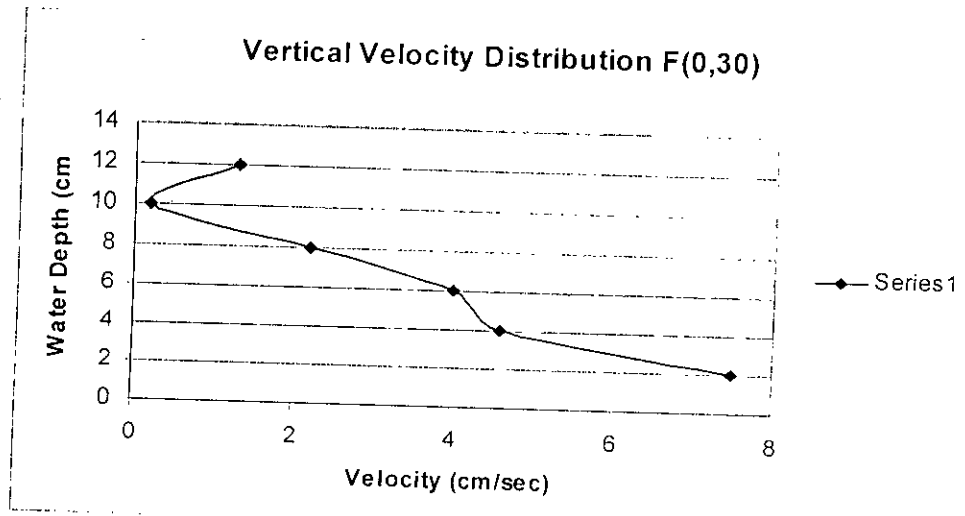


Fig. 3.56 Vertical Velocity Distribution at point 'F' of the structure

3.4 Methodology of Experiment

At the very beginning of the experiment, the channel bed was prepared with fine sand, compaction of the bed occurs promptly with the presence of water over it. Both side of the channel was marked by white color with 1m interval. The slope/vertical structure was placed at the middle of right bank of the channel. The channel was backfilled with water through pipe, then the pump was switched on and the discharge was controlled by gate valve. A calibrated Rehbok weir set at the exit channel was used for measuring discharge. After setting the discharge, the depth of flow was adjusted to the desire level by tail gate. Velocity measurement was started at about three hours from the commencement of run. Bed profile was noted after every two hours.

The pump was turned off after seven hours of flow. After the end of run, the channel bed was dried off and the point gauge reading were collected. Photographs of the bed forms along with the scour hole was also taken.

CHAPTER 4

RESULTS AND DISCUSSION

4.1 Shape / Slope Factor

The relation between scour depth, water depth and flow restriction was analyzed. The scour depth analysis was performed by plotting ds/h values against b/h values. The result was compared with the curves of modified Lacey (1930), Melville (1992), Rahman and Muramoto (1999) and Liu et al. (1961). The plots are shown in Fig. 4.1 to 4.4.

For sloping wall structure, the experimental data of the present study were close to the Lacey's curve. But none data were very close to any curve. The values of ds/h were much higher than the experimental value. However, only the data for 1V: 1H and 1V: 3H slope is consistent with Lacey's curve. For vertical-wall structure, the experimental data of the present study were close to Lacey's curve. The structure of width 60cm is consistent with Lacey's curve.

For the cases of sloping abutment, the experimental data were not consistent with the curves except for slope 1V: 1H. There may be two reasons for this. First, the experiments were not run up to the equilibrium time. Second, the shape factors considered in the formulae were not correct enough for the structures used in the study. Where as, the structures used here were of different type. However, for the present experiment shape factor could not be studied, as the equilibrium depth was not reached.

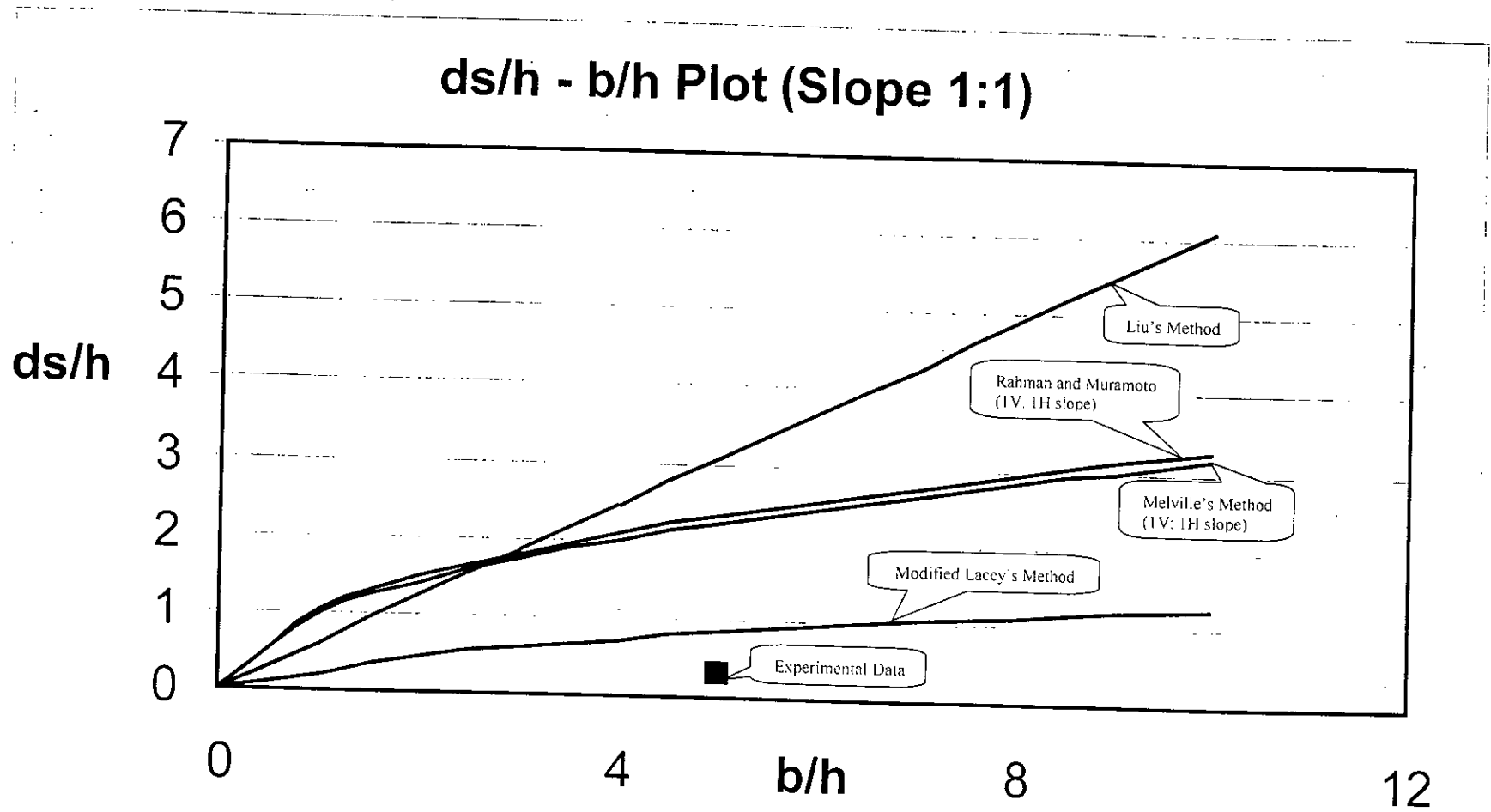


Fig. 4.1 Comparison of experimental Data with curves

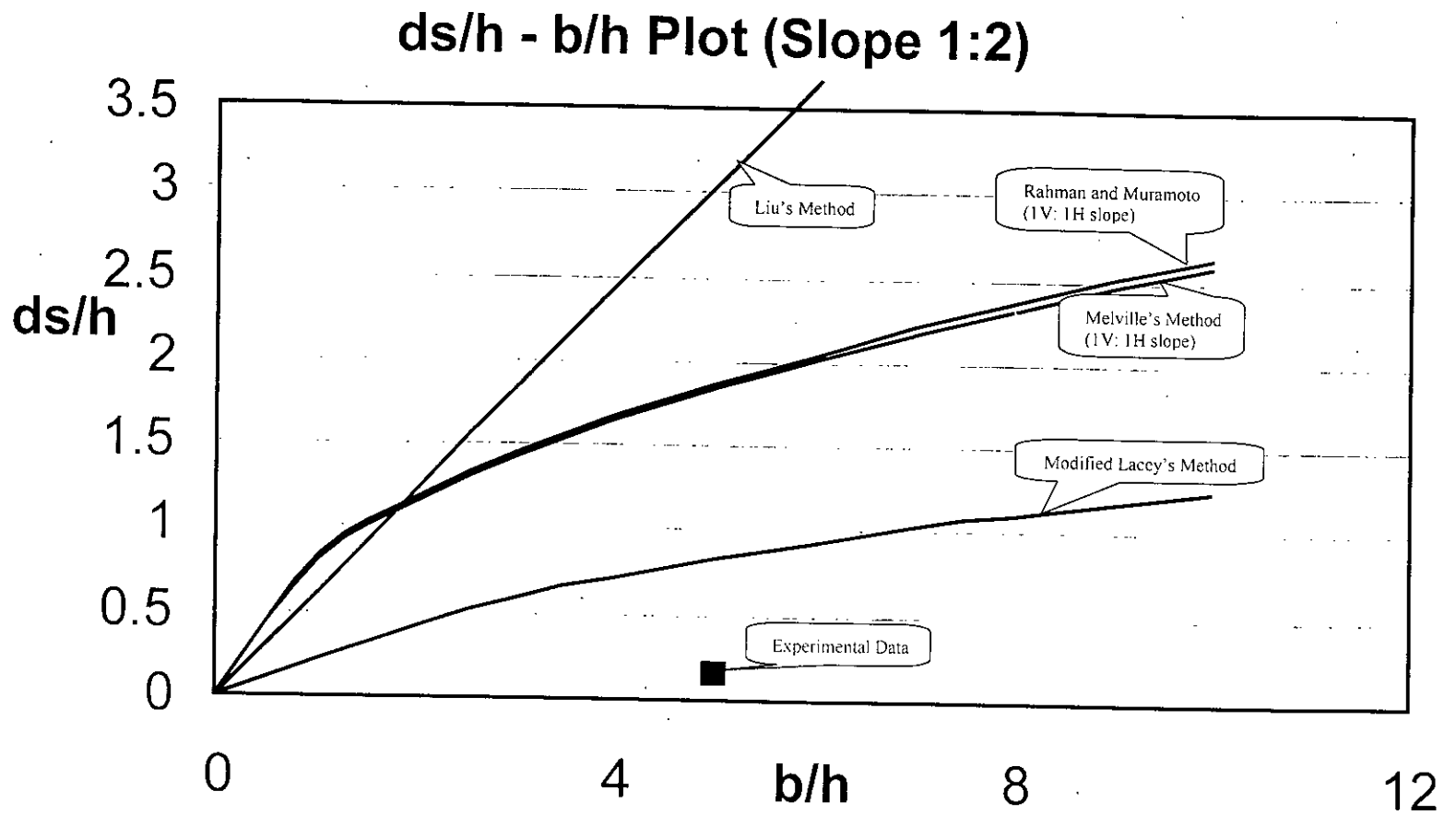


Fig. Comparison of Experimental data with curves

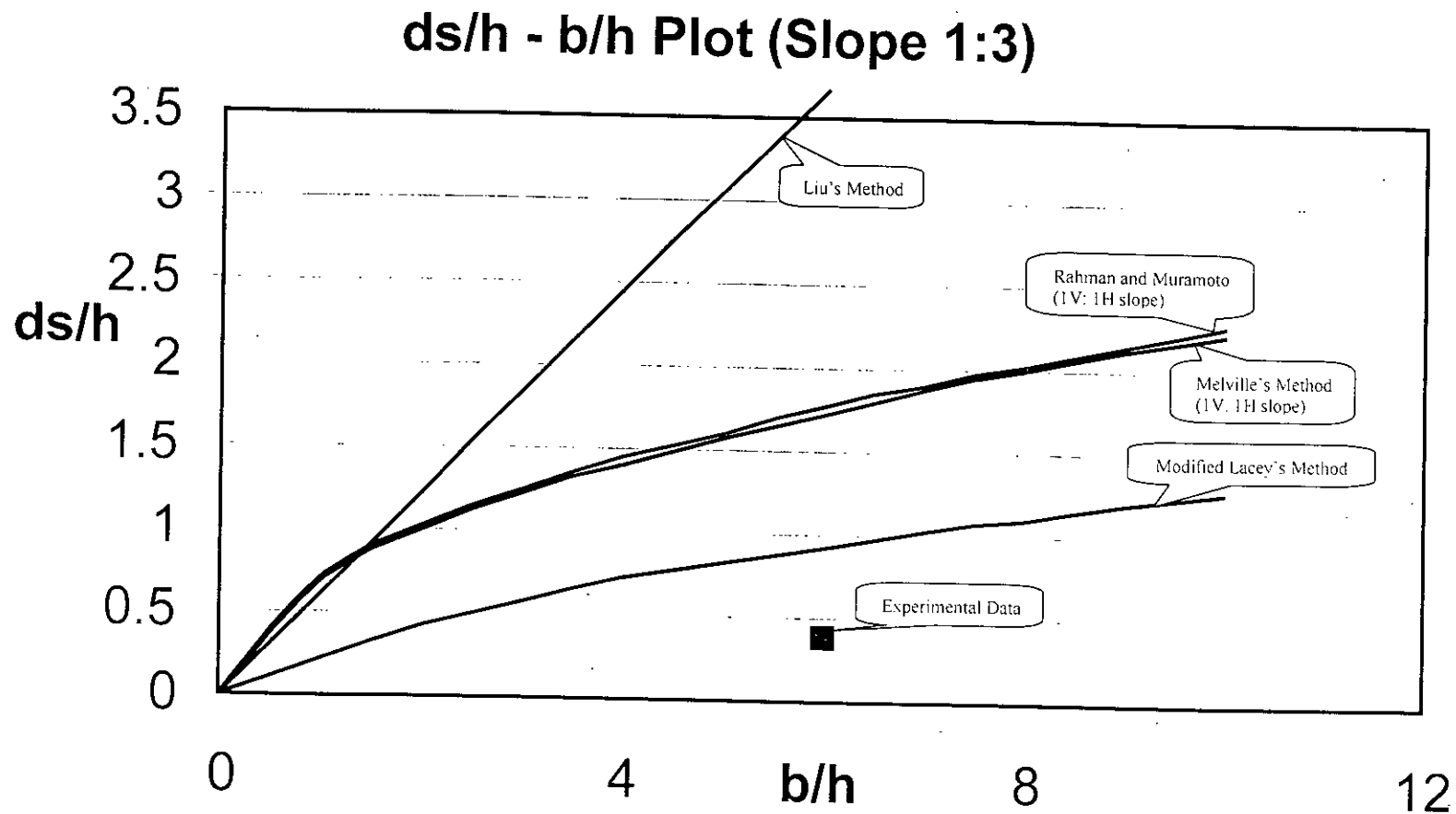


Fig. 4.3 Comparison of Experimental Data with Curves

ds/h - b/h Plot (Vertical)

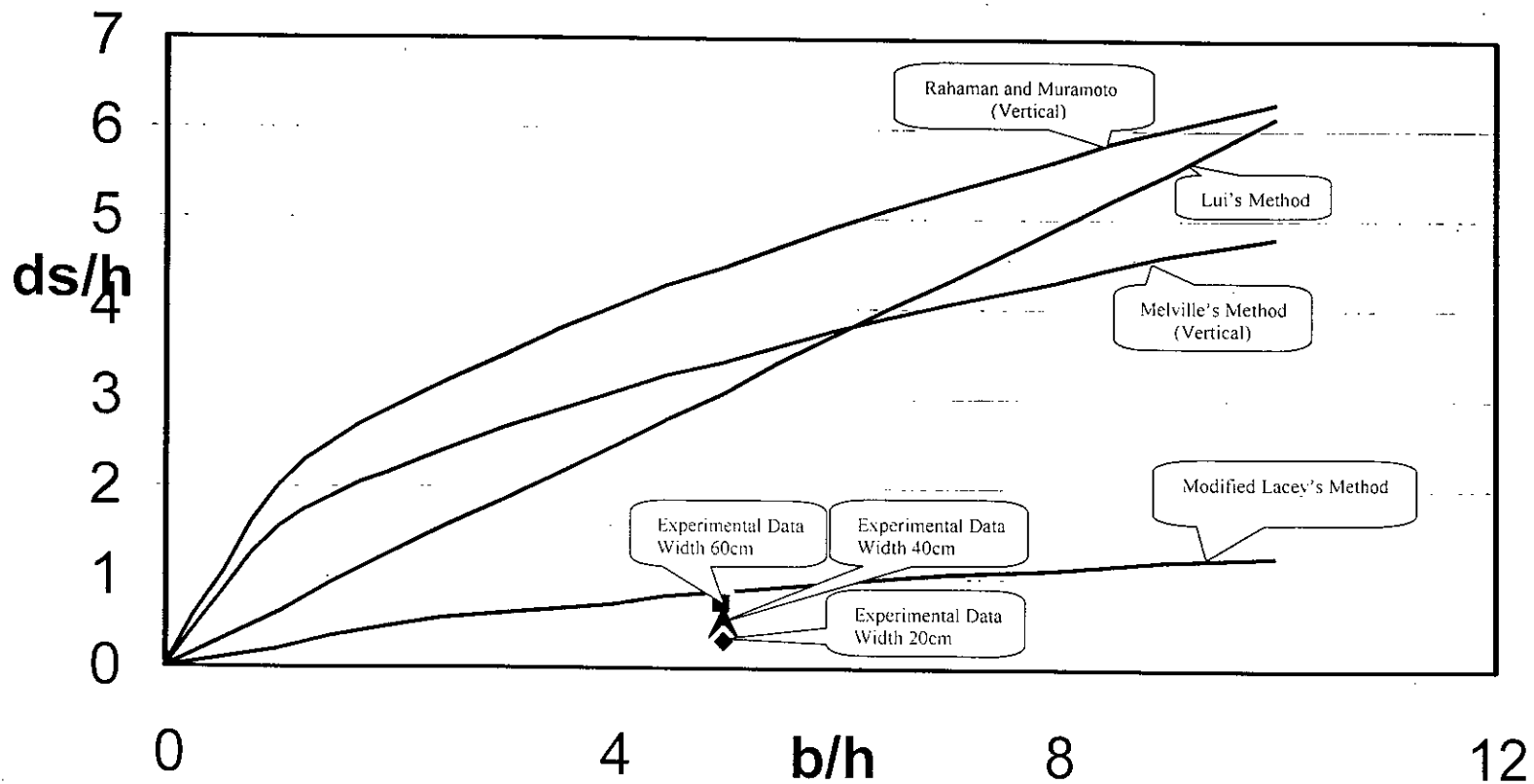


Fig. 4.4 Comparison of Experimental Data with Curve

Table 4.1 Comparison of scour depth with experimented value and equation's value.

Experimented structure	Equation	Equation value(cm)	Experiment value(cm)
Sloping wall 1V: 1H	Lacey	9.9	3.7
	Melville	26.83	
	Rahaman and Muramoto	27.8	
	Liu et al.	36.75	
Sloping wall 1V: 2H	Lacey	9.9	1.7
	Melville	22.05	
	Rahaman and Muramoto	22.43	
	Liu et al.	36.75	
Sloping wall 1V: 3H	Lacey	9.99	4.6
	Melville	18.94	
	Rahaman and Muramoto	30.48	
	Liu et al.	36.75	
Vertical wall	Lacey	9.99	8.5 (b=60cm) 6.3 (b=40cm) 4.6 (b=20cm)
	Melville	40.92	
	Rahaman and Muramoto	53.64	
	Liu et al.	36.75	

4.2 Scour Profile Variation

The longitudinal and lateral scour profiles were shown in chapter 3 (Fig. 3.15 to 3.18). In analyzing these profiles, it was found that, for slope-wall structures, as the slope increased the scour depth also increased at the toe of u/s side at longitudinal direction. But at d/s side lower slope structure shown higher scour. This was the same for lateral direction, as the slopes increased the scour depth also increased but scour length of structure 1V:3H has shown higher than others.

On the other hand, for vertical-wall structure as the flow restriction width, if b increased the scour depth also increased. The effect of the structure b=20cm was negligible than other two structure. This is logical, as due to increased of b, flow concentration or velocity also increased. Therefore, the scour depth increased. The comparisons of scour profile in longitudinal and lateral direction are shown in Fig 4.5 to 4.8.

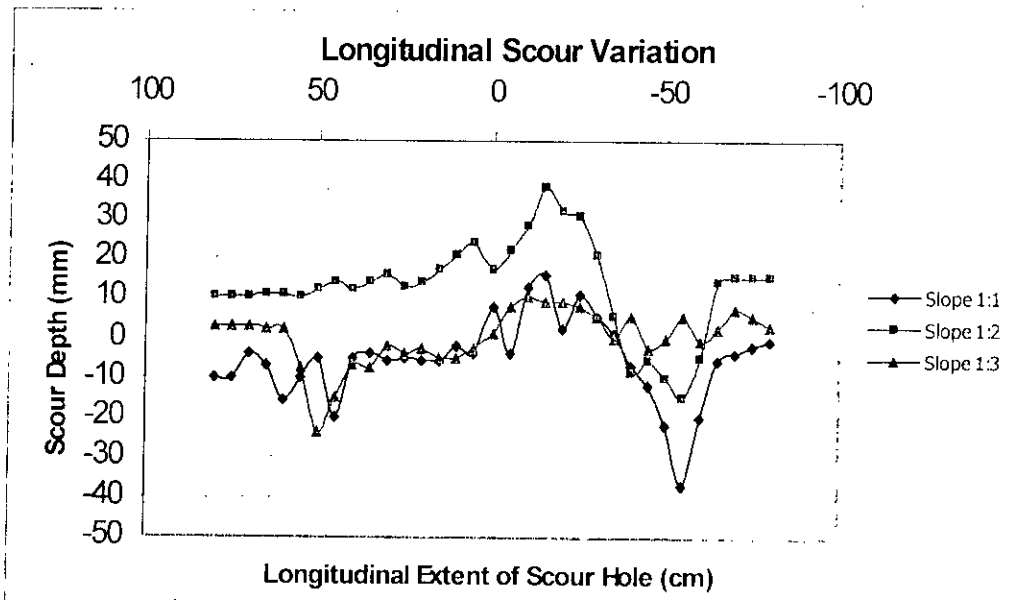


Fig. 4.5 Longitudinal scour variation for sloping-wall Structures

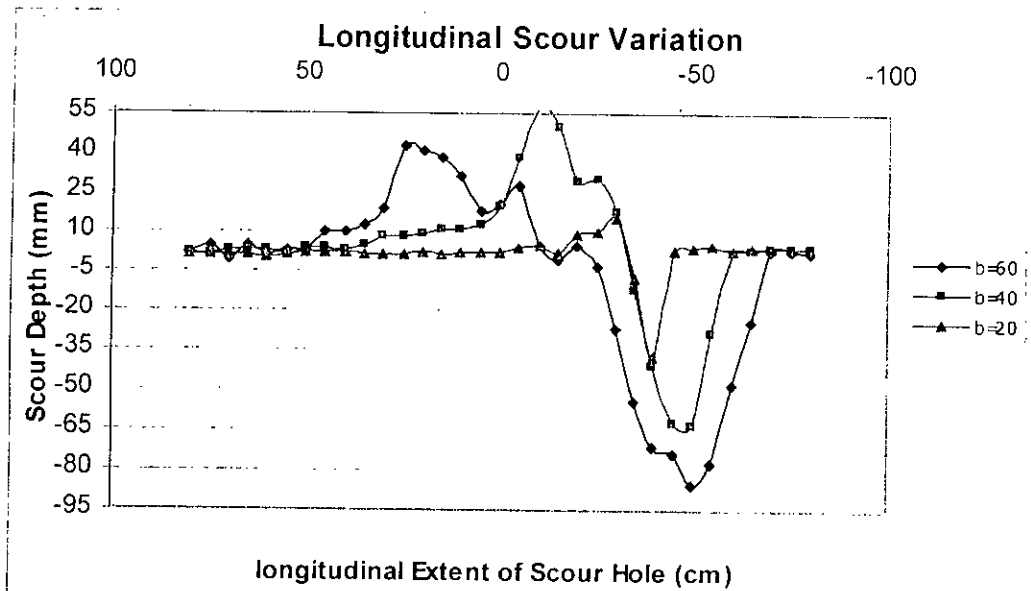


Fig. 4.6 Longitudinal scour variation for vertical-wall structures

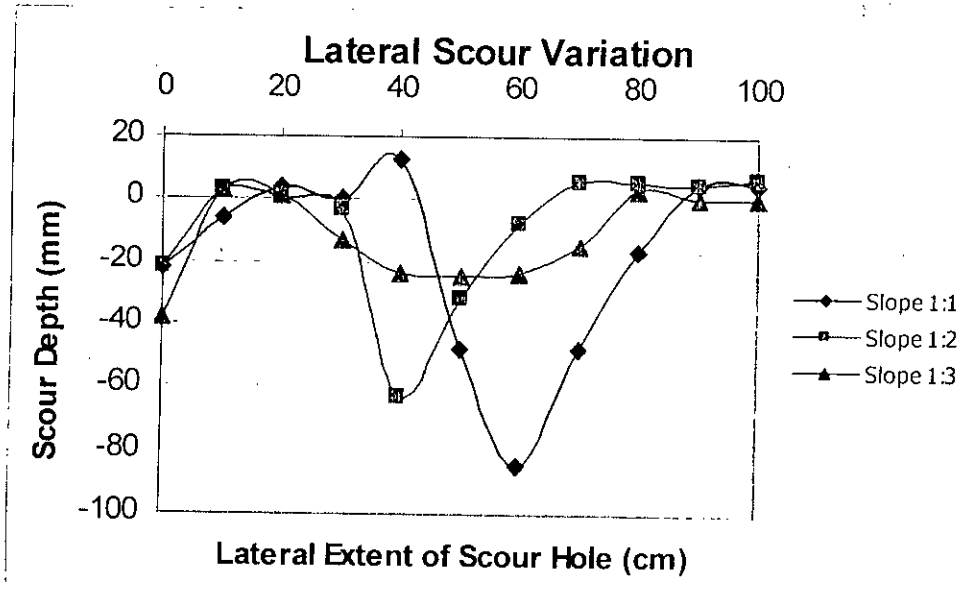


Fig. 4.7 Lateral scour variation for sloping-wall structures

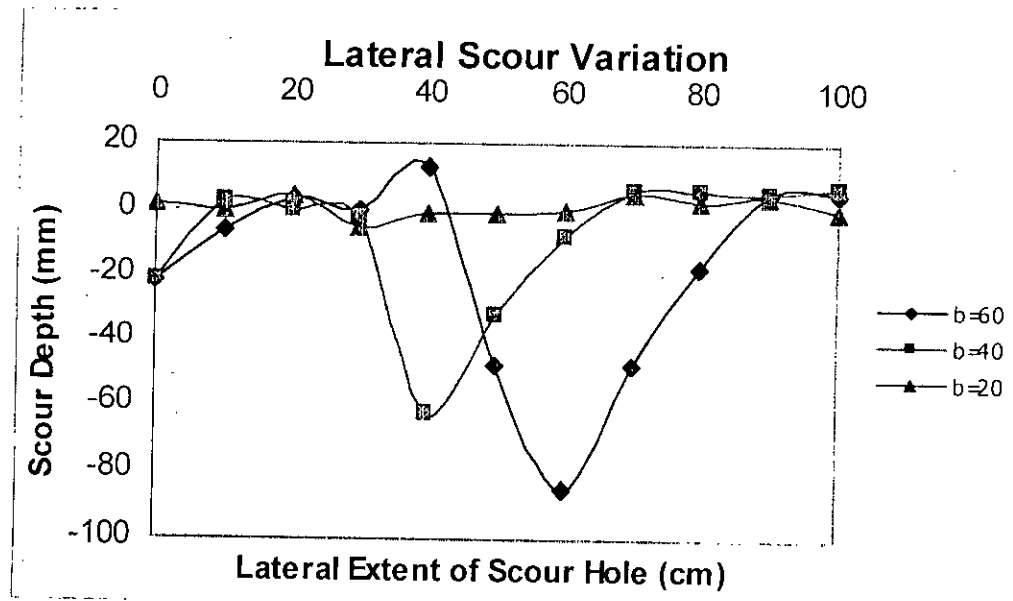


Fig. 4.8 Lateral scour variation for vertical-wall structures

4.2 Scour Area and Characteristics

This discussion is based on the observation made during the study explained in chapter 3. The scour area was measured by scale around the structure by grid formation. For vertical type structure it was seen that the scour area increased with the increasing of flow restriction width. On the other hand, for sloping structure the scour area decreased with increasing slope.

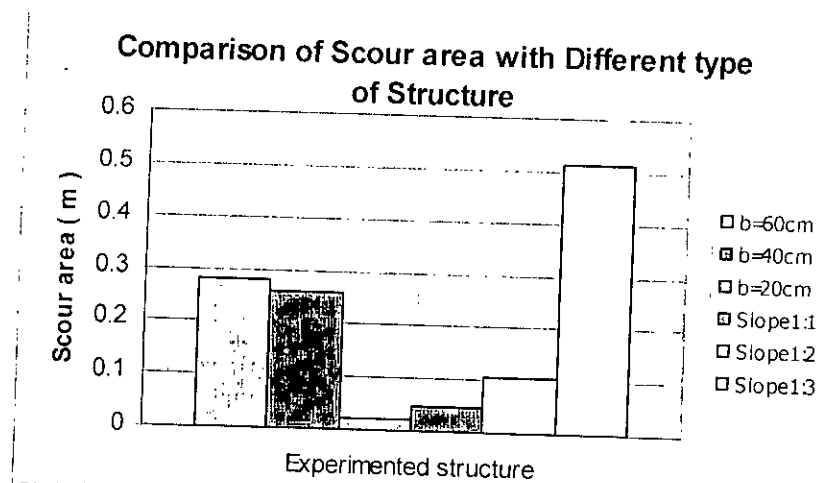


Fig. 4.9 Scour area of different structures

From the photographs of the structures taken at the end of each run, it was seen that for IV: 1H slope structure the scour effect was around at the u/s toe of the structure and there was no noticeable effect of scour at d/s side. But for IV: 2H and IV: 3H structures the scour area increased diagonally and there was noticeable scour hole at the d/s side for IV: 3H structure.

For vertical type structure, it was seen that for 20cm flow restriction width there was no effect of scour at d/s side. But with increasing this width, the scour effect was noticed at d/s side and increased diagonally.

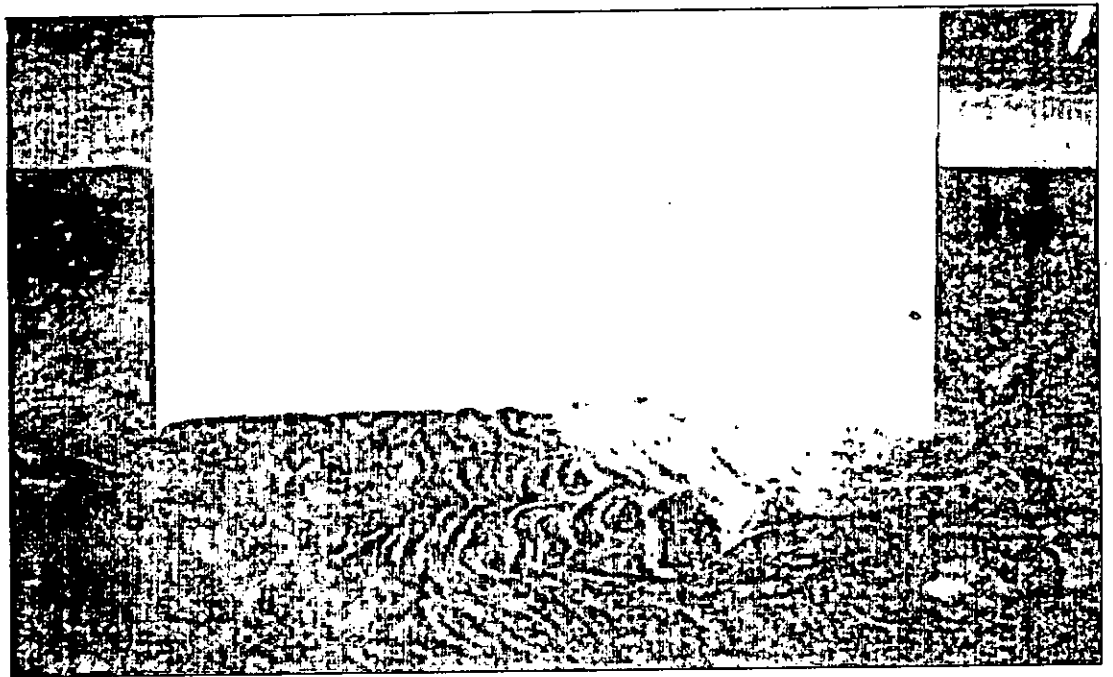
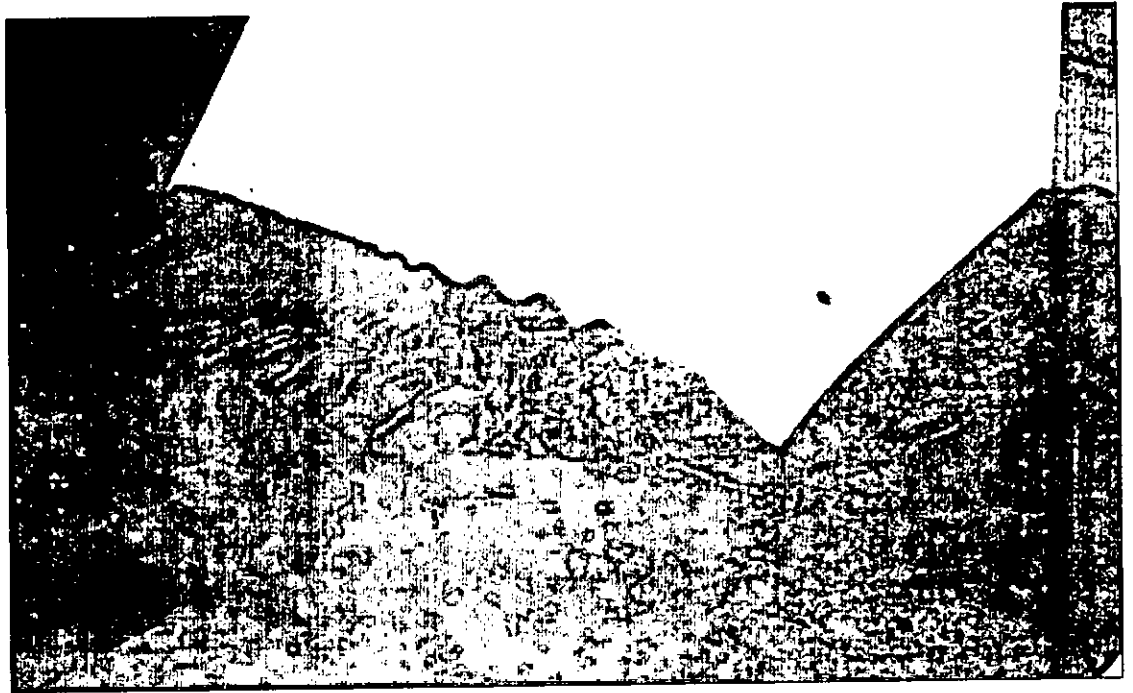


Fig. 4. 10 Scour around the IV: IH slope structure

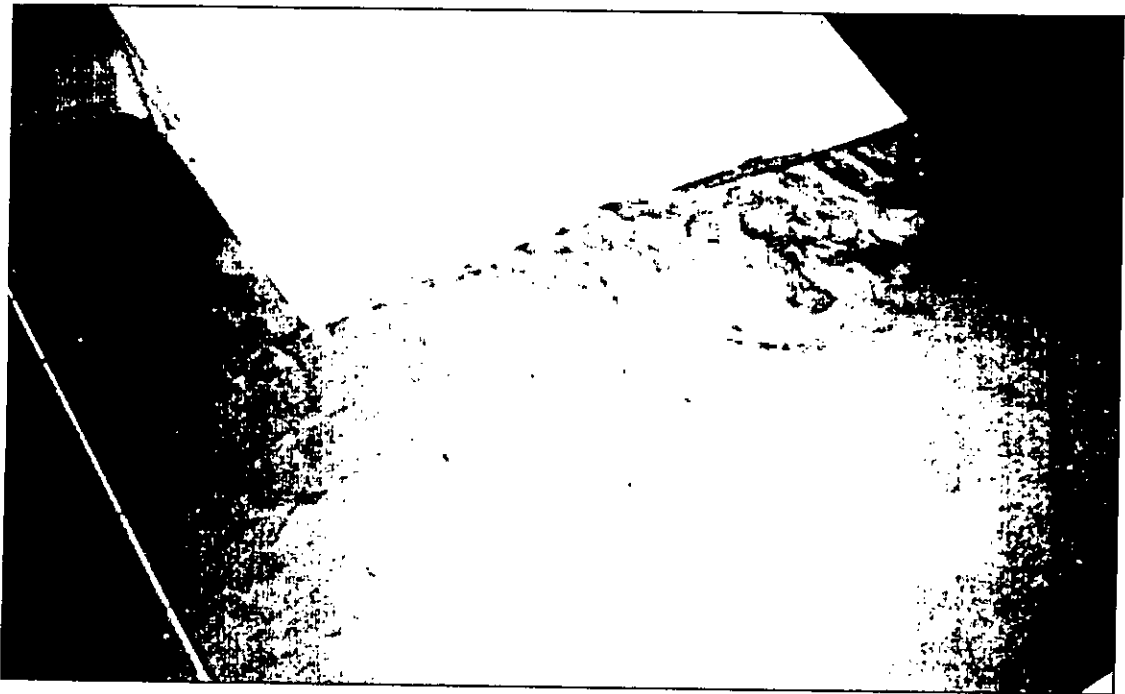


Fig. 4. 11 Scour around the 1V: 2H slope structure

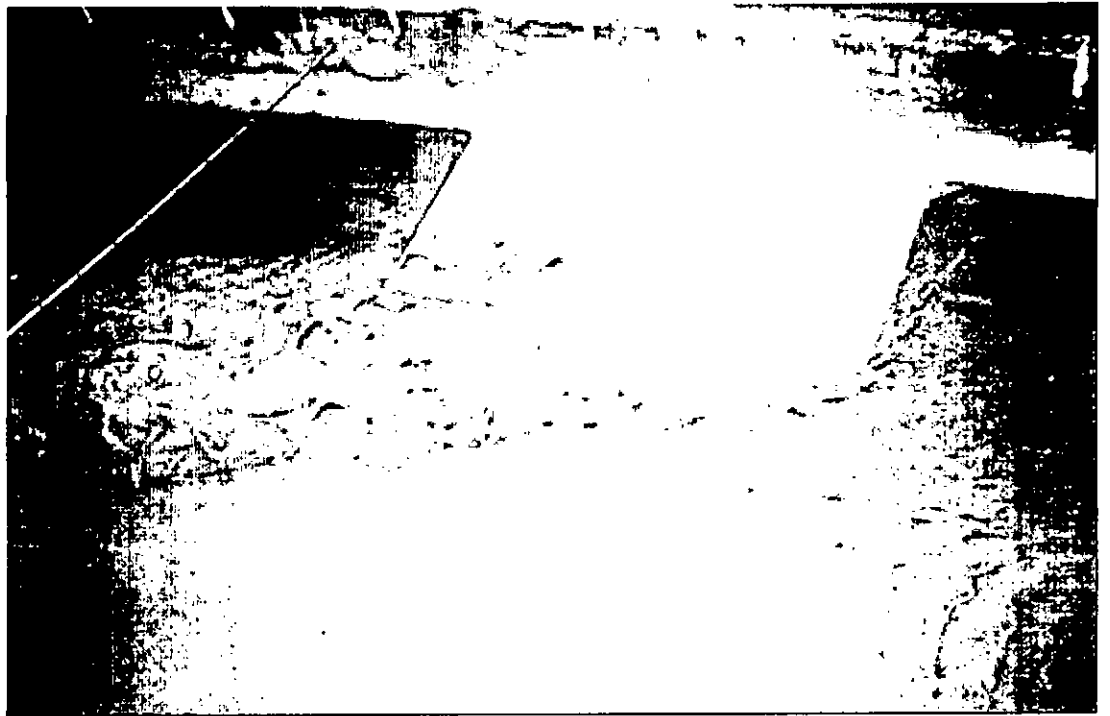
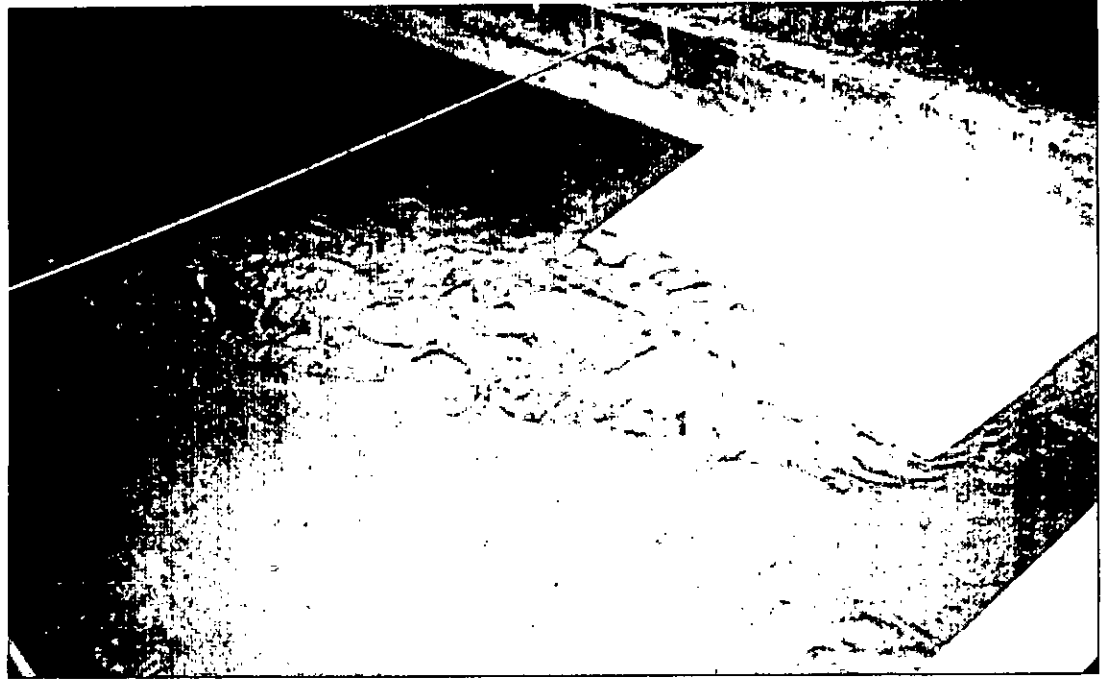


Fig. 4. 12 Scour around the IV: 3H slope structure



Fig. 4. 13 Scour around the vertical structure. $b=60\text{cm}$

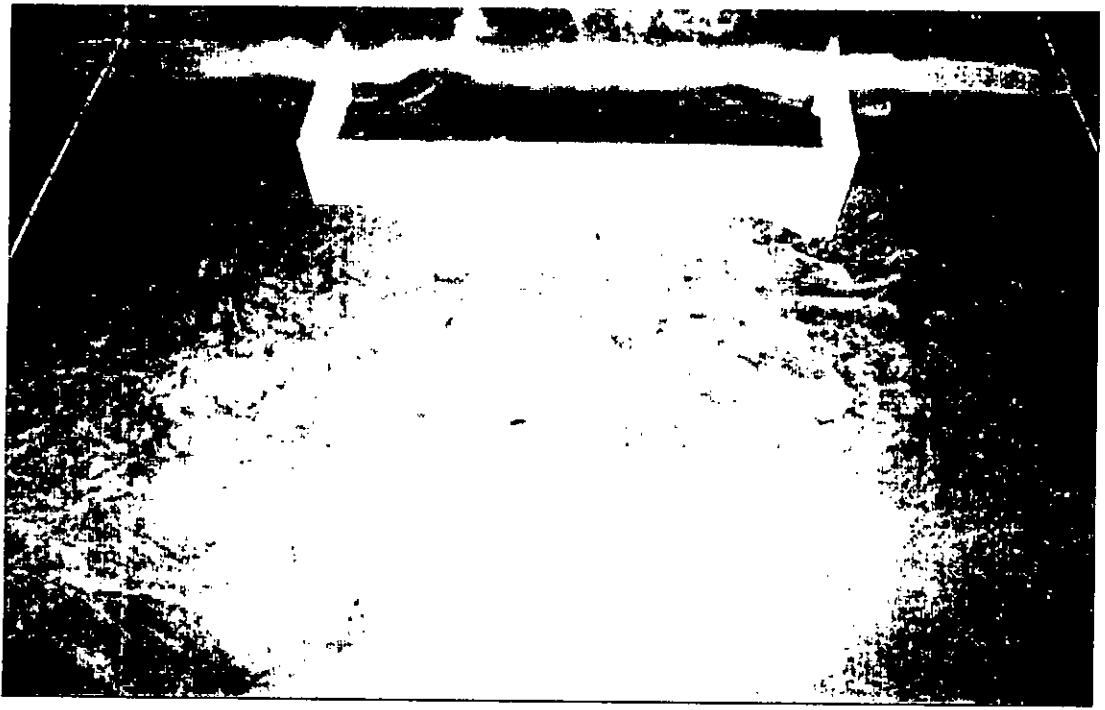


Fig. 4. 14 Scour around the vertical structure, $b=40\text{cm}$

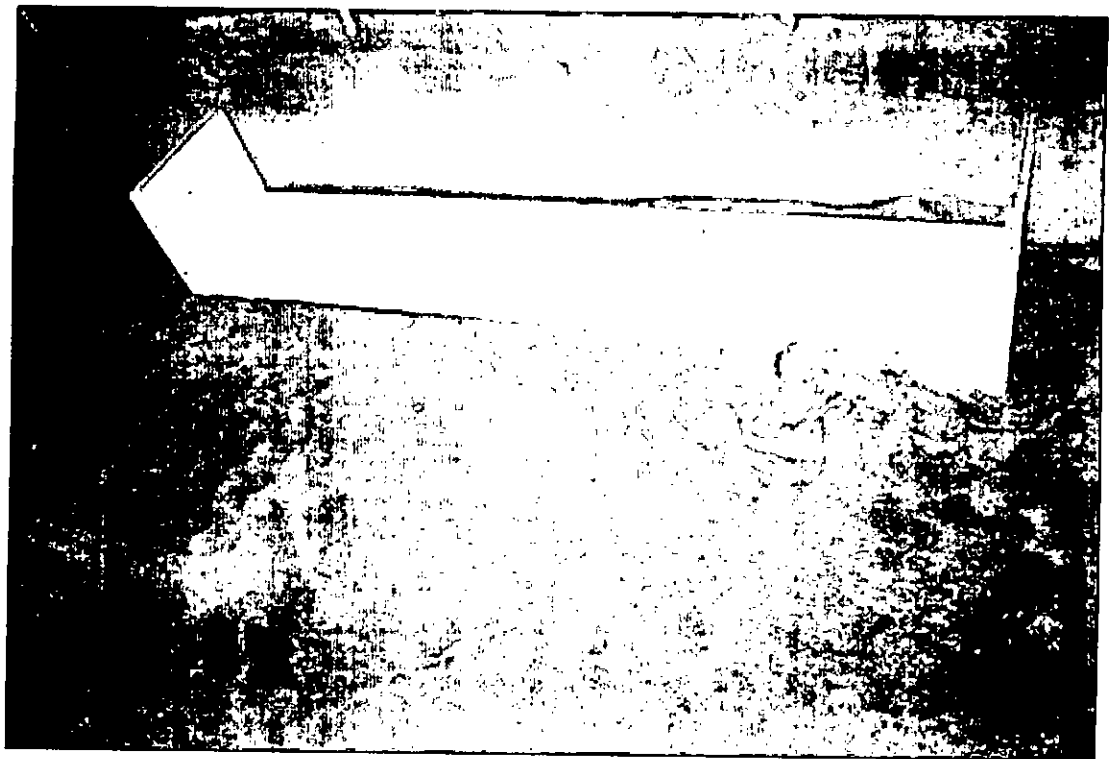
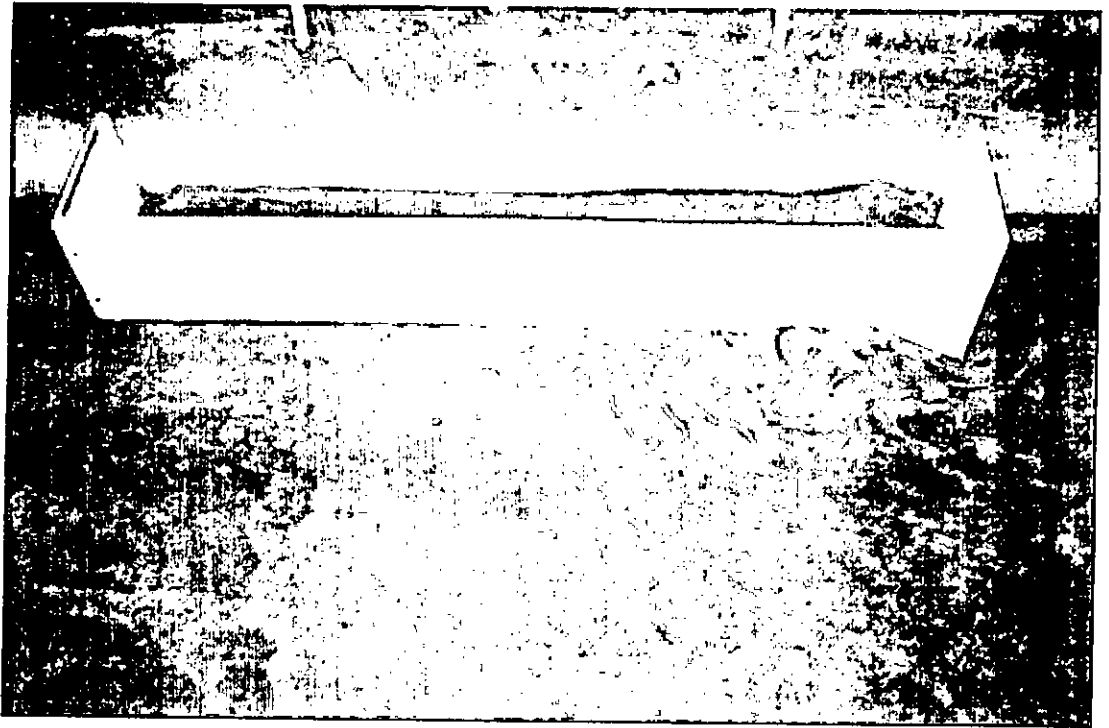


Fig. 4. 15 Scour around the vertical structure, $b = 20\text{cm}$

CHAPTER 5

CONCLUSION AND RECOMMENDATION

5.1 Conclusion

Based on the experimental investigations carried out in the present study, the following conclusion can be made.

- The maximum equilibrium scour depths observed in the experiments of the present study were found to be in good correlation with different prediction equations as follows:
 - i. In case of vertical-wall structure's scour, best correlation was observed with the equation of Lacey (1930). Particularly for the structure width, $b=60\text{cm}$. (Figure 4.4).
 - ii. In case of sloping structure's scour, there was also good correlation with the equation of Lacey (1930). Particularly for 1V: 3H slope structure. (Figure 4.3).
 - iii. From the analysis of scour experiment done at laboratory, it may be concluded that the Lacey's formula is suitable for local scour prediction for embankment-like structure with clear-water condition.
 - iv. Melville's (1992), Rahaman and Muramoto's (1999) and Liu's (1961) formulae were also found to be in good agreement for the prediction of maximum scour depth around vertical as well as sloped-wall structures.

- Scour area, in case of sloping structure increased with decreases of slope. It was noticed that the scour area moved d/s more and more with decreases of slope. In case of vertical structure scour area increased with increase of flow restriction width, b . In all cases, the scour area increased diagonally towards d/s .

- From the observation of the velocity vector at $0.6y$ from the water surface (Figure 3.20 to 3.25), it was clear that the flow concentration occurred close to the structures due to deflection. In case of vertical-wall structures, the angle of deflection was quite significant as compared to the deflection made by sloping-wall. This implies that the shape of the structure has a significant influence in flow concentration, which in turn resulted in greater depth of scour. It was observed that a dead water zone adjacent to the embankment wall existed at d/s corner of the structure.

5.2 Recommendations for Future Studies

Using the present study as a basis, there are wide scopes for future studies. Recommendations for future studies can be made as follows:

- ❖ The study can be made with sediment laden water to conform more with practical cases.
- ❖ The study can be under taken for more longer period to reach quasi equilibrium state of flow.
- ❖ The study can be made with the different angle of inclination of embankment-type structure.
- ❖ The study can be made placing the structure at different position of the channel and with greater flow intensity (V/V_c).
- ❖ Instead of manual measurement of scour depth, electronic bed profiler can be used for better accuracy.

REFERENCES

- Bangladesh Water Development Board (BWDB) "Feasibility Report on the Bogra Polder I Project." Volume -3, Annex C, Civil Engg., Drainage and Flood Control-3 Project (DFC 3-P), Dhaka, PP.C-8-12, 1984.
- Bangladesh Water Development Board (BWDB) "Guide to Planing and Design of River Training and Bank Protection Works" Design Circle-2, 72,Green Road, Dhaka. December 1993.
- Bangladesh Water Development Board, "River Bank Protection Project" Evaluation of Hard Points, Review of Damage during 1999 Flood Season, and Recommended Remedial Works. Halcrow in association with Haskoning, October 1999.
- Chang, H.H "Fluvial Process in River Engineering." John Willey & Sons, Inc. USA, 1988.
- Fischenich, C. and Landers, M. "Computing scour" Technical Notes (ERDC TN- EMRRP-SR-05), U.S, Army Engineer Research and Development Center, Vicksburg, MS. 1999.
- Grade, R.J., Subramanya, K. and Nambudripad, K.D., "Study of scour around spur dikes. J. of the Hydraulic division, ASCE, Vol. 87, Hy6, pp. 23-37. 1961.
- Garg, S.K. "Irrigation Engineering and Hydraulic Structure." 11th edition. Khanna Publishers 2-B, Nath Market, Nai Sarak, New Delhi, 1995.
- Hossain, K.M.S. "Experimental Study of Launching Apron around Abutment." M.Sc. Thesis. Department of Water Resources Engineering, BUET, January 2001.
- Hossain, M.M. and Hossain, K.M.S. "Experimental Study of Launching Aproan around Abutment". Proceeding of the third International Conference on Environmental Hydraulics. Arizona State University, Tampe, USA, December 5-8, 2001.

Islam, M.Z., Salehin, M. "Sedimentation Due to Different Models of Embankment Failure." Technical Report-02. IWFM. Bangladesh University of Engineering and Technology. R04/1998.

Kabir, M.R., Faisal, I.M. and Khatun, "Laboratory Study and Field Investigation of Scour around Bridge Piers in Bangladesh", Proc., International Symposium and Scour of Foundation, IS-Scour 2000, ISSMGE, TC-33, Melbourne, Australia, F. 2000.

Kawn, R.T.F. and Melville, B.W. "Local scour and flow measurements at bridge abutments." J. of Hydraulic Research, IAHR, 32(5), pp. 661-673, 1994.

Khatun, F. "Experimental Study on Local Scour around Bridge Piers and Its Reduction." M.Sc. Thesis, Department of Water Resources Engineering, BUET, April 2001.

Lacey, G. "Stable channels in alluvium." Paper 4736, Minutes of the Proc., Institution of civil Engineers, 229, William Clowes and Sons Ltd., London, Great Britain, 259-92. 1930.

Laursen, E.M. "An analysis of relief bridge scour." J. Hydraulic. Division, ASCE, Vol. 89(3) pp. 93-118, 1963.

Lim, S. Y., "Equilibrium Clear-Water Scour Around an abutment", Journal of Hydraulic Division, ASCE, 123(3), pp. 237-243, 1997.

Liu, H.K., Chang, F.M. and Skinner, M.M. "Effect of bridge constriction on scour and backwater." Engineering Research Center. Colorado State University. CER 60, KHL 22, 1961.

Melville, B.W. "Local Scour at Bridge Abutments." Journal of Hydraulic Engineering, ASCE, 118(4), 615-631, 1992.

Melville, B.W. and Chiew, Y.M. "Time Scale of Local Scour around Bridge Piers." Journal of Hydraulic Engineering, ASCE, 125(1), 59-65, 1999.

- Melville, B.W. and Coleman, S.E. "Bridge Scour". Water Resources Publications, LLC, Colorado, USA, 2000.
- Molinas, A., Kheireldin, K and Wu, B. " Shear Stress around Vertical Wall Abutment." Journal of Hydraulic Engineering, ASCE, Vol. 124, pp. 822-830, 1998.
- Rahaman, M.M., "Studies on Deformation Process of Meandering Channels and Local Scouring Around Spur-dike-like Structures", Doctoral Thesis, Kyoto, Japan, December 1998.
- Rahaman and Haque. "Local scour around sloped-wall spur-dike-like structures in alluvial rivers, revision submitted to the J. of Hydraulic Engg., ASCE, 2002.
- Rahaman, M.M and Muramoto, Y. "Prediction of maximum scour depth around spur-dike-like structures, Annual J. of Hydraulic Engineering, JSCE, Vol. 43, 1999.
- Rahaman, M.M and Haque, A. "Prediction of Scouring Around Abutment-Like Structure." Technical Report-1: Mechanism of scour development. IWFM, BUET, April 2002.
- Rahaman, M.M and Haque, A. "Prediction of Scouring Around Abutment-Like Structure." Technical Report-2: Prediction Methods. IWFM, BUET, June 2002.
- Rajratnam, N. and Nwachuku, B.A. "Flow near groin-like structure." J. of Hydraulic Division, ASCE, Vol. 109, pp. 463-480, 1983a.
- Rajratnam, N. and Nwachuku, B.A. " Erosion near groin-like structure." J. of Hydraulic Research, IAHR, Vol. 21, pp. 277-287, 1983b.
- Sadeque, M.A.F. "A Laboratory Study on Local Scour around Bridge Piers and Abutments." M.Sc. Thesis. Department of Water Resources Engineering, BUET, August 2002.
- Safiullah, A.M.M. "Performance of the Dhaka Narayanganj Demra (DND) Embankment." A Research Report of the Dept. of civil Engg., BUET, Dhaka, PP.3-45, 1977.
- Safiullah, A.M.M. "Failure of Embankment Slope" A Case Study, J. Institution of Engineers Bangladesh, Volume 10, No. 1, PP.17-24, 1982.

- Tobin, G.A. The Levee Love affair: A stormy relationship. Economic and Social Commission for Asia and the Pacific (ESCAP), UNO. Bangkok. PP.15-20. 1995.
- Tobin, G.A. and Ollenburger, J.C. An Examination of stress in a Flood prone Environment. Papers and Proceedings of Applied Geography Conferences. 17:74-81. 1994.
- Vittal, N., Kothiyari, U.C. and Haghightat, M. "Clear Water Scour around Bridge Pier Group". Journal of Hydraulic Engineering, ASCE. Vol.120. No. 11. pp. 1309-1318. 1994.

